ESTONIAN SCIENCE FOUNDATION
GRANT 172

NONHYDROSTATIC ATMOSPHERIC DYNAMICS IN PRESSURE-RELATED COORDINATES

R. Rõõm

Final Report
1993 – 1996

Principal Investigator:

R. Rõõm

TARTU OBSERVATORY
Tõravere EE-2444, Tartumaa, Estonia
1997

ACKNOWLEDGEMENTS

I would like to express cordial gratitude to:

Estonian Science Foundation and its Section of Exact Sciences whose good attitude made this investigation possible;

Professor Thorpe from the University of Reading, who proposed the general idea of this investigation and to whom I owe good scientific contacts with the University of Lisbon and University of Munich;

Professor Miranda from the University of Lisbon, for his support with high-quality numerical program NH3D and visualization package NHGRAF, as well as for many fruitful discussions of the subject;

M.Sc. Anu Ülejõe and B.Sc. Aarne Männik for their contributions to the subject.

All rights reserved

Last revision: December 15, 1997

TABLE OF CONTENTS

INTRODUCTION

The aim of this investigation is to present a comprehensive introduction to nonhydrostatic atmospheric dynamics in the unified pressure-coordinate framework.

The pressure (or isobaric) coordinates (further "p-coordinates" as well as the "p-space" will be often used) were introduced by Eliassen (1949), their adaptation to the non-uniform ground conditions was developed by Phillips (1957). Representation of the hydrostatic (HS) dynamics, which was (and still is) prevailing in climate modeling and weather forecast problems, in pressure-coordinates became instantly popular and is dominating in large-scale atmospheric dynamics up to date. One reason for such popularity is that the p–coordinates are the ones in which the real atmospheric sounding results are recorded. The balloon-borne radio-sounds present temperature, humidity and wind component as functions of pressure p (besides horizontal coordinates, x, y, and time, t) rather than the balloon height, z. Another reason for the popularity of pressure-coordinates, more fundamental for theoretical investigations, is that the atmosphere is incompressible and its dynamics represents circulation of an incompressible liquid in p-space, supposing the governing equations are HS equations. This is understandable because incompressible flows have many advantages in comparison with compressible models: the number of independent functions is less by one; fast acoustic disturbances are removed; mathematical formulation and interpretation of the results is simpler; there exist several nonlinear, nonstationary problems with known exact analytical solutions. These multiple advantages make pressure-space very attractive for theoreticians and fully compensate the only disadvantage: the p-space is a little bit more abstract and it takes some additional efforts to become familiar with it.

The growing resolution of both numerical forecast and climate models as well as the growing requirements to the model precision has brought the transition from hydrostatic dynamics to nonhydrostatic (NH) models into limelight. The development of nonhydrostatic models has been going on for about three decades, it started with the development of NH models for mesoscale-investigations (Ogura and Charney 1962, Dutton and Fichtl 1969, Miller and Pearce 1974, Tapp and White 1976, Klemp and Wilhelmson 1978, Redelsberger and Sommeria 1981, Pielke 1984). The present state of affairs in use of NH models in operational forecast is that they are as a rule high-resolution meso-models and are treated as supporting tools in addition to the main HS forecast models. In the next five to ten year period all HS models are likely to be replaced or updated to NH versions.

For general circulation and local-area forecast models the NH-updating process must go on in the way that the connections with existing models, computing environment and pre- and post-processing utilities were not lost. In such a situation dynamic models

gain primary significance which enable employment of NH dynamics without departure with pressure related coordinate-spaces. Three main trends can be recognized:

i. Models which employ actual pressure of an air-particle for its vertical coordinate (Miller 1974, Miller and Pearce 1974, Miller and White 1984, White 1989, Rõõm 1990). This trend has a longer history.
ii. Models which employ the hydrostatic component of pressure field as a vertical coordinate (Laprise 1992), this coordinate system is used for instance in the Meteo-France model Aladin.
iii. Models which use the hydrostatic mean background pressure field in the role of a vertical coordinate. This coordinate frame is employed in the NH-extension of the Penn State – NCAR model (Dudhia 1993).

The first and probably best known NH model in pressure space is the Miller–Pearce model, hereafter the MPM (Miller 1974, Miller and Pearce 1974). This model abandons the hydrostatic equilibrium assumption in favour of the full vertical momentum equation but postulates the incompressibility of motion in pressure–space and in this way filters the acoustic mode[1]. In a most general form the MPM is presented by White, 1989. Majority of numerical relaxation and physical filtering schemes employ partial linearization with separation of the background and perturbation states. This is needed for explicit revealing of acoustic subsystem of the model. The MPM is not an exclusion in this respect. The White generalization represents an exception in this respect, because it substitutes the horizontally homogeneous background temperature of the original MPM by an optional background temperature field which can represent some real synoptical situation. This generality makes the White version quite valuable. The MPM was originally designed in p–coordinates, sigma–coordinate versions were developed by Miller and White, 1984, and used in numerical modeling by Xue and Thorpe, 1991, and Miranda and James, 1992. Still, there existed many unresolved or theoretically poorly founded aspects of the model, owing their origin to the phenomenological rather than theoretical foundation, like problems with changing geometry and boundary values of different field on these replacing boundaries, and the question of scales of application (is there a limiting scale, below of which the Miller-Pearce model cannot be applied, or is it valid until the laboratory scale?). Therefore, further theoretical investigation in the field of NH p-space dynamics is actual and necessary.

The present technical report makes an attempt to fill some existing gaps in the theory of nonhydrostatic pressure-space dynamics. General nonhydrostatic nonfiltered hydrodynamic equations in pressure coordinates (Rõõm 1989, 1990) yield a ground for such theoretical task. This model, hereafter referred to as the ExM (the Exact Model) is deduced with the help of the direct transformation of complete nonfiltered equations, using the curvilinear coordinate covariant differencing formalism, from the ordinary space to the p–space. It does not assume any preliminary simplification (including the preservation of the full Coriolis force). Using these equations as a starting point, it makes possible a systematic treatment of acoustic relaxation process and rise of incompressible motion in pressure space, as well as reexamination of the boundary value problem. As

[1] In this respect the MPM represents a version of anelastic models.

a result, our understanding of the NH dynamics in p-space should improve, which will result in better numerical forecast and circulation models.

The main objectives of the present technical report are:

– to establish a systematic way of deduction of filtered models in pressure space;

– to estimate quality and domains of applications of different filtered models;

– to examine quality of nonlinear filtered models, especially the geopotential height equation and its boundary value problem;

– give recommendations for creation of numerical algorithms;

– elaborate an example numerical algorithm to prove these recommendations.

The content of the report is as follows.

In Chapter One the basic equations (the ExM) are presented and discussed and the formal transition to the MPM is described.

In Chapters Two to Four the main topics are the filtering problems and the quality estimation of filtered models. In these chapters the treatment is mainly engaged in linear models. In Chapter Two a systematical way of acoustic filtering of the initial complete linear ExM is proposed and elaborated, which bases on the use of the Lagrangian formulation of linear hydrodynamics along with the least action (Hamiltonian) principle. The output of the filtering is a model called the "Elastic filtered model" (EFM) which is different from the common MPM. The most fundamental quality of the EFM is that it supports (weakly) compressible dynamics in pressure-space (this justifies its name). Chapter Three has the assisting nature, its aim is to generalize linear models of the previous chapter (both the complete and filtered versions), designed for resting background, to more general shear-flow background conditions in the presence of the Coriolis force. The aim of this generalization is to get p–space models which are simple and allow analytical solutions and at the same time are close enought to real atmospheric conditions. The corresponding linear equation for the MPM and hydrostatic primitive-equation model (HSM) are deduced as well. All developed models are subject to numerical modeling and mutual comparison in Chapter Four. General conclusions from modeling with linear equations is that **(I)** the EFM can be employed without spacial-scale restrictions, i.e. it is an all-scale model, valid from micro-turbulence ($l \sim$ 10 cm) till planetary scale ($l \sim 10\ 000$ km) dynamics; **(II)** the MPM is applicable in scales $l > 100$ m. The conclusion that the domain of the MPM is restricted from short-scale side is certainly unexpected. Still, the MPM includes all the planetary, synoptic and meso-scale domains, leaving out the small-scale convection and turbulent mixing processes only. Along with the incompressibility of the MPM this means that the MPM claims to be a most useful filtered model.

The general topic of Chapters Five and Six is the numerical modeling of the nonlinear atmospheric dynamics in a limited area with typical dimensions in horizontal directions 100×100 km^2. In Chapter Five the nonlinear equations (both ExM and filtered models) are transformed into the σ-space, which presents a convenient way for the introduction

of orography. Still, the main objective of the chapter is the study of the diagnostical equation for the nonhydrostatic geopotential height distribution. This is a Poisson equation and it represents a most fundamental relationship in all acoustically adjusted (relaxed) nonhydrostatic models, as (the gradient of) its solution determines the main actual force acting on an air-particle in the atmosphere. Much attention is paid to the boundary conditions of this equation. The double character of model geometry – atmosphere is a compressible gas in ordinary physical space with firm lower and free upper boundary, whereas in the p-space it represents an incompressible liquid with fixed upper and free lower boundary – is a potential source for misinterpretations. The main idea used in the present investigation to clear the situation is that the lower boundary (and lateral boundaries, if the model has ones) is treated as an ideal constraint. This leads to the interpretation of normal gradient of the geopotential height at the boundary as forces of constraint reaction. At the upper boundary both the rigid-lid and free-surface conditions are applied in the physical space, which leads to two different models. The rigid-lid model is artificial and it is developed to demonstrate the role of upper boundary condition. The main model is the "free upper boundary model" which assumes that there is no upper boundary in the physical space at all. Corresponding free boundary condition is formulated in the p-space using a special solution-continuation technique. The deduced condition is a generalization of the "radiative" boundary condition.

In Chapter Six ideas of previous Chapters are applied for the creation of a simple adiabatic numerical model in pressure coordinates. As the departure point the numerical model NH3D, elaborated by Miranda (1990), is used. Besides the boundary condition and initialization revision the main modification is that the domain, occupied by the atmosphere in the p-space, is the fixed one during integration. Numerical experiments with the new version and comparison of results with analytical solutions exhibit its good precision and numerical stability. Along with the results of previous chapters this leads to the general conclusion, that the proposed pressure-space models are useful tools in numerical applications and have good perspective to be employed in the future forecast and general circulation models of the atmosphere.

As this investigation represents the first attempt to describe nonhydrostatic acoustically filtered dynamics in pressure-space in an unified framework on the base of general nonhydrostatic p-space equations, the presented material is original in major part and is published first here.

An initial heading of the present investigation, which was carried out as the Grant NO. 172 under the sponsorship of the Estonian Science Foundation, was "Dynamic model of local atmospheric circulation for mesoscale processes and air pollution study". The developed numerical model NHAD, described in the last Chapter, represents the realization of this heading. Still, the actual main trend of the realized investigation turned out to be in the area of pressure-space dynamic foundation rather than in the field of elaboration of specific applications, therefore the final heading was corrected to be more concordant with the actual content.

CHAPTER ONE

Basic Equations in Pressure Coordinates

1.1. Height of the isobaric surface.

In general case the pressure field $p(x, y, z)$ consists of hydrostatic main component, p_s, and a NH correction, p_n: $p = p_s + p_n$. Correspondingly, in pressure coordinates $(\mathbf{x},\ p)$, $\mathbf{x} = (x,\ y)$, the height of an isobaric surface $z(\mathbf{x},\ p,\ t)$ presents in the similar way (Fig. 1.1):

$$z(\mathbf{x},\ p,\ t) \ = \ z_s(\mathbf{x},\ p,\ t) \ + \ z_n(\mathbf{x},\ p,\ t) \ , \tag{1a}$$

$$z_s(\mathbf{x},\ p,\ t) \ = \ h(\mathbf{x}) \ + \ \frac{R}{g} \int_p^{p_0(\mathbf{x},\ t)} \frac{T(\mathbf{x},\ p',\ t)}{p'} \mathrm{d}p' \ . \tag{1b}$$

Here $h(\mathbf{x},\ p,\ t)$ is the height of the ground above sea–level, $p_0(\mathbf{x},\ t)$ represents the atmospheric pressure field at the ground and $T(\mathbf{x},\ p,\ t)$ is the temperature. The hydrostatic height component z_s corresponds to the height, which the particle will have, if the pressure inside that particle is entirely determined by hydrostatic effect, i.e., by the weight of the atmospheric column above that particle. The remaining part of the height, z_n, is defined as the difference of actual and hydrostatic heights of the particle. The independent height–coordinate, p, corresponds to the actual pressure in the particle. Such pressure interpretation performs the most fundamental difference of this model from models of Laprise 1992, with the hydrostatic pressure in the role of vertical coordinate, and Dudhia 1993, with the undisturbed background pressure as the vertical coordinate.

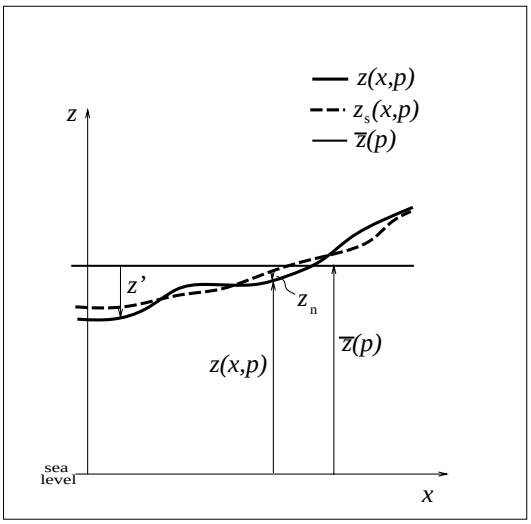

Fig. 1.1

Components of the isobaric height in the NH atmosphere.

The correction term z_n is entirely caused by the nonhydrostatic pressure deviation p_n. Because $|z_n| << z_s$ and $|p_n| << p$ in the atmosphere, the nonhydrostatic pressure and height corrections are related as (Fig. 1.2)

$$\frac{z_n}{H} \approx \frac{p_n}{p} \tag{2}$$

where $H = RT/g$ is the height scale of the atmosphere. For processes with infinitesimal amplitudes (which can be described in the framework of linearized models) this approximate equality may be replaced by the exact one

$$\frac{z_n}{H} = \frac{p_n}{p} \ . \tag{2'}$$

These formulae are useful for comparison of different pressure– and height–coordinate models, as they permit to express pressure–forces via gradients of the geopotential height and vice versa.

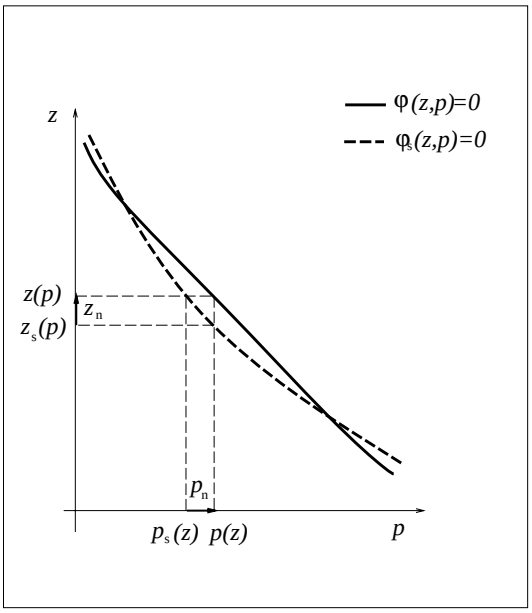

Fig. 1.2

Illustration of formula(2). φ and φ_s are the implicit actual and hydrostatic relationships between z and p for fixed t and $\mathbf{x}$.

1.2. General NH equations in p–coordinates.

If the pressure field is a monotone function of height,

$$\frac{\partial p}{\partial z} < 0 \ ,$$

then it is possible to transform the dynamic equations of the atmosphere from Cartesian coordinates $\{x,\ y,\ z,\ t\}$ to pressure coordinates $\{x,\ y,\ p,\ t\}$, disregarding the hydrostatic assumption. Such transformation can be performed, using the curvilinear coordinate transformation and covariant differencing technique (Rõõm 1989, 1990). The

resulting complete, nonfiltered, nonhydrostatic p–coordinate equations can be presented after minor simplification of the Coriolis force in the form:

$$\frac{\mathrm{d}z}{\mathrm{d}t} \;=\; w \tag{3a}$$

$$n\,\frac{\mathrm{d}w}{\mathrm{d}t} \;=\; g(1\;-\;n)\;, \tag{3b}$$

$$n\,\frac{\mathrm{d}\mathbf{v}}{\mathrm{d}t} \;=\; -\,g\nabla\,z\;-\;nf\hat{\mathbf{z}}\times\mathbf{v}\;, \tag{3c}$$

$$\frac{\mathrm{d}T}{\mathrm{d}t} \;=\; \frac{RT\omega}{c_p p}\;+\;Q\;, \tag{3d}$$

$$\frac{\mathrm{d}n}{\mathrm{d}t} \;=\; -\,n(\nabla\cdot\mathbf{v}\;+\;\partial\omega/\partial p)\;, \tag{3e}$$

$$n \;=\; -\,\frac{p}{H}\frac{\partial z}{\partial p}\;. \tag{3f}$$

Here $\mathbf{v} \;=\; (u,v)$ and w are horizontal wind vector and vertical wind respectively, $\omega \;=\; \mathrm{d}p/\mathrm{d}t$ presents the omega–velocity of an air particle, n is the normalized, nondimensional density in pressure coordinates, which is related to the ordinary air density as:

$$n\delta p \;=\; g\rho\delta z\;,$$

Q is the thermal forcing (heat source divided by c_p), p_0 presents the ground surface pressure, $\hat{\mathbf{z}}$ represents the vertical unit vector, and the total (or Lagrangian) derivative is defined as

$$\frac{\mathrm{d}}{\mathrm{d}t} \;=\; \frac{\partial}{\partial t}\;+\;\mathbf{v}\cdot\nabla\;+\;\omega\frac{\partial}{\partial p}\;.$$

1.3. Boundary conditions

Conditions at the lateral boundaries are the same as in Cartesian coordinate models and do not present special interest in the context of the present study. The main differences with the ordinary model occur in the "horizontal" conditions at the top and at the bottom. The domain occupied by the atmosphere is

$$0 \;<\; p \;< p_0(\mathbf{x},\;t) \tag{4a}$$

where the lower boundary surface in the p–space, p_0, is not fixed, but evolves in accordance with the equation

$$\frac{\mathrm{d}p_0}{\mathrm{d}t} \;=\; \omega|_{p_0}\;, \tag{4b}$$

which expresses the condition that the lower boundary consists all the time of the same air particles. Thus, domain is varying in time and (4b) presents an additional evolutional (prognostic) equation which must be integrated simultaneously with the system (3).

Boundary conditions at $p = p_0(\mathbf{x}, t)$ and $p = 0$ are

$$z|_{p_0} = h(\mathbf{x}) , \tag{5a}$$

$$\omega|_0 = 0 . \tag{5b}$$

The first assumes the existence of rigid underlying surface in the ordinary physical space. The second defines a fixed boundary in the p–space at the level $p = 0$, this boundary condition forbids the mass outflow to the cosmos in the physical space.

Relations (4) and (5) define the prime boundary conditions. Other conditions at boundaries which arise in the course of particular problem formulation, model simplification and discretization must be concordant with the primary one. The most common secondary condition, which will be employed further at mountain-wave simulation and in numerical schemes, is the slipping condition at the lower boundary, which follows at the differencing of (5a) in time:

$$w|_{p_0} = \mathbf{v}_{p_0} \cdot \nabla h . \tag{5a'}$$

If a continuous medium has a bounding surface, which moves in accordance with a differential equation governed by the state of that medium, this surface is called free. In this respect $p_0(\mathbf{x}, t)$ describes a free boundary and in the p–space the atmosphere is a continuous medium with free surface at $p = p_0$. At the same time, at the level $p = 0$ there exists a rigid lid in the p-space in accordance with (5b). The situation in the p-space is just opposite with conditions in the ordinary Cartesian space, where atmosphere has the rigid boundary at the bottom (condition (5a)), but has no definite boundary at the top.

1.4. Diagnostic equation for ω. Time–order lowering

Model (3) presents a closed system consisting of seven equations for seven fields z, u, v, w, T, n and ω. All quantities here, except ω, are prognostic fields, and system (3) includes a single diagnostic equation (3f). This equation must be used for the determination of the diagnostic field ω. As (3f) does not include ω explicitly, the only way to proceed is to differentiate (3f) by t and eliminate time derivatives by the help of other equations in system (3). The result is an explicit equation for ω

$$\alpha \frac{\omega}{p} - \frac{Q}{T} = \frac{p}{nH} \left(\frac{\partial w}{\partial p} - \frac{\partial \mathbf{v}}{\partial p} \nabla z \right) - \nabla \cdot \mathbf{v} \equiv - \mathcal{D} , \tag{6}$$

where

$$\alpha = \frac{c_v}{c_p} .$$

In equation (6) the quantity on the right hand side, denoted as $\mathcal{D}$, represents the divergence of the three–dimensional velocity $\{u, v, w\}$ in the common Cartesian space:

$$\mathcal{D} = \left(\frac{\partial u}{\partial x} \right)_{y,z} + \left(\frac{\partial v}{\partial y} \right)_{x,z} + \left(\frac{\partial w}{\partial z} \right)_{x,y} .$$

Thus, (6) is the general tendency equation for the thermodynamic pressure field, appearing in the isobaric coordinate space as a diagnostic relationship. It is a thermodynamic definition for ω and presents a standard form of the thermodynamic equation, written in terms of $\mathrm{d}p/\mathrm{d}t$ upon application of the continuity equation and the perfect gas law. As the pressure plays the key–role in acoustic adjustment, (6) will be an equation of primary significance for further treatment.

Now, after the diagnostic equation for ω has been derived, the initial relationship for its derivation, equation (3f), has played its role, and, in principal plane, it may be dropped from further treatment. But there exists an alternative possibility – we can employ diagnostic equation (3f) for the determination of one of three dependent variables (z, n, T), and drop the evolutional equation for that variable (ie. (3a), (3e) or (3d)) from consideration. This means, we can go ahead with three different sets of equations, which differ by appearance but are all equivalent to each other. As a result of modification, the time–order of the final model will be five, ie., it will be by one step smaller than in the initial equations (3). The reduced in this way model we shall use in point 3.4.

1.5. The primitive–equation asymptotic

For movements with small vertical accelerations, $\mathrm{d}w/\mathrm{d}t \to 0$,

$$z \ \to \ z_s \ , \quad n \ \to \ 1 \ , \tag{7}$$

where z_s satisfies the hydrostatic condition (equivalent to definition (1b))

$$\frac{\partial z_s}{\partial p} \ = \ -\frac{H}{p} \ . \tag{8}$$

Equations (3) transform at this limit to the ordinary HS model. Formally the HS can be reached, substituting everywhere in (3) n by 1 and z by z_s. The continuity equation (3e) transforms at the hydrostatic limit to the condition of the incompressibility,

$$\nabla \cdot \mathbf{v} \ + \ \partial\omega/\partial p \ = \ 0 \ . \tag{9}$$

The hydrostatic analogue for (6) is

$$\alpha \ \frac{\omega}{p} \ - \ \frac{Q}{T} \ = \ \frac{p}{H} \ \left(\frac{\partial w_s}{\partial p} \ - \ \frac{\partial \mathbf{v}}{\partial p} \nabla \ z_s \right) \ - \ \nabla \cdot \ \mathbf{v} \ . \tag{10}$$

It can be deduced from the HSM in the same way which was used for the deduction of (6), if the definition

$$w_s \ = \ dz_s/dt \tag{11}$$

is assumed for the vertical velocity at hydrostatic limit. Note that (10) is very close in appearance to the original nonhydrostatic version (6) and can be deduced from (6), using limit (7). Though the HSM does not need equation (10), this diagnostic relation may be used for the determination of the hydrostatic vertical velocity, defined by (11).

Due to the assumption of the incompressibility the HSM filters acoustic waves. An exception is presented by the external, or surface waves, which are supported when the pressure at the lower boundary evolves according to nonbalanced equation (4b).

1.6. The Miller–Pearce model

Another model, which filters the sound waves, is the MPM. The MPM was alternatively derived from the Hamilton principle by Salmon and Smith 1994. Here we will outline the deduction of the MPM from the general NH model (3).

The MPM grounds on two fundamental approximations, which are introduced into the initial model (3). The first one is the incompressibility approximation, $n = 1$, which is used everywhere, except the right side of equation (3b). Due to this approximation, equation (3e) transforms to the continuity relation for incompressible fluid :

$$\nabla \cdot \mathbf{v} + \partial\omega/\partial p = 0 \qquad (12a)$$

(which filters acoustic waves by the way). The another approximation stands in the approximate presentation of the total derivative for z in (3a) as follows

$$\frac{\mathrm{d}z}{\mathrm{d}t} \approx \omega \frac{\partial z_s}{\partial p} = -H \frac{\omega}{p} .$$

This enables to reduce the initial evolutional equation (3) to the diagnostic relationship

$$\tilde{w} = -H\frac{\omega}{p} , \qquad (12b)$$

where $\tilde{w}$ stands for for the approximate value of vertical velocity, which is defined by (12b) and which obviously differs (for given $\omega = dp/dt$) from both the exact definition (3a), w, and the quasi-static definition (11), w_s. In momentum equations the density n is approximated by the unit value except the right side of (3b), where it is expressed using (3f):

$$\frac{\mathrm{d}\tilde{w}}{\mathrm{d}t} = g\left(1 + \frac{p}{H}\frac{\partial z}{\partial p}\right) , \qquad (12c)$$

$$\frac{\mathrm{d}\mathbf{v}}{\mathrm{d}t} = -g\nabla z - f\hat{\mathbf{z}} \times \mathbf{v} . \qquad (12d)$$

Finally, the thermodynamic equation takes with the help of (12b) the form

$$\frac{\mathrm{d}T}{\mathrm{d}t} = -\frac{g}{c_p}\tilde{w} + Q . \qquad (12e)$$

The obtained equations coincide with the MPM in its most general form (White 1989).

Differently from HSM, which has an adjusted analogue (10) for equation (6), the MPM lacks such analogue. This occurs due to the use of the (more restrictive) approximation

(12b) instead of the "natural" assumption (11)[1)]. This difference is the main motivation to look further, in point 3, for acoustically filtered models which, differently from the MPM, support the diagnostical relationship (6).

1.7. Energy conservation

The energy conservation law can be presented for (3) in the form

$$n\frac{\mathrm{d}}{\mathrm{d}t}e \;+\; \nabla(\mathbf{v}gz) \;+\; \frac{\partial}{\partial p}(\omega gz) \;=\; nc_pQ \tag{13}$$

where the energy density is

$$e \;=\; \frac{\mathbf{v}^2}{2} \;+\; \frac{w^2}{2} \;+\; c_pT \;+\; \left(1 \;-\; \frac{1}{n}\right) gz \;. \tag{14}$$

The last term here presents additional energy, which atmosphere has due to its compressibility. In both described incompressible models, the HSM and the MPM, this term is absent. In the MPM the energy density turns to the form

$$e \;=\; \frac{\mathbf{v}^2}{2} \;+\; \frac{\tilde{w}^2}{2} \;+\; c_pT \;, \tag{14$'$}$$

the HSM lacks the vertical kinetic energy in addition:

$$e \;=\; \frac{\mathbf{v}^2}{2} \;+\; c_pT \;. \tag{14$''$}$$

[1)] By the way, difference in (11) and (12b) exhibits, that the MPM is not physically identical to the HSM at the long–wave limit.

CHAPTER TWO

Acoustic Filtering

In this Chapter the ExM is linearized and the acoustic filtering is carried out with the help of the least action (Hamiltonian) principle. The least action principle we use represents the classical formulation of the mechanics of continuous medium in the Lagrangian representation (Herivel 1955, Serrin 1959), which is in linear case close to the variational formulation of the classical field theory (Landau and Lifchitz 1987). It should be noted that there exists another way of variational formulation of the continuous mechanics (which is not used in the present investigation): the symplectic formalism which employs the Eulerian representation rather than the Lagrangian one (Salmon 1983, 1988a,b, Salmon and Smith 1994, Roulstone and Brice 1995).

In short, the variational technique is used for filtration task as follows. The nonlinear ExM is linearized and the Lagrangian function is constructed for the linear model. The filtering approximations are introduced promptly into the Lagrangian. Possible approximations, which yield wave–filtration, are not very numerous and they are easily recognizable as they all belong to the approximations, resulting in the time–order lowering. In turn, the filtered Lagrangian generates filtered dynamics, if one moves in opposite direction from the Lagrangian back to the equations with the help of the least action principle. The use of this principle guarantees in accordance with the Noether theorem maintenance of conservation laws of the initial linearized model (assuming, of course, that the filtered Lagrangian has the same temporal and spacial symmetry which has the original, nonfiltered Lagrangian). As a final step, the linear filtered equations are supplemented to a nonlinear model. As it turns out, the Lagrangian function of the initial nonfiltered system is a most fundamental characteristic of the model and its composing represents the central problem. After the Lagrangian is constructed, the remaining part of solution represents a technical task.

In this chapter the Coriolis force will be neglected. This means, the treatment is restricted to the mesoscale domain with horizontal scales $l_x < 100$ km.

2.1. Linear model

Linearization of equations (1.3) according to the hydrostatic equilibrium state, characterised by the mean temperature, $T_0(p)$, yields equations

$$\frac{\partial z'}{\partial t} \;=\; w \;+\; H_0 \frac{\omega}{p} \;, \qquad (1a)$$

$$\frac{\partial w}{\partial t} \;=\; -g\; n' \;, \tag{1b}$$

$$\frac{\partial \mathbf{v}}{\partial t} \;=\; -\; g\nabla\; z' \;, \tag{1c}$$

$$\frac{\partial T'}{\partial t} \;=\; \frac{T_i \omega}{p} \;+\; Q \;, \tag{1d}$$

$$\frac{\partial n'}{\partial t} \;=\; -\; (\nabla \cdot \mathbf{v} \;+\; \partial\omega/\partial p) \;, \tag{1e}$$

$$n' \;=\; -\; \left(\frac{p}{H_0} \frac{\partial z'}{\partial p} \;+\; \frac{T'}{T_0} \right) \;. \tag{1f}$$

Here z' and T' and n' represent isobaric height, temperature and density fluctuations, $H_0 = RT_0/g$, and

$$T_i \;=\; \frac{R}{c_p} T_0 \;-\; p \frac{\partial T_0}{\partial p}$$

is the stability parameter ("stability temperature") of the background state.

2.2. "Horizontal" boundary conditions for linear model

The domain occupied by the atmosphere in the p–space is fixed in linear case:

$$0 \;<\; p \;< \overline{p}_0(\mathbf{x}) \;, \quad -\infty \;<\; x,\; y \;<\; \infty \;.$$

Boundary conditions at the bottom and top are

$$w|_{\overline{p}_0} \;=\; \frac{\mathrm{d}h}{\mathrm{d}t} \;=\; \mathbf{v}|_{\overline{p}_0} \cdot \nabla h \;, \quad \omega|_0 \;=\; 0 \;. \tag{2}$$

The first one represents an extrapolation to the mean lower boundary $\overline{p}_0$ of exact relation $w|_{p_0} = \mathrm{d}h/\mathrm{d}t$, which follows from (1.3a) and (1.5a), the second coincides with (1.5b).

The existence of free boundary in the p–space manifests itself in the bottom condition for z' at the mean lower boundary

$$z'|_{\overline{p}_0} \;=\; H_0(\overline{p}_0) \frac{p'_0}{\overline{p}_0} \;, \tag{3a}$$

where p'_0 represents the ground surface pressure fluctuation. For determination of p'_0 the linearized form of (1.4b) must be employed:

$$\frac{\partial p'_0}{\partial t} \;=\; \omega|_{\overline{p}_0} \;-\; \frac{\mathrm{d}\overline{p}_0}{\mathrm{d}t} \;.$$

As the mean ground surface pressure $\overline{p}_0$ and the ground surface height h are related with the barometric formula

$$\overline{p}(\mathbf{x}) \;=\; a \;\exp\left[-\frac{g}{R} \int_0^{h(\mathbf{x})} \frac{\mathrm{d}z}{T_0(z)} \right]$$

(where a represents the standard sea–level pressure) and, consequently,

$$\frac{\mathrm{d}\overline{p}_0}{\mathrm{d}t} \;=\; -\,\frac{\overline{p}_0}{H_0(\overline{p}_0)}\;\frac{\mathrm{d}h}{\mathrm{d}t} \;=\; -\,\left(\frac{pw}{H_0}\right)_{\overline{p}_0} \;\;,$$

the tendency equation for the ground surface pressure fluctuation can be presented as

$$\frac{\partial p_0'}{\partial t} \;=\; \left(\omega \;+\; \frac{pw}{H_0}\right)_{\overline{p}_0} \;\;. \tag{3b}$$

Equations (3) govern the lower boundary evolution in linear case and are responsible for ground surface pressure waves.

2.3. The reduced linear system

Diagnostic equation for ω can be deduced in the same way as for the nonlinear case and the resulting expression coincides with the linearized version of the equation (6):

$$\alpha\;\frac{\omega}{p} \;=\; \frac{p}{H_0}\;\frac{\partial w}{\partial p} \;-\; \nabla\cdot\;\mathbf{v} \;+\; \frac{Q}{T_0}\;. \tag{4}$$

This equation along with (1f) enable us to get from (1) a reduced set of equations which is closed according to z', w, $\mathbf{v}$, and T' and does not include n' and ω, though equations for these fields, (1f) and (4), remain valid.

We introduce nondimensional fluctuative fields in place of z' and T':

$$\zeta \;=\; \frac{z'}{H_0}\;, \qquad \eta \;=\; \frac{T'}{T_0} \;-\; \frac{T_i z'}{T_0 H_0}\;. \tag{5}$$

ζ presents a relative height fluctuation, scaled in H_0, η can be identified as the relative fluctuation of the entropy. Namely, let us define the nondimensional entropy as the function of the potential temperature, Θ:

$$S(\Theta) \;=\; \ln\Theta\;, \qquad \Theta \;=\; \frac{T}{T_a}\left(\frac{a}{p}\right)^{R/c_p} \;\;,$$

where T_a and a are constants (the mean temperature and pressure at the sea–level), and let $S_0(z)$ presents the background hydrostatic value of S as a function of the geometric height:

$$S_0(z) \;\equiv\; S[\Theta_0(z)]\;.$$

We define the relative entropy as a difference in its actual and background values at the same pressure level:

$$s(\mathbf{x},\;p,\;t) \;=\; S[\Theta(\mathbf{x},\;p,\;t)] \;-\; S_0[z(\mathbf{x},\;p,\;t)] \;\equiv\; \varphi[\Theta(\mathbf{x},\;p,\;t),\;z(\mathbf{x},\;p,\;t)]\;. \tag{6}$$

The defined in this way s is a known functional $\varphi(\Theta, z)$ of the potential temperature and height of the particle. This relative entropy turns zero for background conditions:

$$s_0(p) \;\equiv\; s|_{\Theta_0(p),z_0(p)} \;=\; \varphi[\Theta_0(p), z_0(p)] \;=\; 0\;,$$

and for small temperature and height perturbations it coincides with the defined by (5) field η:

$$s' \;=\; \left(\frac{\partial\varphi}{\partial\Theta}\right)_{\Theta_0,z_0}\Theta' \;+\; \left(\frac{\partial\varphi}{\partial z}\right)_{\Theta_0,z_0}z' \;=$$

$$=\; \frac{\Theta'}{\Theta_0} \;+\; \frac{dS_0}{dz_0}z' \;=\; \frac{T'}{T_0} \;-\; \frac{T_i}{T_0H_0}z' \;,$$

because $dS_0/dz_0 \;=\; T_i/(T_0H_0)$.

Thus, η represents in linearized model, like s in the nonlinear case, the difference between actual entropy of an air particle and the value which the air particle would have at the same height in the background atmosphere.

Using new field variables, the reduced minimal linear model can be presented as

$$\alpha\frac{\partial\zeta}{\partial t} \;=\; \frac{1}{H_0}\left(\alpha \;+\; p\frac{\partial}{\partial p}\right)w \;-\; \nabla\cdot\mathbf{v} \;+\; \frac{Q}{T_0} \;, \tag{7a}$$

$$\frac{\partial\eta}{\partial t} \;=\; -\;\frac{N^2w}{g} \;+\; \frac{Q}{T_0} \;, \tag{7b}$$

$$\frac{\partial w}{\partial t} \;=\; g\left[\left(\frac{\partial}{\partial p}p \;-\; \alpha\right)\zeta \;+\; \eta\right] \;, \tag{7c}$$

$$\frac{\partial\mathbf{v}}{\partial t} \;=\; -\;gH_0\nabla\;\zeta \;, \tag{7d}$$

where $N = \sqrt{RT_i}/H_0$ represents the Väisälä frequency.

Note that the exact nonlinear equation for the relative entropy is

$$\frac{\mathrm{d}s}{\mathrm{d}t} \;=\; -\;S_0'(z)w \;+\; \frac{Q}{T} \;, \tag{7b'}$$

where $S_0' \;\equiv\; dS_0/dz$. Because this derivative can be approximated for small fluctuations of z as

$$S_0'(z) \;\approx\; S_0'(z_0) \;=\; \frac{T_i}{T_0H_0} \;=\; \frac{N^2}{g} \;, \tag{7e}$$

equation (7b) represents the linearized version of equation (7b').

2.4. Wave equations

It is easy to get two second order equations for ζ and η, differentiating (7a) and (7b) according to the time and eliminating the first order time derivatives with the help of (7c) and (7d):

$$\left[H_0^2\left(\frac{1}{c_a^2}\frac{\partial^2}{\partial t^2} \;-\; \nabla^2\right) \;-\; \left(p\frac{\partial}{\partial p} \;+\; \alpha\right)\left(\frac{\partial}{\partial p}p \;-\; \alpha\right)\right]\zeta \;-\; \left(p\frac{\partial}{\partial p} \;+\; \alpha\right)\eta \;=\; Q_\zeta \tag{8a}$$

$$\left(\frac{1}{N^2}\frac{\partial^2}{\partial t^2} + 1\right)\eta + \left(\frac{\partial}{\partial p}p - \alpha\right)\zeta = Q_\eta \ , \qquad (8b)$$

where

$$Q_\zeta = \frac{R}{g^2}\frac{\partial Q}{\partial t} \ , \quad Q_\eta = \frac{RT_0}{g^2 T_i}\frac{\partial Q}{\partial t} \ ,$$

$c_a = \sqrt{RT_0/\alpha}$ is the sound speed[1)] and $(\frac{\partial}{\partial p}p + \alpha)\phi$, where ϕ is an arbitrary function, is the short notation for $\frac{\partial}{\partial p}(p\phi) + \alpha\phi$. These equations can be employed for the modeling of linear wave processes in p–coordinate presentation in a general, nonfiltered case.

2.5. The Lagrangian function and energy

The significance of wave equations for the present study is that they have a Lagrangian function $\mathcal{L}$ and can be deduced with the help of the least action (or Hamiltonian) principle

$$\delta S = \delta \int_{t_0}^{t_1} \mathrm{d}t \int_\Omega \mathrm{d}x\mathrm{d}y\mathrm{d}p \ \mathcal{L} = 0 \quad \text{for optional} \quad \delta\zeta(\mathbf{x},\ p,\ t) \ , \quad \delta\eta(\mathbf{x},\ p,\ t) \ ,$$

as extremes of the Lagrangian action S. The Lagrangian $\mathcal{L}$ is supposed to be a function of field variables ζ, η and their derivatives:

$$\mathcal{L} = \mathcal{L}(\zeta\ , \zeta_t,\ \zeta_x,\ \zeta_y,\ \zeta_p;\ \ \eta\ , \eta_t,\ \eta_x,\ \eta_y,\ \eta_p) \ ,$$

where $\zeta_t = \partial\zeta/\partial t, \zeta_x = \partial\zeta/\partial x$, etc. are short notations for partial derivatives. Action S is varied in variations $\delta\zeta(\mathbf{x},\ p,\ t)$, $\delta\eta(\mathbf{x},\ p,\ t)$, which turn zero at the boundaries of the domain Ω and at the initial and final moments, t_0 and t_1. The condition of extremity $\delta S = 0$ for optional $\delta\zeta$ and $\delta\eta$ yields Lagrangian equations

$$\frac{\partial\mathcal{L}}{\partial\zeta} - \frac{\partial}{\partial t}\frac{\partial\mathcal{L}}{\partial\zeta_t} - \frac{\partial}{\partial x}\frac{\partial\mathcal{L}}{\partial\zeta_x} - \frac{\partial}{\partial y}\frac{\partial\mathcal{L}}{\partial\zeta_y} - \frac{\partial}{\partial p}\frac{\partial\mathcal{L}}{\partial\zeta_p} = 0 \ ,$$

$$\frac{\partial\mathcal{L}}{\partial\eta} - \frac{\partial}{\partial t}\frac{\partial\mathcal{L}}{\partial\eta_t} - \frac{\partial}{\partial x}\frac{\partial\mathcal{L}}{\partial\eta_x} - \frac{\partial}{\partial y}\frac{\partial\mathcal{L}}{\partial\eta_y} - \frac{\partial}{\partial p}\frac{\partial\mathcal{L}}{\partial\eta_p} = 0 \ ,$$

which must coincide with the wave equations (8). For that it is sufficient to choose the Lagrangian function $\mathcal{L}$ in the form

$$\mathcal{L} = \mathcal{T} - \mathcal{V} \ , \qquad (9a)$$

[1)] Following the traditional way of wave–equation representations we have chosen the sound speed c_a for the prime acoustic characteristic of the atmosphere and the Väisälä frequency N for the prime characteristic of the buoyancy. Though most relevant in physical context, such choice is not the best from the point of view of the symmetry (which is always important in Lagrangian formalism). For the maximum symmetry either the characteristic frequency $N_a = c_a/H_0$ instead of c_a, or the characteristic buoyancy–wave phase–speed $c_i = \sqrt{RT_i} = NH_0$ instead of N, should be used.

where the generalized kinetic and potential energy densities, $\mathcal{T}$ and $\mathcal{V}$, are

$$\mathcal{T} \;=\; \frac{1}{2}\left(\frac{H_0}{c_a}\zeta_t\right)^2 \;+\; \frac{1}{2}\left(\frac{\eta_t}{N}\right)^2 \;, \tag{9b}$$

$$\mathcal{V} \;=\; \frac{1}{2}\left(H_0\nabla\zeta\right)^2 \;+\; \frac{1}{2}\left[\left(\frac{\partial}{\partial p}p \;-\; \alpha\right)\zeta \;+\; \eta\right]^2 \;-\; \zeta Q_\zeta \;-\; \eta Q_\eta \;. \tag{9c}$$

The purpose of the described Lagrangian formalism is to provide us with necessary tools for the optimal acoustic filtering. On the one hand, the existence of the Lagrangian guarantees energy conservation for the linearized system. On the other hand, with the help of the Lagrangian formalism it is easy to get filtered versions of the model which are still energy–conserving. The energy in linear system differs from the nonlinear model energy, (1.14). For the linear equations of motion (7) the total energy is

$$E_l \;=\; \int_V e_l \;\mathrm{d}x\mathrm{d}y\mathrm{d}p$$

with the energy density

$$e_l \;\equiv\; F(\zeta,\; \eta,\; \mathbf{v},\; w) \;=\; \frac{1}{2}\left(\frac{g^2H_0^2}{c_a^2}\zeta^2 \;+\; \frac{g^2}{N^2}\eta^2 \;+\; \mathbf{v}^2 \;+\; w^2\right) \;. \tag{10}$$

The first two terms present potential energy which air particle has due to the isobaric height and temperature fluctuations, the remaining two terms are kinetic energy.

Alternatively, the induced by the linear model (7) wave system (8) possesses according to the Noether theorem wave energy

$$E_{\mathcal{L}} \;=\; \int_V \mathcal{H} \;\mathrm{d}x\mathrm{d}y\mathrm{d}p \;,$$

with the density

$$\mathcal{H} \;=\; \zeta_t\frac{\partial\mathcal{L}}{\partial\zeta_t} \;+\; \eta_t\frac{\partial\mathcal{L}}{\partial\zeta_t} \;-\; \mathcal{L} \;=\; \mathcal{T} \;+\; \mathcal{V}. \tag{10$'$}$$

Both E_l and $E_{\mathcal{L}}$ are conservative, if the system is isolated from external forcing, i.e., if $Q \;=\; 0$. Introduced two kinds of energies E_l and $E_{\mathcal{L}}$ are different but still close related. In conservative case, $Q = 0$, consequent densities e_l and $\mathcal{H}$ are bound with the help of the formula

$$g^2\cdot\mathcal{H} \;=\; F(\zeta_t,\; \eta_t,\; \mathbf{v}_t,\; w_t) \;,$$

where F is defined according to (10). This relationship is easy to check, expressing the generalized potential energy density, $\mathcal{V}$, with the help of equations (7c) and (7d) as the function of $\mathbf{v}$ and w. As a consequence, and this presents a matter of primary importance for the present study, the conservation of $E_{\mathcal{L}}$ guarantees always the conservation of E_l, too.

The least action principle for wave equations is formulated here in its first, Lagrangian form. It uses the Lagrangian function, $\mathcal{L}$, as the prime field and results in two Lagrangian equations (8), which are both second order in time. Alternatively, there exists (see Salmon 1983, for example) another, Hamiltonian formulation of the problem, which in that formulation is called the Hamiltonian principle. The Hamiltonian formulation uses $\mathcal{H}$ as the prime function and results in four first order equations. The Hamiltonian equations may turn useful for some applications. For that reason they are presented at the end of this chapter, in section 2.11.

2.6 Acoustic filtering in Lagrangian

For slow atmospheric movements with small Mach number,

$$\mathcal{F} \equiv U^2/c_a^2 << 1 ,$$

where U is the characteristic amplitude of velocity, it is reasonable to filter the model acoustically, i.e. to simplify equations in the way they do not include acoustic–wave solutions anymore, though still maintain other waves and slow movements. Essentially the filtering consists of lowering the time order of the system by two. The filtering task can be solved in a most straightforward manner using the Lagrangian formalism. The main idea is that filtering (ie. time–order reduction) should be carried out in the Lagrangian function, which must be approximated in the way the resulting wave equations do not include acoustic–wave solutions. As the approximate model has still the Lagrangian function, it supports the energy conservation law. The filtered wave equations with the conserving wave energy are the main output of the filtered Lagrangian function. It is easy (though not trivial) to establish simplifications which should be introduced into the initial linear model (7) to get the filtered linear system which originates these wave equations. Finally, it is easy to generalize the linear filtered model to the nonlinear one.

Approximation $c_a \rightarrow \infty$. This model has been introduced by Rõõm and Ülejõe (1996), here it will be presented in an extended version. As the main assumption it employs the approximation that the sound speed can be treated as infinitely large in comparison with slow advective and convective flows.

The physical basis for filtering can be deduced from the scale analysis of the Lagrangian (9a). If the Mach number is small, then the first term in $\mathcal{T}$ is small in comparison with two first terms in $\mathcal{V}$ in all spatial scales and, thus, in the first approximation it can be neglected. The resulting expression for the Lagrangian function is:

$$\mathcal{L} = \frac{1}{2}\left\{\frac{1}{N^2}\left(\eta_t\right)^2 - H_0^2(\nabla\zeta)^2 - \left[\left(\frac{\partial}{\partial p}p - \alpha\right)\zeta + \eta\right]^2\right\} + \zeta Q_\zeta + \eta Q_\eta .$$

2.7. Filtered wave equations

Filtered wave equations, corresponding to this Lagrangian, can be deduced directly from (8) with the help of the formal passage $c_a \rightarrow \infty$ in equation (8a):

$$\left[H_0^2\,\nabla^2 + \left(p\frac{\partial}{\partial p} + \alpha\right)\left(\frac{\partial}{\partial p}p - \alpha\right)\right]\zeta = -\left(p\frac{\partial}{\partial p} + \alpha\right)\eta - Q_\zeta , \qquad (11a)$$

$$\left(\frac{1}{N^2}\frac{\partial^2}{\partial t^2} \ + \ 1\right)\eta \ = \ - \ \left(\frac{\partial}{\partial p}p \ - \ \alpha\right)\zeta \ + \ Q_\eta \ . \qquad (11b)$$

As a result, the time order of the system reduces by two and two solutions of the four of initial model are filtered. The eliminated in this way solutions belong to acoustic modes, as equations (11) do not include sound speed, c_a, anymore. At the same time, buoyancy waves are maintained, as the wave equation, "responsible" for their existence, (11b), maintains its initial appearance and still includes the Väisälä frequency N.

The main consequence of the filtering is that the wave equation (8a) is replaced by the Poisson equation in ζ, (11a). This equation defines ζ as a quasi-static field which is determined by the forcing on the right side of the equation. The name "quasi-static" is justified, because the solution ζ of equation (11a) coincides for stationary forcing with the exact static (time–independent) solution of the exact nonfiltered equations (8) in stationary conditions. For nonstationary conditions the quasi-static ζ depends on time parametrically, via Q and η (and, perhaps, via nonstationary boundary conditions). In general, the quasi-static ζ is different from the hydrostatic height fluctuation ζ_s, which corresponds to the fluctuative part of the hydrostatic height, (1b), and which represents a solution of the hydrostatic equation. The hydrostatic equation reads in terms of η, ζ (instead of common T', z'):

$$\left(\frac{\partial}{\partial p}p \ - \ \alpha\right)\zeta_s \ = \ - \ \eta \ . \qquad (12)$$

As it can be seen, the solution $(\zeta_s, \ \eta)$ of this equation is a solution of system (11) at the limit of infinitely slow processes ($\partial^2\eta/\partial t^2 \to 0$, $\partial Q/\partial t \to 0$) with sufficiently large horizontal scales ($\nabla^2\zeta \to 0$).

The described filtering scheme is optimal in the sense it enables exact solutions for infinitely slow processes. For finite speed processes the filtered model yields approximate solutions, of course. Meanwhile, these solutions can be further improved, if needed, and the filtering scheme shows a natural way for the improvement. Let us write (11a) as a linear operator equation for ζ

$$\hat{P}\zeta \ = \ - \ A \ ,$$

where the source term A is known function of η and Q_ζ. Then the nonfiltered equation (8a) can be represented as

$$\hat{P}\zeta \ = \ - \ A \ + \ \varepsilon \ \frac{\partial^2\zeta}{\partial t^2} \ .$$

The last term on the right hand side can be treated for slow processes as a perturbation with the small perturbation parameter $\varepsilon \ = \ H_0^2/c_a^2$, and the solution of this equation can be presented as a series

$$\zeta \ = \ \zeta_0 \ + \ \zeta_1 \ + \ \zeta_2 \ + \ ...$$

where $\zeta_i \sim \varepsilon^i$. The first term ζ_0 represents a solution of the filtered equation (11a). Other members of the series are successive correction terms, which can be calculated from equations

$$\hat{P}\zeta_i \ = \ \varepsilon \ \frac{\partial^2\zeta_{i-1}}{\partial t^2} \ , i \ = \ 1, 2, ... \ .$$

Most meaningful is the first correction term, ζ_1, which can be interpreted as an acoustic component of the motion, generated by slow dynamics.

2.8. The linear filtered dynamics

The linear model, corresponding to the filtered wave equations (11), can be derived from (7) substituting equation (7a) by the balance condition

$$\frac{1}{H_0}\left(\alpha \ + \ p\frac{\partial}{\partial p}\right) w \ - \ \nabla\cdot\mathbf{v} \ + \ \frac{Q}{T_0} \ = \ 0 \ . \tag{13}$$

This relation presents a diagnostic equation for ζ. The explicit equation for ζ can be obtained, differentiating (13) by t. This results in the Poisson equation (11a). After this equation for ζ is employed, relation (13) can be used instead of (7c) for the determination of the vertical wind w.

As (13) is deduced from the initial linearized system with the help of the passage $\partial\zeta/\partial t \rightarrow 0$, it can be treated as a consequence of the equation (4) and

$$\frac{w}{H_0} \ = \ - \ \frac{\omega}{p} \ . \tag{14}$$

Equations (7b) – (7d) along with diagnostic relations (13) and (14) represent the closed linear acoustically filtered system of equations, which is most close to initial nonfiltered linear model and which yields filtered wave–equations (11). Therefore, this set of equations will be a basis for nonlinear generalization.

The energy density filtered model (7b) – (7d), (13), (14) is

$$e_l \ = \ \frac{1}{2}\left(\frac{g^2}{N^2}\eta^2 \ + \ \mathbf{v}^2 \ + \ w^2\right) \ . \tag{15}$$

In comparison with the nonfiltered version (10) it lacks the term, proportional to ζ^2.

2.9. Compressibility in filtered model

Relation (14) presents the adjusted version of equation (1a) and coincides with the MPM equation (12b). That means, the vertical velocity w is, like in the MPM, an approximated field. Still, differently from the MPM, our model preserves the thermodynamic relationship for ω, (4). This is achieved due to the maintenance of the compressibility. For the three–dimensional divergence of velocity in the p–space,

$$\mathcal{D} \ \equiv \ \nabla\cdot\mathbf{v} \ + \ \frac{\partial\omega}{\partial p} \ , \tag{16}$$

from (4) and (14) a diagnostic equation follows

$$\mathcal{D} \ = \ - \ \frac{N^2}{g}w \ + \ \frac{Q}{T_0} \ . \tag{17}$$

The right hand term has the amplitude 10^{-7} – 10^{-4} s^{-1}. Thus, $\mathcal{D}$ is really a small term. Nevertheless, it differs from the exact zero and the medium is compressible. Thus, the developed model can be called as the "Elastic Filtered Model" (EFM). As we will be convinced in the section 4, for many cases of importance this compressibility is dynamically unsubstantial, and the medium can be treated with high efficiency as incompressible. Nevertheless, there exist situations (various short-scale flows), where incompressibility assumption in the p-space yields distortions of modelled dynamics in comparison with the reality.

Comparison of equation (7b) with (16), (17) exhibits that η satisfies equation

$$\frac{\partial \eta}{\partial t} \; - \; \nabla \cdot \mathbf{v} \; - \; \frac{\partial \omega}{\partial p} \; = \; 0 \; .$$

Because the density fluctuation, n', satisfies the continuity equation (1e) (this is a matter of the definition of continuous medium), the sum $\eta_0 = n' + \eta$ presents a local invariant, which is constant in time at every point of the medium. This detailed balance of entropy and density fluctuations is that mechanism, which eliminates the acoustic waves.

2.10. Nonlinear filtered model

Because the linear filtered model is compressible in the p–space, there is no deep sense to try to build incompressible nonlinear extensions to it.

If the compressibility is supported, then the nonlinear generalization of the linear model (7b) – (7d), (13), (14) can be obtained in straightforward manner, complementing the system with the nonlinear continuity equation and substituting everywhere the local time derivative $\partial/\partial t$ by the construct nd/dt. To maintain the conservation law for the energy density in quadratic form (15) it is reasonable, before generalization of local time derivative to the Lagrangian one, to rewrite the linear entropy–equation (7b) in the more symmetric way:

$$\frac{\partial}{\partial t}\frac{\eta}{N} \; = \; - \; \frac{N}{g} w \; + \; \frac{Q}{N T_0} \; . \tag{18}$$

The resulting model is:

$$n \frac{\mathrm{d}}{\mathrm{d}t}\frac{\eta}{N} \; = \; - \; \frac{N}{g} w \; + \; n \; \frac{Q}{N T_0} \; , \tag{19a}$$

$$n \frac{\mathrm{d}w}{\mathrm{d}t} \; = \; g \left[\left(\frac{\partial}{\partial p} p \; - \; \alpha \right) \frac{z'}{H_0} \; + \; \eta \right] \; , \tag{19b}$$

$$n \frac{\mathrm{d}\mathbf{v}}{\mathrm{d}t} \; = \; - \; g \nabla \; z' \; - \; n f \hat{\mathbf{z}} \times \mathbf{v} \; , \tag{19c}$$

$$\frac{\mathrm{d}n}{\mathrm{d}t} \; + \; n \left(\nabla \cdot \mathbf{v} \; + \; \frac{\partial \omega}{\partial p} \right) \; = \; 0, \tag{19d}$$

$$\frac{1}{H_0} \left(\alpha \; + \; p \frac{\partial}{\partial p} \right) w \; - \; \nabla \cdot \mathbf{v} \; + \; \frac{Q}{T_0} \; = \; 0 \; , \tag{19e}$$

$$\frac{w}{H_0} \;=\; -\,\frac{\omega}{p}\;. \qquad (19f)$$

We have restored in the nonlinear version the Coriolis force and turned back to the height fluctuation, z'.

The entropy equation (19a) includes in nonlinear case an additional term, which is introduced especially for the energy conservation. To demonstrate that, one can rewrite (19a) as

$$n\frac{\mathrm{d}\eta}{\mathrm{d}t} \;=\; -\,\frac{N^2}{g}w \;+\; n\frac{d\ln N}{dz_0}\eta w \;+\; n\,\frac{Q}{T_0}\;. \qquad (19a')$$

Comparison of this equation with the exact one, (7b'), exhibits, that beside the linearized definition for entropy (η is used instead of s), and the approximation (7e), an additional approximation is made by introduction of the second term onto the right hand side of equation (19a'). The only purpose of this term is to maintain the energy conservation law for the density (15). As it includes the product $w\cdot\eta$, this term is second–order in dependent variables and thus, it is small in slow processes in comparison with the first term on right hand side, which is linear in perturbation terms. Additionally, for many realistic situations the vertical derivative dN/dz_0 is small, and the discussed correction term represents a third order small quantity (By the way, it turns zero for models with constant N). Another possibility to overcome difficulties with energy–conservation is to maintain the filtered entropy equation in its initial linearized form (18). That variant was discussed in Rõõm and Ülejõe, 1996. Because they were aware of the exact equation for the relative entropy, (7b'), they lack a possibility to estimate accuracy of different approximations. The present model (19) presents as a more realistic version because it includes the entropy advection.

It is possible to substitute the horizontally homogeneous background temperature $T_0(p)$ by the nonhomogeneous, time-dependent field $T_s(\mathbf{x},\ p,\ t)$ (corresponding to some realistic synoptical situation, for instance) along with the simultaneous substitutions of $H_0(p)$, $N(p)$ by the nonhomogeneous parameters $H_s(\mathbf{x},\ p,\ t)$ and $N_s(\mathbf{x},\ p,\ t)$.

2.11. Hamiltonian principle for linear model

Generalized momenta for Lagrangian (9) are

$$\pi_\zeta \;=\; \frac{\partial\mathcal{L}}{\partial\zeta_t} \;=\; \frac{\partial\mathcal{T}}{\partial\zeta_t} \;=\; \frac{H_0^2}{c_a^2}\zeta_t\;, \qquad \pi_\eta \;=\; \frac{\partial\mathcal{L}}{\partial\eta_t} \;=\; \frac{\partial\mathcal{T}}{\partial\eta_t} \;=\; \frac{1}{N^2}\eta_t\;.$$

Using these definitions, kinetic energy (9b) can be presented as a function of π_ζ, π_η

$$\mathcal{T} \;=\; \frac{1}{2}\frac{c_a^2}{H_0^2}\pi_\zeta^2 \;+\; \frac{1}{2}N^2\pi_\eta^2$$

and the Hamiltonian (10') turns to a function of ζ, η, π_ζ, π_η.

The Hamiltonian principle is a variational extremum condition in the form

$$\delta \int_{t_0}^{t_1} \mathrm{d}t \int_V \mathrm{d}x\mathrm{d}y\mathrm{d}p \, (\zeta_t \pi_\zeta \, + \, \eta_t \pi_\eta \, - \, \mathcal{H}) \, = \, 0 \, , \quad \forall \, \delta\zeta, \, \delta\eta, \, \delta\pi_\zeta, \, \delta\pi_\eta \, .$$

where variations of all fields must be zero at initial and final moments and variations of ζ, η must be zero at the boundary of the domain V. Solutions of this extremum problem are the Hamiltonian equations

$$\frac{\partial \zeta}{\partial t} \, = \, \frac{\delta \mathcal{H}}{\delta \pi_\zeta} \, , \quad \frac{\partial \eta}{\partial t} \, = \, \frac{\delta \mathcal{H}}{\delta \pi_\eta} \, ,$$

$$\frac{\partial \pi_\zeta}{\partial t} \, = \, - \, \frac{\delta \mathcal{H}}{\delta \zeta} \, , \quad \frac{\partial \pi_\eta}{\partial t} \, = \, - \, \frac{\delta \mathcal{H}}{\delta \eta} \, .$$

Because

$$\frac{\delta \mathcal{H}}{\delta \pi_\zeta} \, = \, \frac{\delta \mathcal{T}}{\delta \pi_\zeta} \, = \, \frac{c_a^2}{H_0^2} \pi_\zeta \, , \quad \frac{\delta \mathcal{H}}{\delta \pi_\eta} \, = \, \frac{\delta \mathcal{T}}{\delta \pi_\eta} \, = \, N^2 \pi_\eta \, ,$$

$$\frac{\delta \mathcal{H}}{\delta \zeta} \, = \, \frac{\delta \mathcal{V}}{\delta \zeta} \, = \, - \, H_0^2 \nabla^2 \zeta \, - \, \left(\alpha \, + \, p \frac{\partial}{\partial p} \right) \left[\left(\frac{\partial}{\partial p} p \, - \, \alpha \right) \zeta \, + \, \eta \right] \, - \, Q_\zeta \, ,$$

$$\frac{\delta \mathcal{H}}{\delta \eta} \, = \, \frac{\delta \mathcal{V}}{\delta \eta} \, = \, \left(\frac{\partial}{\partial p} p \, - \, \alpha \right) \zeta \, + \, \eta \, - \, Q_\eta \, ,$$

an explicit form of Hamiltonian equations is

$$\frac{\partial \zeta}{\partial t} \, = \, \frac{c_a^2}{H_0^2} \pi_\zeta \quad , \quad \frac{\partial \eta}{\partial t} \, = \, N^2 \pi_\eta \, ,$$

$$\frac{\partial \pi_\zeta}{\partial t} \, = \, H_0^2 \nabla^2 \zeta \, + \, \left(\alpha \, + \, p \frac{\partial}{\partial p} \right) \left[\left(\frac{\partial}{\partial p} p \, - \, \alpha \right) \zeta \, + \, \eta \right] \, + \, Q_\zeta \, ,$$

$$\frac{\partial \pi_\eta}{\partial t} \, = \, - \, \left(\frac{\partial}{\partial p} p \, - \, \alpha \right) \zeta \, - \, \eta \, + \, Q_\eta \, .$$

Elimination of generalized momenta from the obtained equations turns them to the Lagrangian equations (8). An acoustically filtered variant follows, if $\partial\zeta/\partial t$ and π_ζ are put to zero.

2.12. Model with nonzero adjustment. It is possible to express z' as a sum of hydrostatic fluctuation z'_s and nonhydrostatic component z_n (see (1.1a)):

$$z' \;=\; z'_s \;+\; z_n \;, \tag{20a}$$

where the hydrostatic component satisfies the quasi-static equation

$$\frac{p}{H_0}\frac{\partial z'_s}{\partial p} \;+\; \frac{T'}{T_0} \;=\; 0 \;. \tag{20b}$$

This expansion generates analogous representations for the field variables ζ and η:

$$\zeta \;=\; \zeta_s \;+\; \zeta_n \;, \quad \eta \;=\; \eta_s \;+\; \eta_n \;, \tag{21a}$$

$$\zeta_s \;=\; \frac{z'_s}{H_0} \;, \quad \eta_s \;=\; \frac{T}{T_0}' \;-\; \frac{T_i z'_s}{T_0 H_0} \;, \tag{21b}$$

$$\zeta_n \;=\; \frac{z_n}{H_0} \;, \quad \eta_n \;=\; -\,\frac{T_i z_n}{T_0 H_0} \;. \tag{21c}$$

Among the defined four field variables ζ_s, ζ_n, η_s and η_n, only two are functionally independent. As independent variables ζ_s and ζ_n can be chosen, in which case

$$\eta_s \;=\; -\,\left(\frac{\partial}{\partial p}p \;-\; \alpha\right)\zeta_s \;, \eta_n \;=\; -\,\frac{T_i}{T_0}\zeta_n \;. \tag{21d}$$

2.12.1. Basic approximations. For the long–wave domain, $l_x >> H_0$, the atmosphere is with good accuracy in hydrostatic balance and $\zeta_n \approx 0$. This means, $\zeta \approx \zeta_s$, and $\eta \approx \eta_s$. As a consequence, in this domain the tendencies ζ_t and η_t are adjusted to the hydrostatic values ζ_{st}, η_{st} as well. We hypothesise that these adjustments of time derivatives can be extended into the mesoscale domain:

$$\frac{\partial \zeta}{\partial t} \;\approx\; \frac{\partial \zeta_s}{\partial t} \;, \quad \frac{\partial \eta}{\partial t} \;\approx\; \frac{\partial \eta_s}{\partial t} \;=\; -\,\frac{\partial}{\partial t}\left(\frac{\partial}{\partial p}p \;-\; \alpha\right)\zeta_s \;. \tag{22}$$

The first approximation, $\zeta_t \approx \zeta_{st}$, represents a modification of the main filtering assumption of the previous model[1)]. As the first term in the Lagrangian (23b) is always small, this modification does not cause a large variation in the filtered model. The main modification is a consequence of the second approximation $\eta_t \approx \eta_{st}$. To justify this approximation we note that in the short–scale limit the relative pressure fluctuations are small in comparison with the relative temperature fluctuations: $|\delta p/p| << |T'/T_0|$. Thus,

$$|\eta_n| \;=\; (T_i/T_0)|\zeta_n| \;\sim\; (T_i/T_0)|\delta p/p| \;<<\; |T'/T_0| \;\sim\; |\eta_s| \;.$$

[1)] Because ζ_s is in general different from ζ_0, the approximation presented here differs for ζ from the solution $\zeta_0 \;+\; \zeta_1 \;+...$, discussed in section 2.7.

2.12.2. Lagrangian function and wave equations. The use of (22) in (23) yields an approximate Lagrangian which can be expressed as a functional of ζ_s and ζ_n as

$$\mathcal{L} \;=\; \frac{1}{2}\left\{\left(\frac{H_0}{c_a}\zeta_{st}\right)^2 \;+\; \left[\frac{1}{N}\left(\frac{\partial}{\partial p}p \;-\; \alpha\right)\zeta_{st}\right]^2 \;-\right.$$

$$\left. -\; \left[H_0^2\nabla(\zeta_s \;+\; \zeta_n)\right]^2 \;-\; \left[\left(\frac{\partial}{\partial p}p \;-\; \alpha^*\right)\zeta_n\right]^2\right\} \;-\; \frac{p}{gT_i}\,\frac{\partial H_0\zeta_s}{\partial p}\frac{\partial Q}{\partial t}\;, \qquad (23)$$

where

$$\alpha^* \;=\; \alpha \;+\; \frac{T_i}{T_0}\;.$$

The corresponding wave equations are

$$H_0^2\nabla^2(\zeta_s \;+\; \zeta_n) \;+\; \left(\alpha^* \;+\; p\frac{\partial}{\partial p}\right)\left(\frac{\partial}{\partial p}p \;-\; \alpha^*\right)\zeta_n \;=\; 0\;, \qquad (24a)$$

$$\frac{\partial^2}{\partial t^2}\left[\left(\alpha \;+\; p\frac{\partial}{\partial p}\right)\frac{1}{N^2}\left(\frac{\partial}{\partial p}p \;-\; \alpha\right) \;-\; \frac{H_0^2}{c_a^2}\right]\zeta_s \;+\; H_0^2\nabla^2\left(\zeta_s \;+\; \zeta_n\right) \;=$$

$$=\; -\;\frac{H_0}{g}\frac{\partial}{\partial p}\left(\frac{p}{T_i}\frac{\partial Q}{\partial t}\right)\;. \qquad (24b)$$

In appearance these equations are quite different from the exact ones, (22), and from the wave equations ofthe previous model, (11). As will be demonstrated in the next section, the dynamic model which corresponds to system (24) is the MPM.

2.12.3. Filtered nonlinear hydrodynamics

It is easy to prove the identities

$$\left[\left(\alpha \;+\; p\frac{\partial}{\partial p}\right)\frac{1}{N^2}\left(\frac{\partial}{\partial p}p \;-\; \alpha\right) \;-\; \frac{H_0^2}{c_a^2}\right]\varphi \;=\; \left(H_0\frac{\partial}{\partial p}\frac{p^2}{c_i^2}\frac{\partial}{\partial p}H_0\right)\varphi\;,$$

$$\frac{1}{H_0}\left(\alpha^* \;+\; p\frac{\partial}{\partial p}\right)\varphi \;=\; \frac{\partial}{\partial p}\left(\frac{p}{H_0}\varphi\right)\;,$$

$$\left(\frac{\partial}{\partial p}p \;-\; \alpha\right)\zeta_n \;=\; \frac{p}{H_0}\frac{\partial z_n}{\partial p}\;,$$

where φ is any function. Equations (24) can be transformed with the help of these relations to the equivalent system

$$\nabla^2\left(z_s' \;+\; z_n\right) \;+\; \frac{\partial}{\partial p}\left(\frac{p^2}{H_0^2}\frac{\partial z_n}{\partial p}\right) \;=\; 0\;, \qquad (24a')$$

$$\frac{\partial^2}{\partial t^2}\frac{\partial}{\partial p}\left(\frac{p^2}{c_i^2}\frac{\partial z_s'}{\partial p}\right) \;-\; \frac{\partial}{\partial p}\left(\frac{p^2}{H_0^2}\frac{\partial z_n}{\partial p}\right) = \;-\;\frac{1}{g}\frac{\partial}{\partial p}\left(\frac{p}{T_i}\frac{\partial Q}{\partial t}\right)\;. \qquad (24b')$$

It is clear that the Poisson equation in z_n, (24a'), is a consequence of the balance condition

$$\nabla \cdot \mathbf{v} \; - \; \frac{\partial}{\partial p} p \frac{v_z}{H_0} \; = \; 0, \tag{25a}$$

supposing the linear momentum equations are

$$\frac{\partial w}{\partial t} \; = \; g \frac{p}{H_0} \frac{\partial z_n}{\partial p} \; , \tag{25b}$$

$$\frac{\partial \mathbf{v}}{\partial t} \; = \; - \, g \nabla (z_s' \; + \; z_n) \; . \tag{25c}$$

The remaining equation, (24b'), is satisfied if the temperature equation has the form

$$\frac{\partial}{\partial t} T' \; = \; - \, T_i \frac{w}{H_0} \; + \; Q \; . \tag{25d}$$

Finally, comparison of this equation and the exact linear temperature equation, (15d), shows that w and ω are related according to equation

$$\frac{w}{H_0} \; = \; - \, \frac{\omega}{p} \; . \tag{25e}$$

The received model (25) represents the linearized version of the MPM. Thus, the filtered Lagrangian (23) yields the nonlinear MPM. In turn, wave equations (24) along with the Lagrangian (23) follow from the MPM at the linear limit.

CHAPTER THREE

Linear Shear Flow

In previous chapter linearized models where treated, where linearization was performed according to the resting background state without Coriolis force. For different applications it is highly recommended to get linearizations according to some sounding profile which represents a uniform flow and include the Coriolis term into linear version. In this chapter we will develop such linearizations. The material will represent a link between ideas of the previous chapter and the next one, where the obtained in this chapter results will be used for numerical modeling and model evaluation.

In the first section general linear shear flow model in pressure coordinate framework is presented. This general treatment is useful, as all particular shear-flow models can be easily derived from this one. Special efforts are undertaken to get wave equations which possess Lagrangian. The situation is a little complicated with the presence of the Coriolis force. Due to this complication, the trivial local invariant of linear models in Chapter 1, the non-divergent horizontal flow $\mathbf{v}_\psi = \nabla\times\psi$, which enabled the time-order reduction to the fourth order, must be replaced by the more general local invariant – the linearized potential vorticity.

In Section 3.3 general model is simplified to the inertial background flow with a wind profile, depending on the height only. These equations will present special interest for stability problems of different kind.

Finally, the maximum simplified model equations with the uniform height-independent background wind are described in 3.4 and 3.5. background flow is presented

3.1. Linearization according to stationary shear flow. General case

Up to now our treatment included the simplest resting background in full hydrostatic equilibrium. Here we will study situations, where medium flows, for instance, over smooth low orography which causes small perturbations in that medium.

The sounding state of the atmosphere is as follows:

$$z = z_0(y,p)\ ,\quad T = T_0(y,p)\ ,\quad \mathbf{V} = \hat{\mathbf{x}}U(y,p)\ ,\quad w = 0\ ,\quad n = 1\ , \tag{1}$$

$$\frac{\partial z_0}{\partial p} = -\frac{H_0(y,p)}{p}\ ,\quad \frac{\partial z_0}{\partial y} = -\frac{f(y)}{g}U(y,p)\ . \tag{2}$$

This is a stationary regime, which satisfies exact equations. If there exist small additional perturbations in the atmosphere (which will be denoted with the prime), the

complete fields are

$$z \;=\; z_0 \;+\; z' \;, \quad T \;=\; T_0 \;+\; T' \;, \quad \mathbf{V} \;=\; \hat{\mathbf{x}}U \;+\; \mathbf{v} \;, \quad w \;=\; w' \;, \quad n \;=\; 1 \;+\; n' \;,$$

$$\frac{\mathrm{d}}{\mathrm{d}t} \;=\; \frac{\mathrm{d}_0}{\mathrm{d}t} \;+\; \hat{a} \;, \quad \frac{\mathrm{d}_0}{\mathrm{d}t} \;=\; \frac{\partial}{\partial t} \;+\; U\frac{\partial}{\partial x} \;, \quad \hat{a} \;=\; \mathbf{v}\cdot\nabla \;+\; \omega\frac{\partial}{\partial p} \;, \tag{3}$$

Linearization of the complete equations (1.3) according to perturbations yields equations

$$\frac{\mathrm{d}_0 z'}{\mathrm{d}t} \;=\; w \;+\; H_0\frac{\omega}{p} \;-\; v_y\frac{\partial z_0}{\partial y} \;, \tag{4a}$$

$$\frac{\mathrm{d}_0 w}{\mathrm{d}t} \;=\; -g\; n' \;, \tag{4b}$$

$$\frac{\mathrm{d}_0 \mathbf{v}}{\mathrm{d}t} \;=\; -\; g\nabla\; z' \;-\; f\hat{\mathbf{z}}\times\mathbf{v} \;-\; \hat{\mathbf{x}}\left(v_y\frac{\partial U}{\partial y} \;+\; \omega\frac{\partial U}{\partial p}\right) \;, \tag{4c}$$

$$\frac{\mathrm{d}_0 T'}{\mathrm{d}t} \;=\; \frac{T_i\omega}{p} \;+\; Q \;-\; v_y\frac{\partial T_0}{\partial y} \;, \tag{4d}$$

$$\frac{\mathrm{d}_0 n'}{\mathrm{d}t} \;=\; -\;(\nabla\cdot\mathbf{v} \;+\; \partial\omega/\partial p) \;, \tag{4e}$$

$$n' \;=\; -\;\left(\frac{p}{H_0}\frac{\partial z'}{\partial p} \;+\; \frac{T'}{T_0}\right) \;. \tag{4f}$$

As we can see, equations include terms which describe advection of the perturbation wields by the background flow.

Material derivative $\frac{\mathrm{d}_0}{\mathrm{d}t}$ commutates with all background fields U, T_0, z_0, f, but it is not commutable with the differential operators $\frac{\partial}{\partial y}$ and $\frac{\partial}{\partial p}$, except special cases where U is not a function of the consequent coordinate y or p. This non-computability must be taken into account at derivation of the diagnostical equation for ω:

$$\alpha\frac{\omega}{p} \;=\; \frac{p}{H_0}\frac{\partial w}{\partial p} \;-\; \nabla\cdot\mathbf{v} \;+\; \frac{p}{H_0}\frac{\partial z_0}{\partial y}\frac{\partial v_y}{\partial p} \;+\frac{p}{H_0}\frac{\partial U}{\partial p}\frac{\partial z'}{\partial x} \;+\; \frac{Q}{T_0} \;. \tag{5}$$

Again, this equation, deduced from the linear system (4), coincides with the linearized version of relation (1.6).

The reduced linearized model for η, ζ, $\mathbf{v}$, w reads

$$\alpha\frac{\mathrm{d}_1\zeta}{\mathrm{d}t} \;=\; \frac{1}{H_0}\left(\alpha \;+\; p\frac{\partial}{\partial p}\right)\left(w \;-\; v_y\frac{\partial z_0}{\partial y}\right) \;-\; \nabla\cdot\mathbf{v} \;-\; v_y\frac{1}{T_0}\frac{\partial T_0}{\partial y} \;+\; \frac{Q}{T_0} \;, \tag{6a}$$

$$\frac{\mathrm{d}_0\eta}{\mathrm{d}t} \;=\; -\;\frac{N^2}{g}\left(w \;-\; v_y\frac{\partial z_0}{\partial y}\right) \;-\; v_y\frac{1}{T_0}\frac{\partial T_0}{\partial y} \;+\; \frac{Q}{T_0} \;, \tag{6b}$$

$$\frac{\mathrm{d}_0 w}{\mathrm{d}t} \;=\; g\left[\left(\frac{\partial}{\partial p}p \;-\; \alpha\right)\zeta \;+\; \eta\right] \;, \tag{6c}$$

$$\frac{\mathrm{d}_0 \mathbf{v}}{\mathrm{d}t} \;=\; -\; gH_0\nabla\,\zeta \;-\; f\hat{\mathbf{z}}\times\mathbf{v} \;-\; \hat{\mathbf{x}}\left(v_y\frac{\partial U}{\partial y} \;+\; \omega\frac{\partial U}{\partial p}\right) \;. \tag{6d}$$

where the notation is used

$$\frac{\mathrm{d}_1}{\mathrm{d}t} \;=\; \frac{\mathrm{d}_0}{\mathrm{d}t} \;+\; \frac{p}{\alpha}\frac{\partial U}{\partial p}\frac{\partial}{\partial x} \;. \tag{6e}$$

It is worth to underline onse more that derived linear equations represent the exact adiabatic model in the p–space, which include all the spectrum of possible motions of small amplitude in a uniform steady background flow. They can be employed, for instance, for the investigation of stability problems at all spatial and temporal scales.

Notable difference in comparison with the resting background model is the material derivative $\mathrm{d}_1/\mathrm{d}t$ on the left hand side in (6a). This derivative may become large, if the vertical gradient of U makes large. Other additional terms in η and ζ equations which include derivatives of z_0 and T_0 in y are not so important, as usually horizontal gradients are much smaller in the atmosphere than vertical gradients. An important problem with these derivatives is that they are to be omitted, if one wants to introduce the EFM. It is clear that this is justified only, if all referred terms are moderate.

To get the corresponding to (6) wave equations, we deduce from (6d) equations for divergence and vorticity

$$D \;=\; \nabla\cdot\mathbf{v} \;, \qquad \Omega_r \;=\; \hat{\mathbf{z}}\cdot(\nabla\times\mathbf{v}) \;, \tag{7}$$

acting on (6d) with $\nabla\cdot$ and $\hat{\mathbf{z}}\cdot(\nabla\times\;\;)$:

$$\frac{\mathrm{d}_0 D}{\mathrm{d}t} \;=\; -gH_0\nabla^2\zeta \;+\; f\Omega_r \;-\; \beta v_x \;-\; 2\frac{\partial v_y}{\partial x}\frac{\partial U}{\partial y} \;-\; \frac{\partial\omega}{\partial x}\frac{\partial U}{\partial p} \tag{8a}$$

$$\frac{\mathrm{d}_0\Omega_r}{\mathrm{d}t} \;=\; -\;\left(f \;-\; \frac{\partial U}{\partial y}\right)D \;-\; v_y\frac{\partial}{\partial y}\left(f \;-\; \frac{\partial U}{\partial y}\right) \;+\; \frac{\partial}{\partial y}\left(\omega\frac{\partial U}{\partial p}\right) \;. \tag{8b}$$

The last equation coincides (without the last term on the right hand side) with the linearized version of the shallow water model absolute vorticity equation

$$\frac{\mathrm{d}\Omega}{\mathrm{d}t} \;+\; D\cdot\Omega \;=\; 0 \;, \quad \Omega \;=\; f \quad +\; \hat{\mathbf{z}}(\nabla\times\mathbf{v}) \;= f \;+\; \Omega_r \;.$$

Let us introduce the potential vorticity

$$J \;=\; -\;\Omega_r \;+\; \alpha f\zeta \;+\; \frac{fg}{H_0}\left(\frac{\partial}{\partial p}p - \alpha\right)\frac{\eta}{N^2} \;, \tag{9}$$

as the independent dynamic field instead of relative vorticity Ω_r. Equations (8) read in terms of D, J as

$$\frac{\mathrm{d}_0 D}{\mathrm{d}t} \;=\; -gH_0\nabla^2\zeta \;-\; \beta v_x \;-\; 2\frac{\partial v_y}{\partial x}\frac{\partial U}{\partial y} \;-\; \frac{\partial \omega}{\partial x}\frac{\partial U}{\partial p} \;+$$

$$f\left[-\,J \;+\; \alpha f\zeta \;+\; f\left(\frac{\partial}{\partial p}p\frac{T_0}{T_i} \;-\; 1\right)\eta\right] \;, \qquad (10a)$$

$$\frac{\mathrm{d}_0 J}{\mathrm{d}t} \;=\; -\frac{\partial U}{\partial y}D \;-\; \frac{\partial}{\partial y}\left(\omega\frac{\partial U}{\partial p}\right) \;+\; v_y\frac{\partial}{\partial y}\left(f \;-\; \frac{\partial U}{\partial y}\right) \;+$$

$$f\left\{p\frac{\partial U}{\partial p}\frac{\partial}{\partial x}\frac{T'}{T_i} \;-\; \frac{\partial}{\partial p}\left[\frac{p}{T_i}\left(v_y\frac{\partial T_0}{\partial y} \;-\; Q\right)\right]\right\} \;. \qquad (10b)$$

Now we are ready to perform the final step and to deduce wave equations for η and ζ from (6a) – (6d). For that we act on (6a) and (6b with $\mathrm{d}_0/\mathrm{d}t$ and eliminate d_0w/dt ja d_0D/dt using (6c) and (10a):

$$\left(\hat{L} \;+\; \hat{P}^+\hat{P}^-\right)\zeta \;+\; \hat{P}^+\left(1-\frac{f^2}{N^2}\right)\eta \;=$$

$$\frac{H_0}{g}\left(\frac{p}{H_0}\frac{\partial U}{\partial p}\frac{\partial w}{\partial x} \;-\; 2\frac{\partial v_y}{\partial x}\frac{\partial U}{\partial y} \;-\; \frac{\partial \omega}{\partial x}\frac{\partial U}{\partial p}\right) \;+\; \frac{H_0}{g}\frac{\mathrm{d}_0}{\mathrm{d}t}\left(\frac{1}{H_0}\hat{P}^+ v_y\frac{\partial z_0}{\partial y} \;+\; \frac{v_y}{T_0}\frac{\partial T_0}{\partial y}\right) \;-$$

$$\frac{\beta H_0}{g}v_x \;-\; \frac{R}{g^2}\frac{\mathrm{d}_0 Q}{\mathrm{d}t} \;-\; \frac{H_0 f}{g}J \;, \qquad (11a)$$

$$\left[\left(\frac{1}{N}\frac{\mathrm{d}_0}{\mathrm{d}t}\right)^2 \;+\; 1\right]\eta \;+\; \hat{P}^-\zeta \;=\; \left(\frac{N^2}{g}\frac{\partial z_0}{\partial y} \;-\; \frac{1}{T_0}\frac{\partial T_0}{\partial y}\right)\frac{\mathrm{d}_0 v_y}{\mathrm{d}t} \;+\; \frac{1}{N^2}\frac{\mathrm{d}_0}{\mathrm{d}t}\frac{Q}{T_0} \;, \qquad (11b)$$

where

$$\hat{L} \;=\; H_0^2\left(\nabla^2 \;-\; \frac{1}{c_a^2}\frac{\mathrm{d}_0}{\mathrm{d}t}\frac{\mathrm{d}_1}{\mathrm{d}t} \;-\; \frac{f^2}{c_a^2}\right) \;, \qquad (11c)$$

$$\hat{P}^+ \;=\; p\frac{\partial}{\partial p} \;+\; \alpha \;, \qquad \hat{P}^- \;=\; \frac{\partial}{\partial p}p \;-\; \alpha \;. \qquad (11d)$$

The deduced wave system (11) is central in many different ways. First, it represents non-filtered dynamics and in this sense it is an exact linear model. Secondly, despite the linearity it is quite representative in the sense it is capable of modeling different real situations like stationary flows over complex orography, generation of instabilities in shear flows etc. Thirdly, it is convenient for the use in filtration study. Particularly, the EFM can be deduced from it with a minimum number of simplifications.

Model (11) includes all linear terms. In many cases horizontal shear of the background fields can be omitted, which yield simplification. These will be treated in the next section.

3.2. Linearization according to quasi-inertial shear flow

The simplest model, which incorporates the Coriolis effect simultaneously with the lack of horizontal shear of the background wind, can be presented as

$$f \;=\; const.\;,\quad T_0 \;=\; T_0(p)\;,\quad z_0(y,p) \;=\; -\,\frac{f}{g}U(p)\cdot y\;. \tag{12a}$$

Nevertheless, in most cases the horizontal gradient $\partial z_0/\partial y$ is so small in comparison with other competing terms that we can disregard it and introduce a quasi-inertial background

$$f \;=\; const.\;,\quad T_0 \;=\; T_0(p)\;,\quad z_0 \;=\; z_0(p) \;=\;,\quad U \;=\; U(p)\;. \tag{12b}$$

This background model enables, for instance, investigation of baroclinic and symmetric instabilities in the presence of acoustic effects. Its barotropic sub-case,

$$f \;=\; const.\;,\quad T_0 \;=\; T_0(p)\;,\quad z_0 \;=\; z_0(p)\;,\quad U \;=\; const, \tag{12c}$$

will be treated in the next sections, here we present the model (6) – (11) for background (12b).

The reduced linear system (6a), (6b), (10b), (10a) simplifies to

$$\alpha\frac{\mathrm{d}_1\zeta}{\mathrm{d}t} \;=\; \frac{1}{H_0}\left(\alpha \;+\; p\frac{\partial}{\partial p}\right)w \;-\; D + \;\frac{Q}{T_0}\;, \tag{13a}$$

$$\frac{\mathrm{d}_0\eta}{\mathrm{d}t} \;=\; -\,\frac{N^2}{g}w \;+\; \frac{Q}{T_0}\;, \tag{13b}$$

$$\frac{\mathrm{d}_0 w}{\mathrm{d}t} \;=\; g\left[\left(\frac{\partial}{\partial p}p \;-\; \alpha\right)\zeta \;+\; \eta\right]\;, \tag{13c}$$

$$\frac{\mathrm{d}_0 D}{\mathrm{d}t} \;=\; -gH_0\nabla^2\zeta \;-\; \frac{\partial\omega}{\partial x}\frac{\partial U}{\partial p} \;+\; f\left[-\;J \;+\; \alpha f\zeta \;+\; f\left(\frac{\partial}{\partial p}p\frac{T_0}{T_i} \;-\; 1\right)\eta\right]\;, \tag{13d}$$

$$\frac{\mathrm{d}_0 J}{\mathrm{d}t} \;=\; -\,\frac{\partial\omega}{\partial y}\frac{\partial U}{\partial p} \;+\; f\left[p\frac{\partial U}{\partial p}\frac{\partial}{\partial x}\frac{T'}{T_i} \;+\; \frac{\partial}{\partial p}\left(\frac{p}{T_i}Q\right)\right]\;. \tag{13e}$$

The corresponding wave equations (11a) and (11b) have simpler right hand terms

$$\left(\hat{L} \;+\; \hat{P}^+\hat{P}^-\right)\zeta + \hat{P}^+\left(1 - \frac{f^2}{N^2}\right)\eta \;=\; \frac{H_0}{g}\left(\frac{p}{H_0}\frac{\partial w}{\partial x} \;-\; \frac{\partial\omega}{\partial x}\right)\frac{\partial U}{\partial p} - \frac{R}{g^2}\frac{\mathrm{d}_0 Q}{\mathrm{d}t} - \frac{H_0 f}{g}J\;, \tag{14a}$$

$$\left[\left(\frac{1}{N}\frac{\mathrm{d}_0}{\mathrm{d}t}\right)^2 \;+\; 1\right]\eta \;+\; \hat{P}^-\zeta \;=\; +\,\frac{1}{N^2}\frac{\mathrm{d}_0}{\mathrm{d}t}\frac{Q}{T_0}\;. \tag{14b}$$

Equations (14) represent the ExM for background (12b). The corresponding EFM can be obtained, putting the left hand side of (13a) to zero, which in (14a) results with the simplification $\hat{L} \Rightarrow \hat{L}_0$:

$$\hat{L}_0 \;=\; H_0^2 \left(\nabla^2 \;-\; \frac{f^2}{c_a^2} \right) \;. \tag{15}$$

This approximation of $\hat{L}$ (and consequently, the EFM) is valid, if

$$\varepsilon \;=\; || \frac{1}{c_a^2} \frac{\mathrm{d}_0}{\mathrm{d}t} \frac{\mathrm{d}_1}{\mathrm{d}t} || / || \nabla^2 ||$$

represents a small quantity. Using estimations

$$||\nabla^2|| \;\sim\; 1/L^2 \;,\quad ||\frac{\mathrm{d}_0}{\mathrm{d}t}|| \;\sim\; U/L \;,\quad ||\frac{\mathrm{d}_1}{\mathrm{d}t}|| \;\sim\; ||p \frac{\partial U}{\partial p} \frac{\partial}{\partial x}|| \;\sim\; (H_0/L) \cdot U/L \;,$$

ε can be evaluated with a formula

$$\varepsilon \;\sim\; \frac{H_0}{L} \cdot \frac{U^2}{c_a^2} \;.$$

For $L = 100$ m, $U = 10$ m/s this estimate yields $\varepsilon \sim 0.1$. Thus, for such a small spacial scale of background fields the EFM can cause notable errors.

If one wants to maintain the accuracy of the EFM, he (she) has to use a more complicated operator $\hat{L}_1$ instead of $\hat{L}_0$

$$\hat{L}_1 \;=\; H_0^2 \left(\nabla^2 \;-\; \frac{1}{c_a^2} \frac{\mathrm{d}_0}{\mathrm{d}t} \frac{p}{\alpha} \frac{\partial U}{\partial p} \frac{\partial}{\partial x} \;-\; \frac{f^2}{c_a^2} \right) \;. \tag{15$'$}$$

which corresponds to the approximation

$$\frac{\mathrm{d}_0}{\mathrm{d}t} \frac{\mathrm{d}_1}{\mathrm{d}t} \;=\; \frac{\mathrm{d}_0}{\mathrm{d}t} \left(\frac{\mathrm{d}_0}{\mathrm{d}t} \;+\; \frac{p}{\alpha} \frac{\partial U}{\partial p} \frac{\partial}{\partial x} \right) \;\rightarrow\; \frac{\mathrm{d}_0}{\mathrm{d}t} \;\frac{p}{\alpha} \frac{\partial U}{\partial p} \frac{\partial}{\partial x} \;.$$

3.3. Wave equation for vertical velocity in simplest shear flow model

In the special case of the barotropic background, (12c), and adiabatic model, $Q = 0$, J turns to a local invariant

$$\frac{\mathrm{d}_0 J}{\mathrm{d}t} \;=\; 0 \;.$$

Restricting the further treatment with

$$J \;=\; 0 \;,$$

(14) turn to homogeneous closed wave equations for η and ζ, which are identical to consequent equations of the model with the resting background, (2.11), except that $\partial/\partial t$ is changed by a more general material derivative d_0/dt:

$$\left(\hat{L} \;+\; \hat{P}^+ \hat{P}^- \right) \zeta \;+\; \hat{P}^+ \left(1 - \frac{f^2}{N^2} \right) \eta \;=\; 0 \;, \tag{16a}$$

$$\left[\left(\frac{1}{N}\frac{\mathrm{d}_0}{\mathrm{d}t}\right)^2 \;+\; 1\right]\eta \;+\; \hat{P}^-\zeta \;=\; 0\;. \qquad (16b)$$

keeping in mind further numerical comparison of different filtered models in shear flow regime, it is advantageous to deduce a single fourth order in t scalar wave equation for one dynamical field. Here we choose vertical wind speed w for that independent dynamical variable. The equation for w can be deduced in two steps. First, action on (16a) with $\hat{P}^-(1/H_0^2)\cdot$ and use of (16b) yields

$$\mathcal{L}\left(\frac{1}{N^2}\frac{\mathrm{d}_0^2}{\mathrm{d}t^2} \;+\; 1\right)\eta \;+\; \mathcal{M}\left(\frac{1}{N^2}\frac{\mathrm{d}_0^2}{\mathrm{d}t^2} \;+\; \frac{f^2}{N^2}\right)\eta \;=\; 0\;, \qquad (17)$$

where

$$\mathcal{L} \;=\; \hat{L}/H_0^2 \;=\; \nabla^2 \;-\; \frac{1}{c_a^2}\frac{\mathrm{d}_0^2}{\mathrm{d}t^2} \;-\; \frac{f^2}{c_a^2}\;, \quad \mathcal{M} \;=\; \hat{P}^-\frac{1}{H_0^2}\hat{P}^+$$

(it is assumed here at the definition of $\mathcal{L}$, that $\mathrm{d}_1/\mathrm{d}t = \mathrm{d}_0/\mathrm{d}t$). Action on equation (17) with $\mathrm{d}_0/\mathrm{d}t$ (an essential attribute of the barotropic model is that $\mathrm{d}_0/\mathrm{d}t$ commutates with all operators in this equation) and use of (6b) yields

$$\left(\frac{\mathrm{d}_0^2}{\mathrm{d}t^2} \;+\; N^2\right)\mathcal{L}w \;+\; \left(\frac{\mathrm{d}_0^2}{\mathrm{d}t^2} \;+\; f^2\right)\mathcal{M}w \;=\; 0\;. \qquad (18)$$

The presented equations (17) and (18) correspond to the ExM. The EFM can be obtained, omitting the second term in the $\mathcal{L}$ definition. The error of this approximation, ε, does not exceed 1 – 2 % at the present case with constant U.

For some theoretical purpoces and practical applications it is convenient to have a equation for $\hat{\omega} \equiv -pw/H_0$. For filtered models $\hat{\omega}$ coinsides with the true omega–velocity, still, for the exact model it represents an artificial construction. Using operator–identities

$$\hat{P}^-\frac{1}{H_0}\varphi \;=\; \frac{p}{H_0}\left(\frac{\partial}{\partial p} + \frac{T_i}{pT_0}\right)\varphi\;, \quad \frac{1}{H_0}\hat{P}^+\varphi \;=\; \left(\frac{\partial}{\partial p} - \frac{T_i}{pT_0}\right)\frac{p}{H_0}\varphi\;,$$

it is straightforward to get from (18) an equation

$$\left(\frac{\mathrm{d}_0^2}{\mathrm{d}t^2} \;+\; N^2\right)\mathcal{L}\hat{\omega} \;+\; \left(\frac{\mathrm{d}_0^2}{\mathrm{d}t^2} \;+\; f^2\right)\left(\frac{p^2}{H_0^2}\frac{\partial^2}{\partial p^2} \;-\; m(p)\right)\hat{\omega} \;=\; 0\;, \qquad (18')$$

where

$$m(p) \;=\; \left(\frac{T_i}{pT_0}\right)^2 \;+\; \frac{\partial(T_i/pT_0)}{\partial p}\;.$$

3.4. Linear MPM and HSM in simplest shear flow model

Linearization of MPM in according to the background state (2) is

$$\frac{\mathrm{d}_0 w}{\mathrm{d}t} \;=\; g\;\left(\frac{p}{H_0}\frac{\partial z'}{\partial p} \;+\; \frac{T'}{T_0}\right)\;, \qquad (19a)$$

$$\frac{\mathrm{d}_0 T'}{\mathrm{d}t} \;=\; \frac{T_i \omega}{p} \;+\; Q \;, \tag{19b}$$

$$D \;+\; \frac{\partial \omega}{\partial p} \;=\; 0 \;, \tag{19c}$$

$$\frac{w}{H_0} \;=\; -\,\frac{\omega}{p} \;, \tag{19d}$$

to which horizontal wind equations (6d) ja (6e) are to be added.

Potential vorticity is

$$J \;=\; f\,\frac{\partial}{\partial p} p \frac{T'}{T_i} \;-\; \Omega_r \;, \tag{20a}$$

and it evolves according to the equation

$$\frac{\mathrm{d}_0 J}{\mathrm{d}t} \;=\; f\,\left(\frac{\partial}{\partial p} p \frac{Q}{T_i} \;-\; \frac{\partial U}{\partial p}\frac{p}{T_i}\frac{\partial T'}{\partial x}\right) \;-\; \frac{\partial}{\partial y}\omega\frac{\partial U}{\partial p} \;. \tag{20b}$$

The wave equations are

$$\left(\frac{1}{N^2}\frac{\mathrm{d}_0^2}{\mathrm{d}t^2} \;+\; 1\right)\frac{T'}{T_0} \;+\; \frac{p}{H_0}\frac{\partial z'}{\partial p} \;=\; \frac{1}{N^2}\frac{\mathrm{d}_0}{\mathrm{d}t}\frac{Q}{T_0} \;, \tag{21a}$$

$$\left(\frac{\partial}{\partial p}\frac{p^2}{H_0^2}\frac{\partial}{\partial p} \;+\; \nabla^2\right)\, z' \;+\; \frac{\partial}{\partial p}\left[\frac{p}{H_0}\left(1 \;-\; \frac{f^2}{N^2}\right)\frac{T'}{T_0}\right] \;=\; -\,\frac{2}{g}\frac{\partial \omega}{\partial x}\frac{\partial U}{\partial p} \;-\; \frac{f}{g} J \;. \tag{21b}$$

Assuming that background is (12c)a, and $Q = 0$, $J = 0$, it is easy to deduce from these equations a scalar wave equation for T'/T_0, second oder in t:

$$\nabla^2\left(\frac{1}{N^2}\frac{\mathrm{d}_0^2}{\mathrm{d}t^2} \;+\; 1\right)\frac{T'}{T_0} \;+\; \hat{M}\left(\frac{1}{N^2}\frac{\mathrm{d}_0^2}{\mathrm{d}t^2} \;+\; \frac{f^2}{N^2}\right)\frac{T'}{T_0} \;=\; 0 \;, \tag{22}$$

where

$$\hat{M} \;=\; \frac{p}{H_0}\frac{\partial}{\partial p}\frac{\partial}{\partial p}\frac{p}{H_0} \;.$$

Equation for w follows, after acting on (22) with $\mathrm{d}_0/\mathrm{d}t$, with the help of the relation

$$\frac{1}{N^2}\frac{\mathrm{d}_0}{\mathrm{d}t}\frac{T'}{T_0} \;=\; -\,\frac{w}{g} \;.$$

The wanted equation is

$$\left(\frac{\mathrm{d}_0^2}{\mathrm{d}t^2} \;+\; N^2\right)\nabla^2 w \;+\; \left(\frac{\mathrm{d}_0^2}{\mathrm{d}t^2} \;+\; f^2\right)\hat{M} w \;=\; 0 \;. \tag{23}$$

Obviously, (22) represents the analogue of (17) and (23) – the analogue of (18).

Analoque of (18') for ω (hat can be omitted in the case of the MPM) is

$$\left(\frac{\mathrm{d}_0^2}{\mathrm{d}t^2} \; + \; N^2\right) \nabla^2\omega \; + \; \left(\frac{\mathrm{d}_0^2}{\mathrm{d}t^2} \; + \; f^2\right) \frac{p^2}{H_0^2}\frac{\partial^2}{\partial p^2}\omega \; = \; 0 \; . \tag{23'}$$

Wave equation in HSM. Because this is the very standard case which is presented in different copy-books, we reproduce the final equation for T'/T_0 only

$$\hat{M}\frac{1}{N^2}\frac{\mathrm{d}_0^2}{\mathrm{d}t^2}\frac{T'}{T_0} \; + \; \left(\nabla^2 \; + \; \hat{M}\frac{f^2}{N^2}\right)\frac{T'}{T_0} \; = \; 0 \; , \tag{24}$$

This equation is a long-wave asymptote of (22). Thus, in the linear case there is no need to treat the HSM as an independent model but as the long-wave asymptote of the MPM.

3.5. Boundary conditions for vertical velocity equation

The condition for w at the ground follows from (15a'):

$$w|_{p_0} \; = \; \frac{\mathrm{d}_0 h}{\mathrm{d}t} \; = \; U\frac{\partial h}{\partial x} \; , \tag{25}$$

where h is the ground height above the sea level.

On the top of the atmosphere, $p \; \to 0$, we employ the "radiation condition" for the separation among possible wave solutions physically relevant ones. This condition specifies that the waves radiate "out of the top" without reflection and there is no downward propagation of wave energy in the vicinity of the upper boundary. The radiation condition can be quantitatively formulated in the spectral space. An comprehensive discussion of the topic can be found in the monograph by P. Baines (1995). For acoustically relaxed models EFM and MPM the most general upper boundary condition for vertical velocity can be deduced from the "regularity requirement", that geopotential height fluctuation, ζ lacks exponentially growing modes near $p = 0$. The regularity requirement will be discussed in detail in Chapter Five. Here we accept without detailed proof that in linear models the radiation condition is an consequence of the regularity requirement.

At the lateral boundaries periodic conditions will be used.

CHAPTER FOUR

Testing of Filtration Accuracy

In this chapter the model tests are carried out. For that wave solutions of equations (3.18) and (3.23) are compared. Equation (3.18) supplies us with exact solutions and (for $c_a = \infty$) with EFM-solutions, while (3.23) yields solutions for the MPM and (in long-wave limit) – for the HSM.

We will study waves in the model atmosphere with homogeneous stratification:

$$H_0 \;=\; 10^4 \;\; \mathrm{m} \;\;, \quad N \;=\; 10^{-2} \;, \;\; 2 \cdot 10^{-2} \;\; \mathrm{s}^{-1} \;, \quad U \;=\; 10 \;, \; 25 \; \mathrm{m/s} \;. \tag{1}$$

General solution of (3.18) and (3.23) can be presented as a sum of the stationary particular solution w_s with nonhomogeneous lower boundary condition (3.25) and general nonstationary solution w_g with homogeneous lower condition (3.25):

$$(\mathbf{x},\; p,\; t) \;=\; w_s(\mathbf{x},\; p) \;+\; w_g(\mathbf{x},\; p,\; t) \;. \tag{2}$$

In this representation the nonstationary general solution, which represents propagating wave component, is not affected by the orography. In following, stationary and nonstationary solutions are treated separately.

4.1. Propagating waves in different models

Wewill look for nonstationary waves $w_g$in the form

$$w \;\sim\; \left(\frac{p}{p_0}\right)^{-1/2} \sin(\mu \ln p_0/p) \cdot \exp(-i\mathbf{kx} \;+\; i\nu t) \;. \tag{3}$$

Substitution of this assumed solution into (3.18) or (3.13) yields dispersion relationships between wave numbers μ, $\mathbf{k}$ and frequency ν. Solution of the dispersion relationship with regard to μ gives

$$\mu \;=\; \sqrt{q} \tag{4a}$$

where q is for the ExM:

$$q \;=\; H_0^2 k^2 \cdot \left(1 \;+\; \frac{f^2}{c_a^2 k^2} \;-\; \frac{\nu_*^2}{c_a^2 k^2}\right) \cdot \frac{N^2 \;-\; \nu_*^2}{\nu_*^2 \;-\; f^2} \;-\; (\alpha \;-\; 1/2)^2 \;, \tag{4b}$$

for the EFM:

$$q \;=\; H_0^2 k^2 \cdot \left(1 \;+\; \frac{f^2}{c_a^2 k^2}\right) \cdot \frac{N^2 \;-\; \nu_*^2}{\nu_*^2 \;-\; f^2} \;-\; (\alpha \;-\; 1/2)^2 \;, \tag{4c}$$

for the MPM:

$$q \;=\; H_0^2 k^2 \cdot \frac{N^2 \;-\; \nu_*^2}{\nu_*^2 \;-\; f^2} \;-\; 1/4 \qquad (4d)$$

and for the HSM:

$$q \;=\; H_0^2 k^2 \cdot \frac{N^2}{\nu_*^2 \;-\; f^2} \;-\; 1/4 \;. \qquad (4e)$$

It is instructive to complement this series with consequent formulae for the anelastic model without Coriolis force:

$$q \;=\; H_0^2 k^2 \cdot \frac{N^2 \;-\; \nu_*^2}{\nu_*^2} \;-\; 1/4 \;, \qquad (4f)$$

for the Boussinesq (shallow convection model):

$$q \;=\; H_0^2 k^2 \cdot \frac{N^2 \;-\; \nu_*^2}{\nu_*^2} \qquad (4g)$$

and for the Euler linear model of incompressible laboratory fluid:

$$q \;=\; -\; H_0^2 k^2 \;. \qquad (4h)$$

The intrinsic frequency ν_* in these formulae,

$$\nu_* \;=\; \nu \;-\; Uk \;, \qquad (4g)$$

represents the frequency which is recorded by a observer moving along with the wind.

As it can be seen, all models are simplified forms of the general model (4b).

Dimensionless vertical wave-number μ determines the vertical wavelength of the wave. Its difference from the exact one, (4a), is a good indicator of the quality of approximate model. Results of comparison of $\mu^2 = q$ as function of ν_* for different horizontal scales $l_x = 1/k$ are presented on Fig. 1.1a – 1d for parameters $H_0 \;=\; 10$ km, $N = 10^{-2}\ s^{-1}$. Because orography is for propagating waves irrelevant (in linear case, of course), we can take without loss of generality $\nu_* = \nu$. As it may be concluded from these figures, all filtered models have notable error for very long waves, $1/k \sim 10\ 000$ km. This is the domain of planetary waves, where the used approximation of constant Coriolis parameter f is not the very best choice. In more shorter scales up to $1/k = 10$ km filtered models coincide with the exact one with a good accuracy.

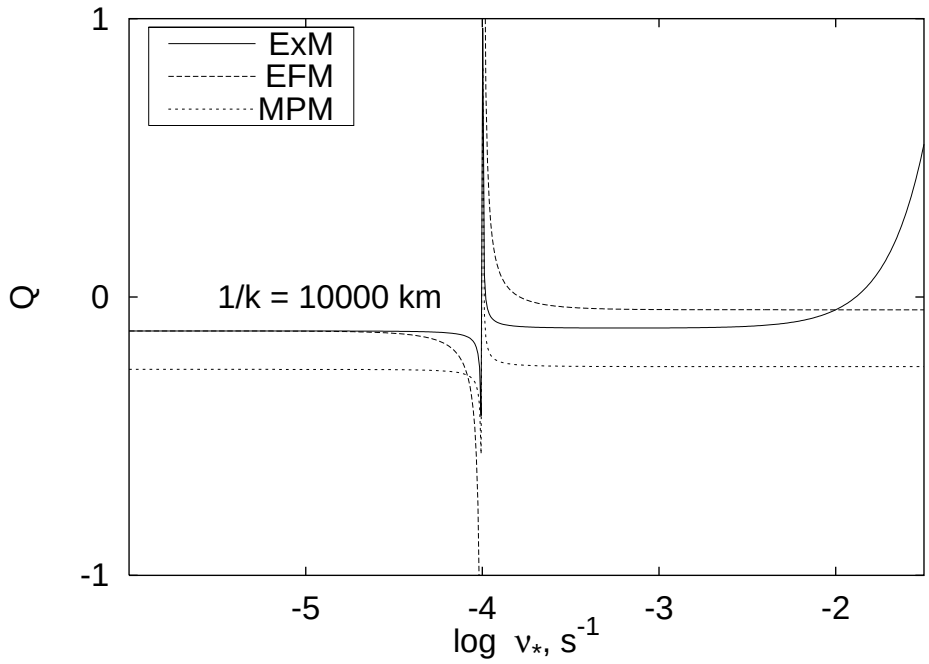

Fig. 4.1a

$\mu^2 = q$ as a function of intrinsic frequency ν_* for horizontal scale $1/k = 10^4$ km.

$H_0 = 10$ km, $N = 0.01$ 1/s.

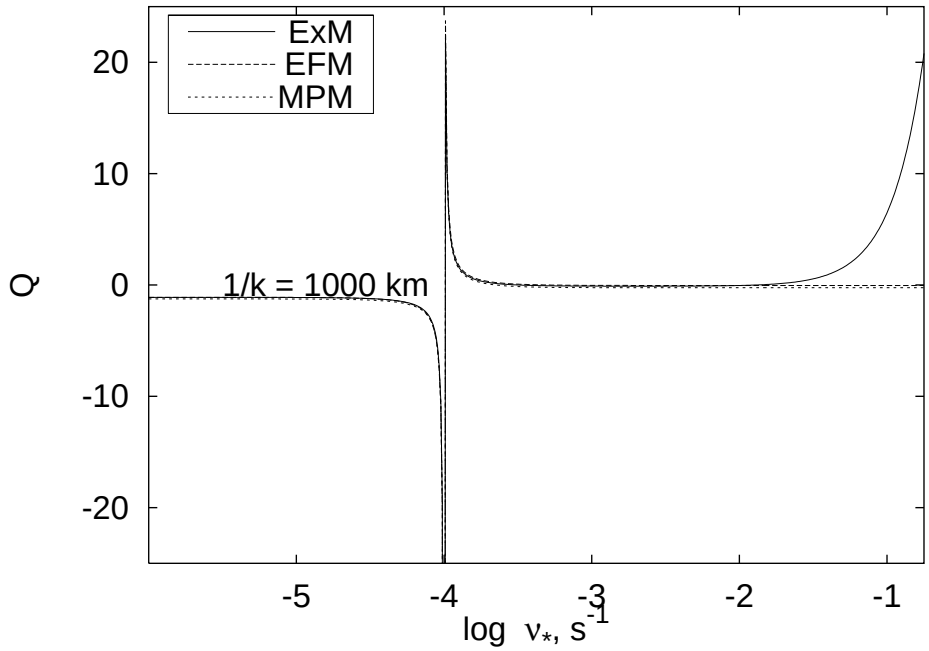

Fig. 4.1b

The same as Fig. 4.1a, except $1/k = 10^3$ km.

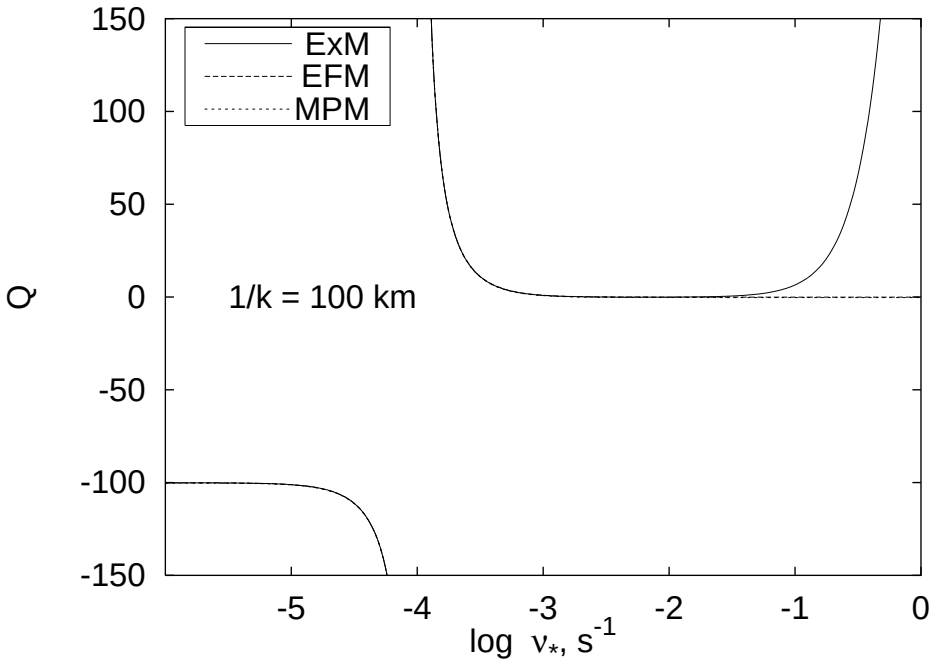

Fig. 4.1c

The same as Fig. 4.1a, except $1/k = 10^2$ km.

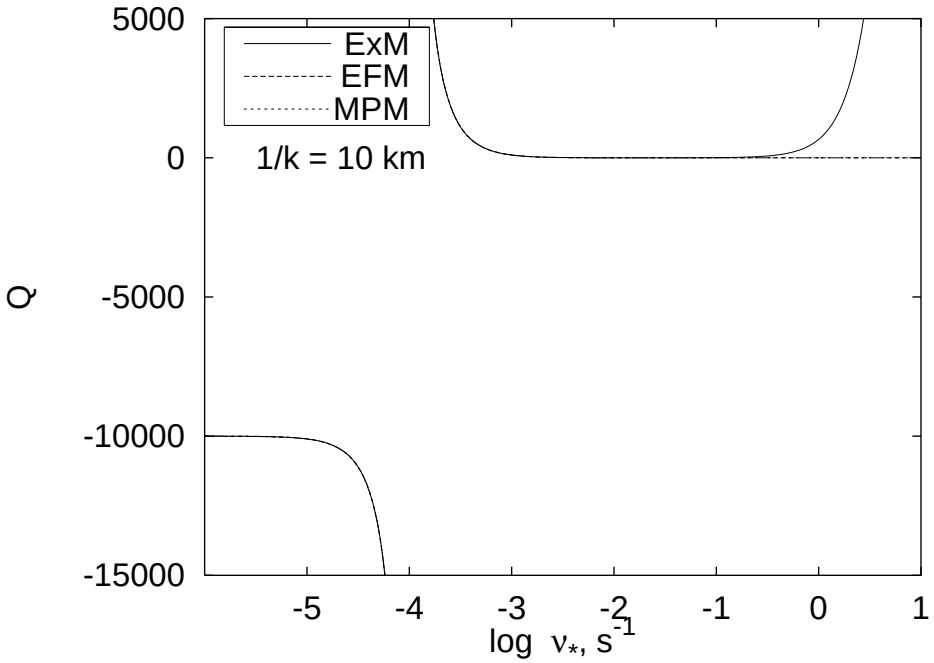

Fig. 4.1d

The same as Fig. 4.1a, except $1/k = 10$ km.

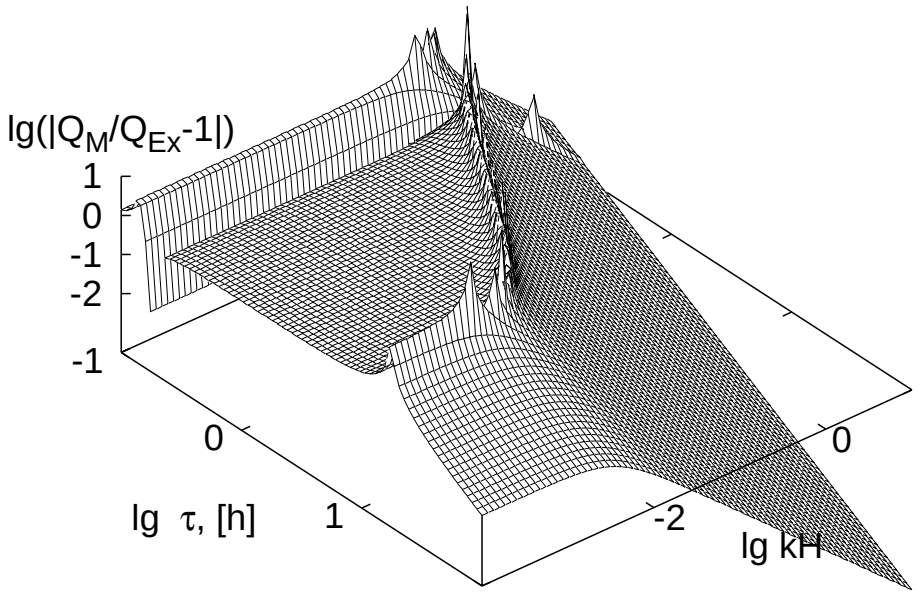

Fig. 4.2a. Model EFM: Relative error of q as a function of intrinsic period $\tau = 2\pi/\nu_*$ and nondimensional horizontal wave-number $k \cdot H_0$. $H_0 = 10$ km, $N = 0.01$ 1/s.

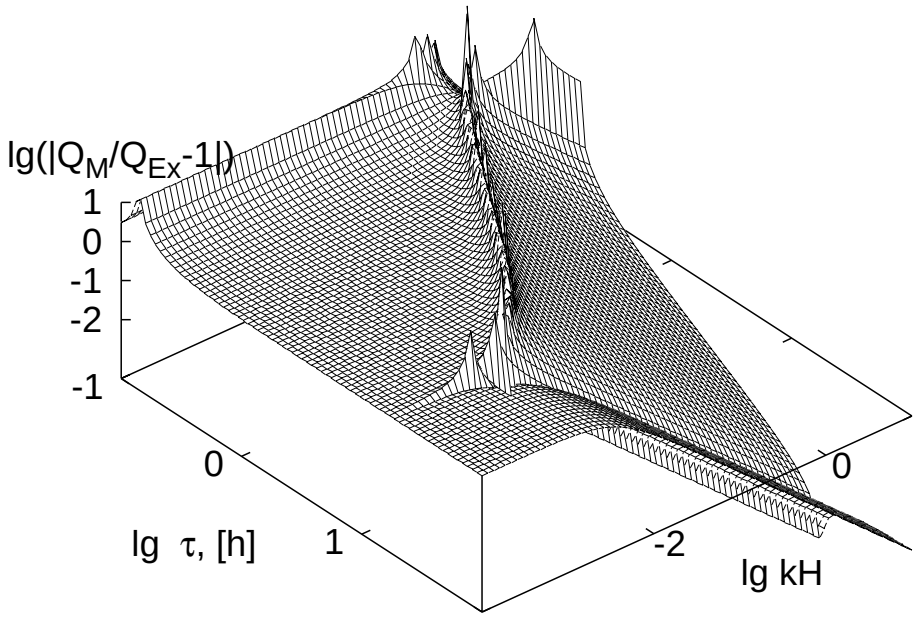

Fig. 4.2b. The same as fig. 4.2a for the MPM.

In Fig. 4.2a and 4.2b are presented relative absolute errors of q for the EFM and MPM. The diagonally oriented ridge on both figures corresponds to ultimate case of two-dimensional waves with infinite vertical wave-length, $Q_{ExM} = 0$. The error of any approximation is large by the definition in this case. Two additional ridges parallel to the k-axis correspond to frequencies $\nu_* = N$ and $\nu_* = f$. The relative error of both filtered models is large in the vicinity of these ridges as well (still, on the frequency ν_* $= N$ the error of EFM turns to exact zero). The plateau surrounded with this three ridges corresponds to the domain $kH \to 0$, $f \ << \nu_* << \ N$. Relative error of both approximations are large at this plateau ($\sim \ 1$). The real domain of application of filtered models for transient waves lies to the right of the ridge, ie. to waves with lower frequencies and shorter horizontal wave-lengths. This is the domain of gravity waves. In addition, the MPM has large error, which was documented on Fig. 1a already, for $kH < 10^2$ at frequencies $\nu_* < f$.

4.2. Stationary orographic waves. Sinusoidal orography

Though the studied in the previous section transient free modes are interesting in theoretical aspect, in real atmosphere they are rarely exited to large amplitudes and thus represent a relatively exotic phenomenon. In numerical models they arise more often from nonbalanced initial conditions and should be eliminated at the initialization.

Much more essential for slow dynamics are (quasi-)stationary orographic waves, which are in real atmosphere permanently exited, interact (in nonlinear models) with the large-scale wind fields and cause the wave-drag.

Stationary orographic and mountain waves have elementary representation for one-dimensional harmonical (sinusoidal) orography

$$h \ = \ h_k \mathrm{e}^{-i\ kx} \tag{5}$$

More complex (but still one-dimensional) orography can be presented as the sum of elementary oscillations (5). Due to the linearity of wave equation the solution with complex orography is a sum of elementary solutions corresponding to elementary modes (5).

The elementary solution to (5) has the same structure for all models:

$$w_k(x,p) \ = \ \frac{\mathrm{d}_0 a}{\mathrm{d}t} \ = \ -ikU \ a_k(x,p) \ , \tag{6a}$$

where

$$a_k(x,p) \ = \ h_k \left(\frac{p_0}{p}\right)^{1/2} \mathrm{e}^{-i(kx \ + \ \sqrt{q}\ln p_0/p)} \ . \tag{6b}$$

For $q > 0$ this solution satisfies the radiative boundary condition at the top, for $q < 0$ it yields a trapped wave, if

$$\sqrt{q} \ = \ \sqrt{-|q|} \ = \ -i\sqrt{|q|} \tag{6c}$$

(Baines, 1995; Holton, 1992). Expression for q coincides with (4) for $\nu = 0$ and $\nu_* = -Uk$. For different models it has the following representation
– the exact model:

$$q(k) \;=\; \left[\left(1 \;-\; \frac{U^2}{c_a^2}\right) H_0^2 k^2 \;+\; \frac{c_f^2}{c_a^2}\right] \cdot \frac{c_i^2/U^2 \;-\; H_0^2 k^2}{H_0^2 k^2 \;-\; c_f^2/U^2} \;-\; (\alpha \;-\; 1/2)^2 \;, \qquad (7a)$$

– the EFM:

$$q(k) \;=\; \left(H_0^2 k^2 \;+\; \frac{c_f^2}{c_a^2}\right) \cdot \frac{c_i^2/U^2 \;-\; H_0^2 k^2}{H_0^2 k^2 \;-\; c_f^2/U^2} \;-\; (\alpha \;-\; 1/2)^2 \;, \qquad (7b)$$

– the MPM:

$$q(k) \;=\; H_0^2 k^2 \;\cdot \frac{c_i^2/U^2 \;-\; H_0^2 k^2}{H_0^2 k^2 \;-\; c_f^2/U^2} \;-\; 1/4 \;, \qquad (7c)$$

– the HSM:

$$q(k) \;=\; H_0^2 k^2 \;\cdot \frac{c_i^2/U^2}{H_0^2 k^2 \;-\; c_f^2/U^2} \;-\; 1/4 \;, \qquad (7d)$$

– the anelastic model:

$$q(k) \;=\; c_i^2/U^2 \;-\; H_0^2 k^2 \;-\; 1/4 \;, \qquad (7e)$$

– the Boussinesq model:

$$q(k) \;=\; c_i^2/U^2 \;-\; H_0^2 k^2 \;. \qquad (7f)$$

Constant $c_i = \sqrt{RT_i} \sim 100$ m/s represents the characteristic phase speed of internal buoyancy waves (real phase speed is proportional to it), and $c_f = fH_0 \sim 1$ m/s. The anelastic and Boussinesq model q are presented for the check, no special modeling is carried out with these two approximations. Note that for the Boussinesq model the factor $(p_0/p)^{1/2}$ in (6b) must be left out.

Like in the nonstationary case, q plays again the central role. This function is presented for different U and N on Fig.3. As it turns out, q of the EFM is very close to the exact model in stationary case at all spatial scales so far as $U^2/c_a^2 << 1$. Because in the atmosphere this condition holds at all spatial scales with high accuracy, one can conclude that for slow (stationary and quasi-stationary) flows the EFM represents the filtered model of the global range, ie., it is valid at all spatial scales from micro-turbulence till planetary scale motions. The same is true for the MPM, except the very long waves, $H_0 k \to 0$, where slight difference appear: For the ExM and EFM $q \to -[c_i^2/c_a^2 + (\alpha - 1/2)^2] \approx$ –0.15, whereas for the MPM $q \to$ –0.25. Still, as it will be demonstrated in the next section, this difference is irrelevant because it causes very small(really negligible) difference of wave pattern in comparison with the exact case. Thus, so far as q is the only characteristic of the solutions, the EFM and MPM are not distinguishable from the exact model and from each other.

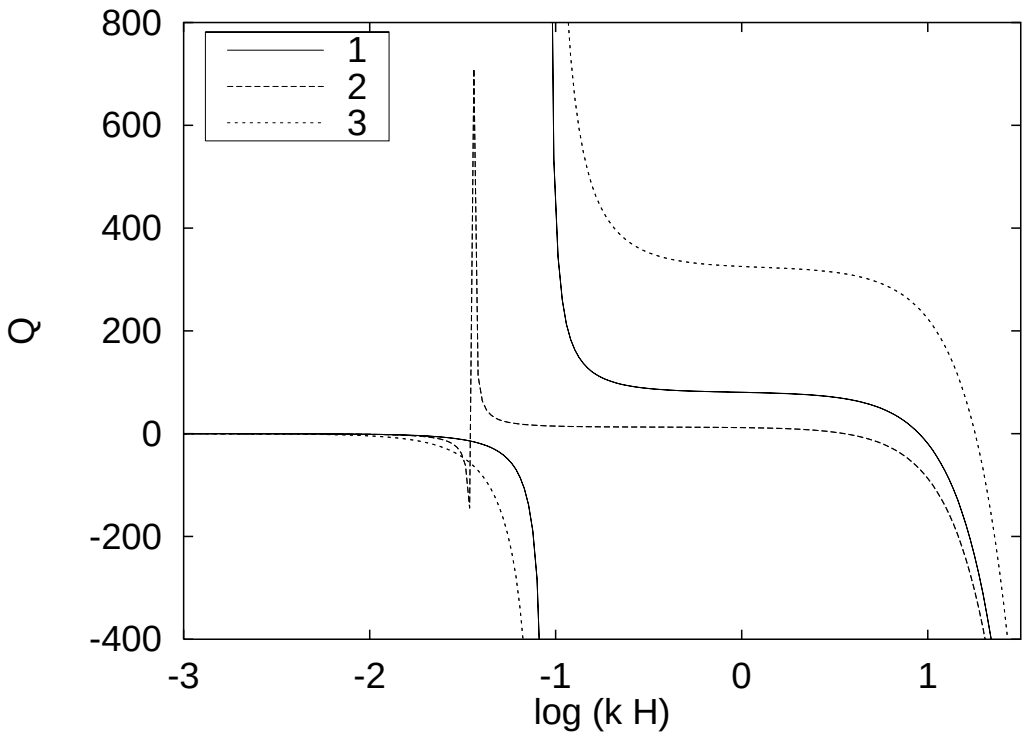

Fig. 4.3 $q(kH_0)$ for stationary orographic waves. Curves correspond to the exact model (7a). Other two models, the EFM (7b), and the MPM (7c), are so close to the ExM that their curves would coincide with the curves on the figure.
1 – $N = 10^{-2}$ 1/s, $U = 10$ m/s; 2 – $N = 10^{-2}$ 1/s, $U = 25$ m/s; 3 – $N = 2{\cdot}10^{-2}$ 1/s, $U = 10$ m/s.

Summarising, we can conclude, that the field of vertical velocity w is in similar conditions practically same for all compared models, ExM, EFM and MPM.

For other quantities the similarity is not so close anymore, as the algorithm of their calculation from primary field w will depend on the model. Formula for η follows from (3.13b) with $Q = 0$, it is of the same appearance for ExM and EFM (the MPM does not define this field):

$$\eta_k(x,p) \;=\; -\frac{N^2}{g}\, a_k(x,p)\;, \tag{8a}$$

Formula for ζ of the ExM and EFM results from (3.13c) with the help of (8a):

$$\zeta_k(x,p) \;=\; \frac{N^2 - k^2U^2}{g(1/2 - \alpha + i\sqrt{q})}\, a_k(x,p) \tag{8b}$$

and (1.5) yields for the relative temperature fluctuation

$$T'_k/T_0 \;=\; -\;(1\;+\;d_k)\;\frac{N^2}{g} a_k(x,p)\;, \tag{8c}$$

where

$$d_k \;=\; \frac{T_i}{T_0}\;\frac{k^2U^2/N^2\;-\;1}{1/2-\alpha+i\sqrt{q}}\;. \tag{9}$$

At the same time, from (3.19b) and (3.19d) with the help of (6a) it follows a formula for the temperature fluctuation in MPM:

$$T_k'/T_0 \;=\; -\frac{T_i}{T_0}\;\frac{a_k(x,p)}{H_0} \;=\; -\frac{N^2}{g}\;a_k(x,p)\;. \tag{10}$$

Which is clearly different from (8c). The exact model and EFM have in comparison with the MPM an additional term, proportional to the "correction factor" d_k (9). Temperature fluctuations of the ExM and EFM, (8c), and of the MPM, (10), are close, if this correction factor is small. As it may be convinced from Fig. 4.4a, 4.4b, which represent the real- and imaginary parts of d_k respectively, d_k is small everywhere except at very short scales. The level $|d_k| \;>\; 0.1$ is reached (depending upon background parameters) at spatial scales $l_x \;\sim\; 1/k \;\sim\; 100 \;--\; 500$ m, and it increases rapidly towards shorter scales.

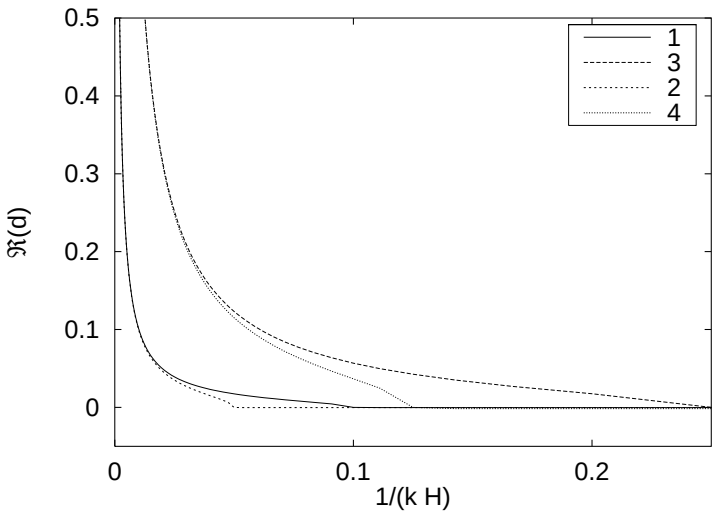

Fig. 4.4a

Real part of the correction factor d_k.
1 – $N = 10^{-2}$ 1/s, $U = 10$ m/s; 2 – $N = 2{\cdot}10^{-2}$ 1/s, $U = 10$ m/s; 3 – $N = 10^{-2}$ 1/s, $U = 25$ m/s; 4 – $N = 2{\cdot}10^{-2}$ 1/s, $U = 25$ m/s.

Differently from the real part, the imaginary part of d (Fig. 4.4b) is zero for short waves and restricted at long scales.

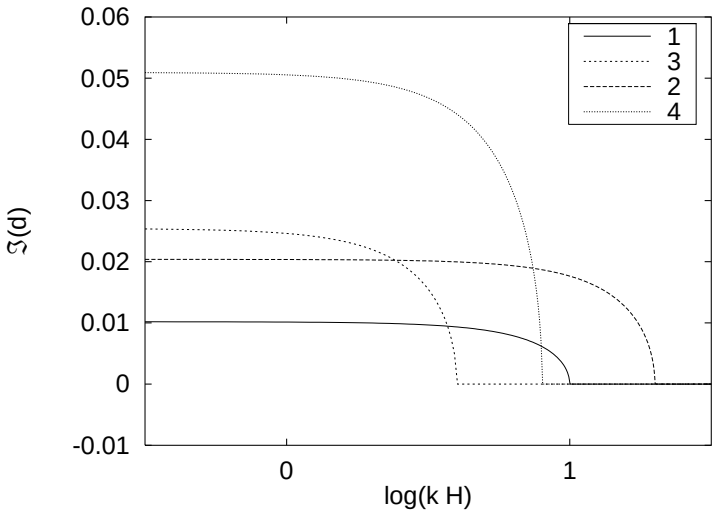

Fig. 4.4b

Imaginary part of the correction factor d.
Notation is the same as on Fig. 4a.

The general conclusion from this treatment is that temperature fluctuations differ depending on the model choice. This is an example of the situation, where a particular field – temperature in this example – is differently calculated and yields different values for different models. Another example, which is just opposite to this, represents the relative entropy fluctuation. For the EFM and ExM this is η, defined as (2.5) and represented by formula (8a). For the MPM the (relative) entropy fluctuation is defined as s' $= T'/T_0$, which is obviously quite different from (2.5). At the same time, its particular representation in the present model case is (10), ie., numerically it coincides with η!

With the help of formula

$$\frac{p}{H_0}\frac{\partial z'}{\partial p} \;=\; \left(p\frac{\partial}{\partial p} \;+1\;-\;\alpha^*\right)\zeta\;, \qquad \alpha^* \;=\; \alpha \;+\; T_i/T_0\;,$$

and treating α^* at the integration as a constant, from (3.21) and (10) an expression for ζ in MPM framework follows:

$$\zeta_k(x,p) \;=\; \frac{N^2-k^2U^2}{g(1/2-\alpha^*+i\sqrt{q})}\;a_k(x,p)\;. \tag{11}$$

The only difference of this approximate formula in comparison with the exact one, (8b) is the use of α^* instead α. This difference in value of α is not large, approximately 10 % , and has influence on the amplitude of ζ, if $q \approx 0$, ie., in the vicinity of the critical wave-number k_c. Critical wave-number k_c is determined with the condition $q(k_c) = 0$ and it is approximately

$$k_c \;\approx\; c_i/(UH_0)\;,$$

which yields $l_c \;=\; 1/k_c \;\sim 10^3$ m. Thus, vertical accelerations in MPM have most significant deviations (about 10 %) from exact value in the region $l_f \sim 1$ km.

The hydrostatic/nonhydrostatic character of the dynamics depends much on the horizontal scale of the orography l_x $(= 1/k$ for sinusoidal surface). For long waves atmosphere is with good accuracy in hydrostatic balance, and $\zeta \approx \zeta_s$ (see (2.12)), for short

waves departure from hydrostatic state, determined with the amplitude of $\zeta_n = \zeta - \zeta_s$, should be comparable with ζ. The transition from hydrostatic state to nonhydrostatic with the decrease of the characteristic scale is demonstrated for ExM[(1)] on Fig. 4.5a-f.

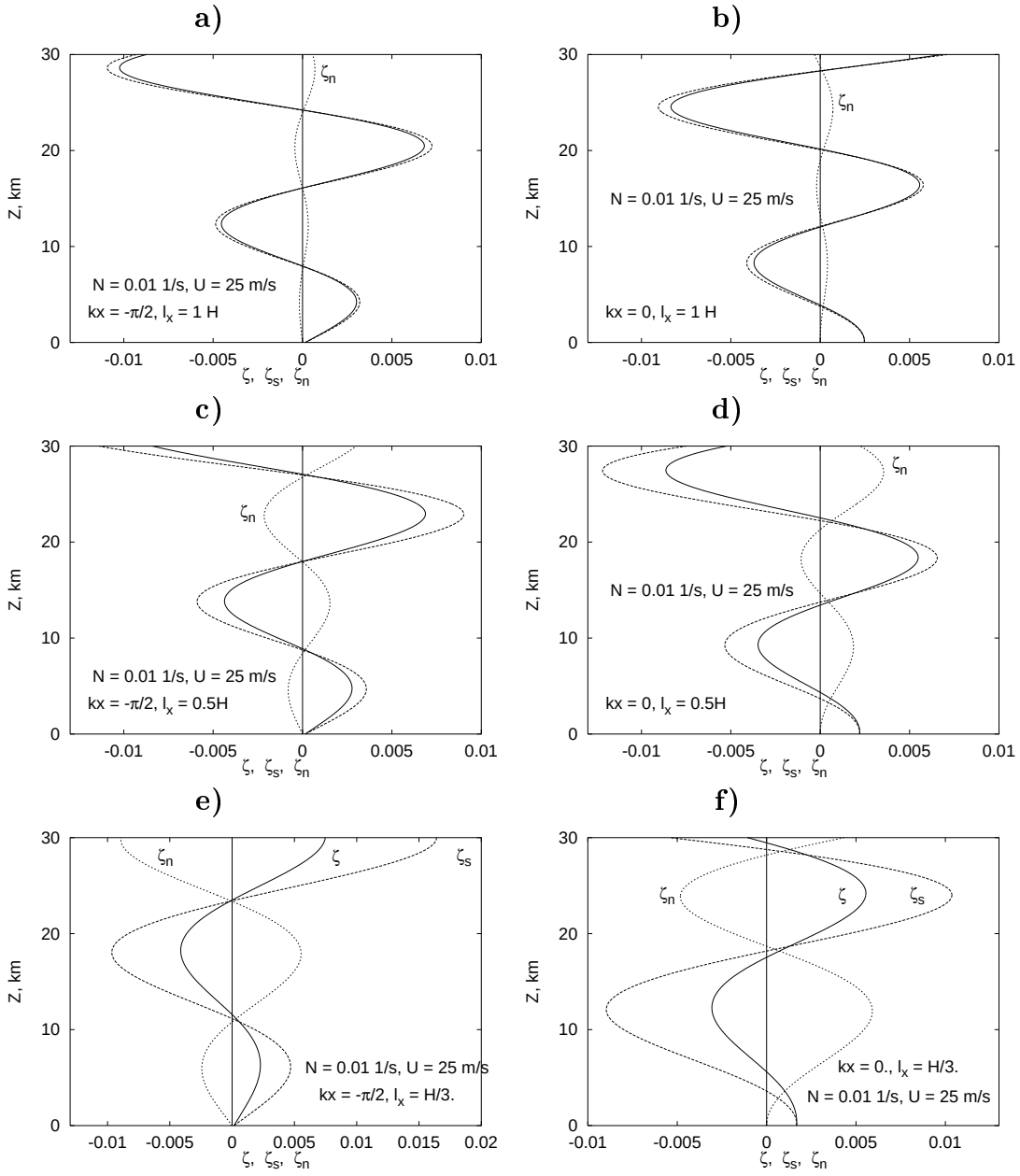

Fig. 4.5

Relative fluctuation of geopotential, ζ, and its hydrostatic and nonhydrostatic components, ζ_s and ζ_s, as functions of the geometrical height, Z.
a), c), e) – x corresponds to the valley; b), d), f) – x corresponds to the hill-slope.

The departure from hydrostatic state is small but observable, if $l_x = H \approx 10$ km, and it makes substantial for $l_x \approx 5$ km and less. It is remarkable, that nonhydrostatic correction, ζ_n, is oppositely signed to the hydrostatic component, ζ_s and tries to cancel it.

(1) Transition is not sensitive to the model choice.

As a result, the total deviation, ζ, is always smaller than it would be in the hydrostatic approximation.

4.3. Stationary flow over isolated mountain

Sinusoidal profile is an artificial idealization. More close to the reality is the case of an isolated mountain. In the following we will represent results of the modeling of the uniform flow over the two-dimensional bell-shaped mountain, so called "Witch of Agnesi":

$$h(x) \;=\; \frac{h_0}{1+(x\;-\;x_0)^2/l^2}\;. \tag{12}$$

Parameter h_0 is the maximum height, l is the half-width and x_0 is the location of the mountain top. Beginning with classical works by Queney, 1948, Scorer, 1949 – 1956, Long, 1953 and Alaka, 1960, a vast amount of papers is published on the modeling of two-dimensional flows over isolated topography, both linear and nonlinear, analytical and numerical content (see overviews by R. Smith 1979, and P. Baines 1995). Our examples do not represent in this respect nothing new and original. The only purpose of following is a model comparison. The use of well-documented examples is justified as it increases authenticity of the results. Due to the known analytical solutions, mountain waves are common popular objects for model tests (Laprise and Peltier 1989, Lin and Wang 1996, Hereil and Laprise 1996).

Modeling is carried out with background parameters (1) and with l, h_0 in domain: $l \in$ [10 m, 1000 km], $h_0 \in$ [10 m, 1.5 km]. The modelled field is the total entropy, defined as

$$\Theta \;=\; \Theta_0(p)\left(1\;+\;\frac{T'}{T_0}\right)\;, \tag{13a}$$

where the background profile Θ_0 is a solution of the differential equation

$$\frac{g}{\Theta_0}\frac{\mathrm{d}\Theta_0}{\mathrm{d}z} \;=\; N^2\;. \tag{13b}$$

For constant N– and H_0 (as it is assumed everywhere in this Chapter):

$$\ln[\Theta_0(p)/T_0(p_0)] \;=\; \frac{N^2}{g}\;Z \;=\; \frac{T_i}{T_0}\ln(p_0/p)\;, \tag{13c}$$

where $Z = Z(p)$ represents isobaric height in the undisturbed atmosphere. Thus,

$$\Theta(x,p) \;=\; T_0(p_0)\mathrm{e}^{N^2 z/g}[1\;+\;T'(x,p)/T_0]\;. \tag{13d}$$

Results of the modelling are represented on Fig. 4.6 – 4.16, beginning with the longest scale, $l = 1000$ km, $h_0 = 1$ km (Fig. 6a - 6b), and then continuing toward shorter scales, until $l = h_0 = 10$ m.

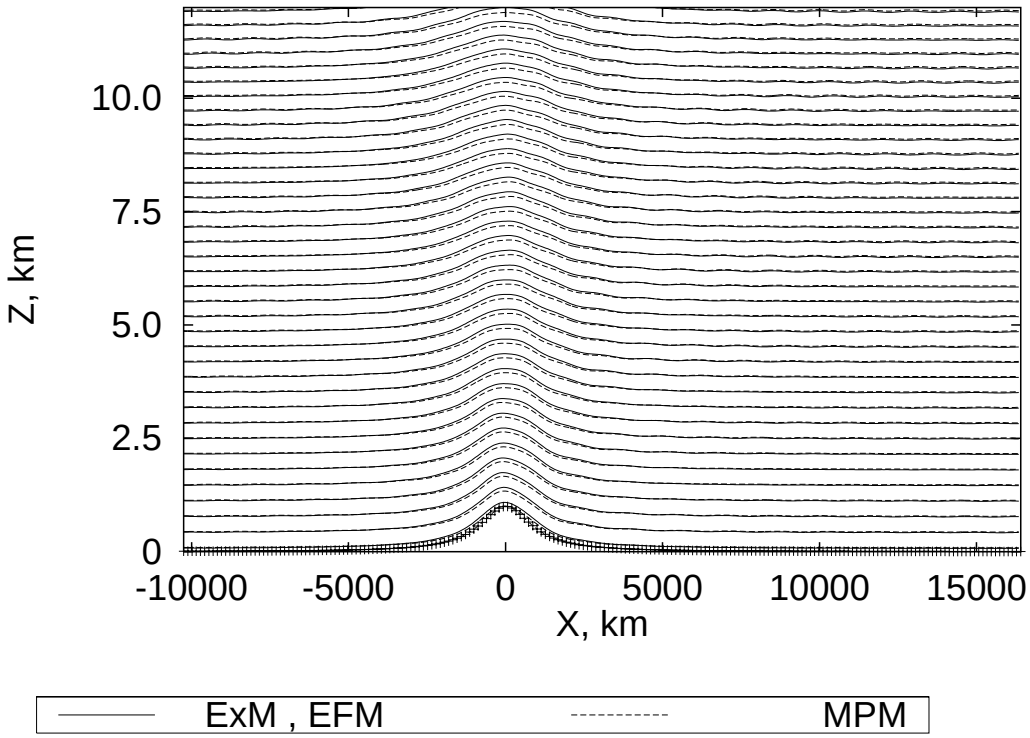

Fig. 4.6a. Very long trapped waves. $l = 1000$ km, $h_0 = 1$ km, $U = 25$ m/s, $N = 0.01$ 1/s, $\Delta\Theta = 1.0$ K. Differences are caused by different asymptotes in q. MPM isolines are slightly lower.

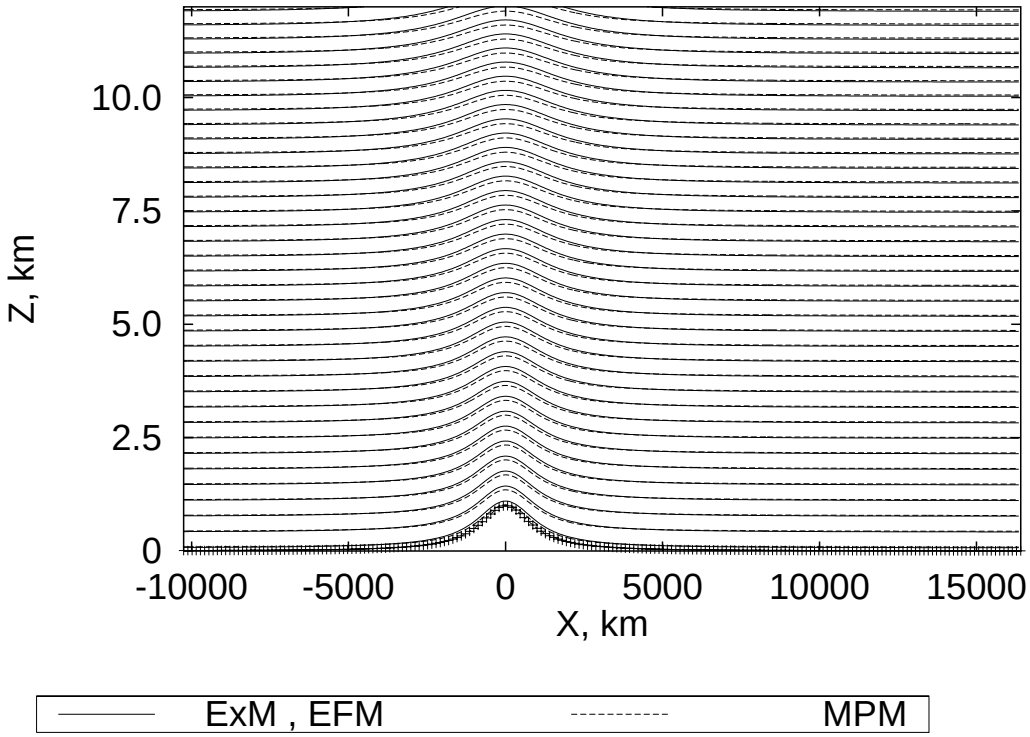

Fig. 4.6b. Same as Fig. 4.6a, except $U = 10$ m/s.

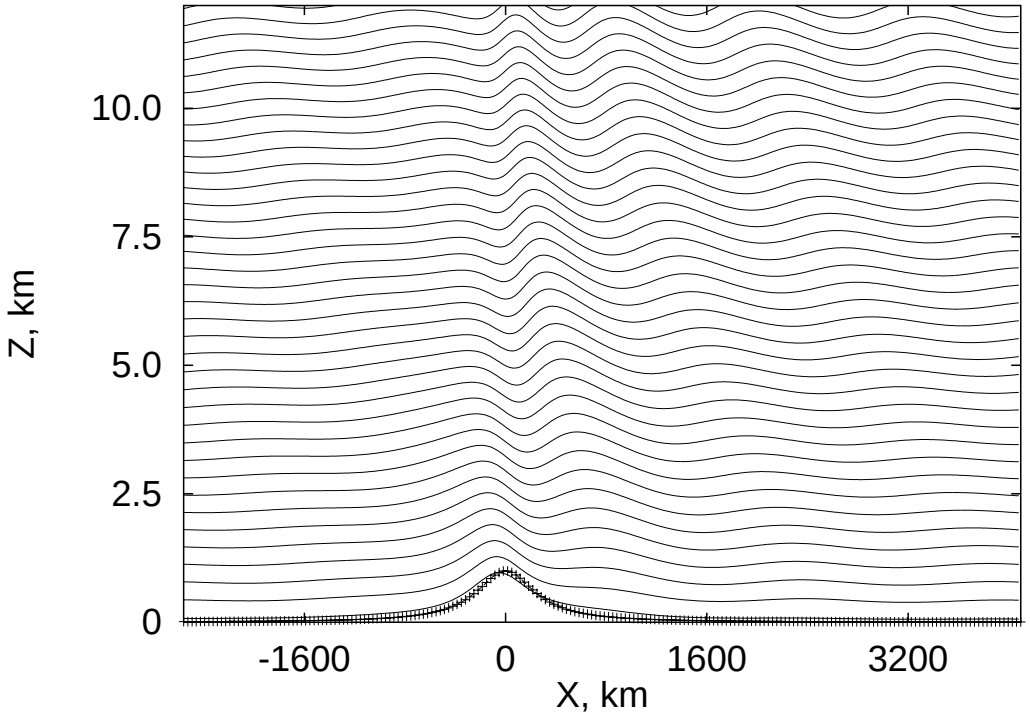

Fig. 4.7a. All models coincide. $l = 300$ km, $h_0 = 1$ km, $U = 25$ m/s, $N = 0.01$ 1/s, $\Delta\Theta = 1.0$ K.

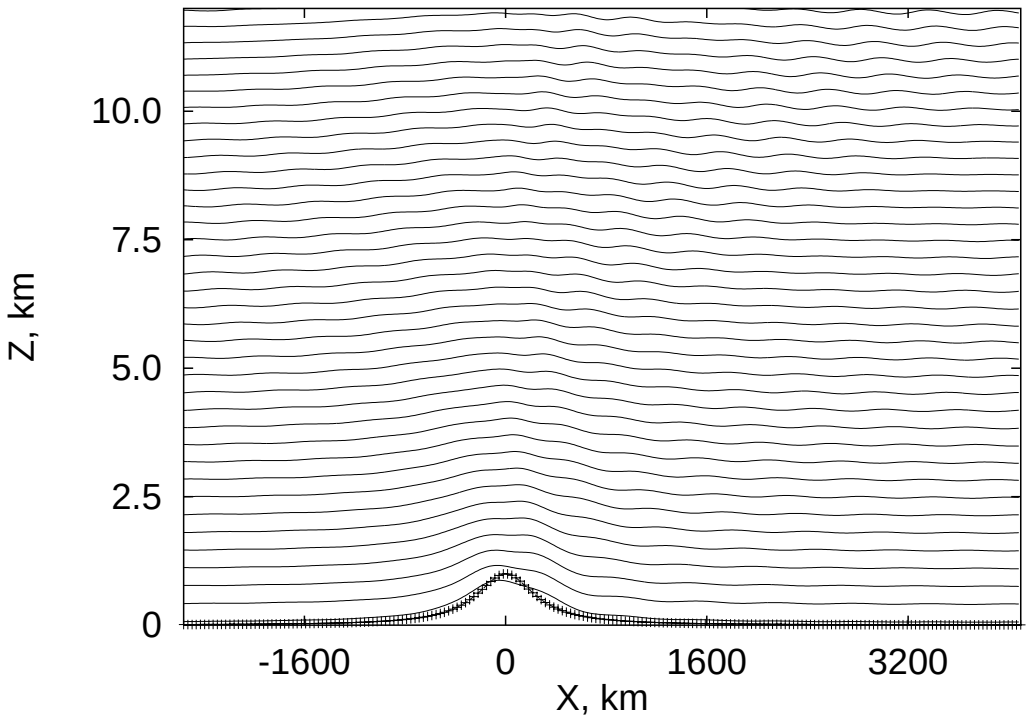

Fig. 4.7b. Same as Fig. 4.7a, except $U = 10$ m/s.

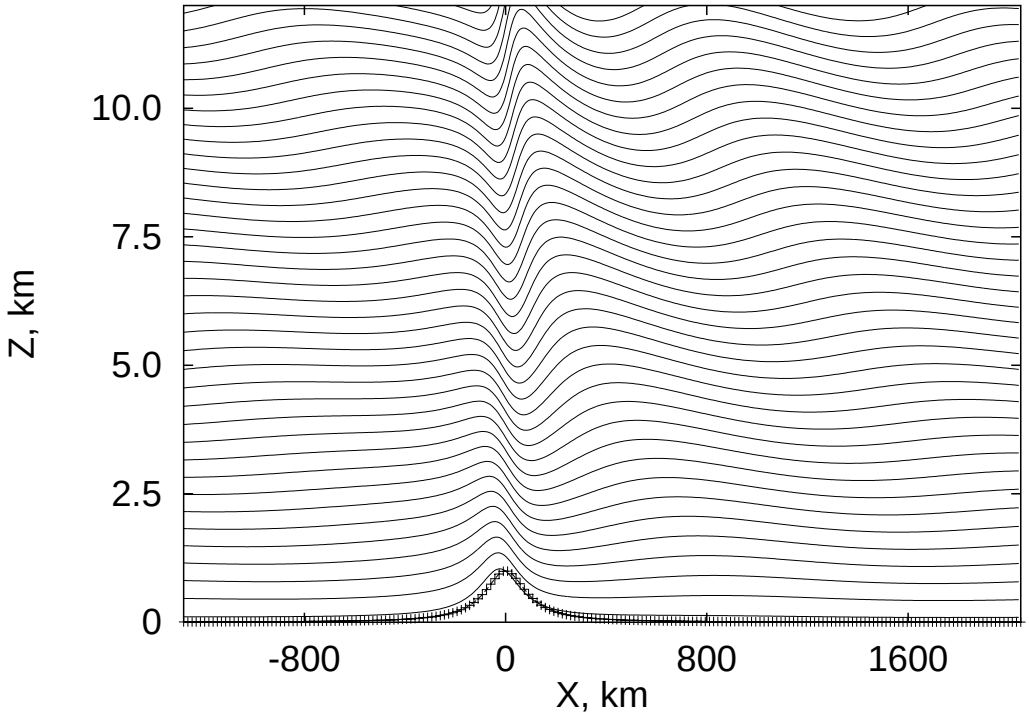

Fig. 4.8a. All models coincide. $l = 100$ km, $h_0 = 1$ km, $U = 25$ m/s, $N = 0.01$ 1/s, $\Delta\Theta = 1.0$ K.

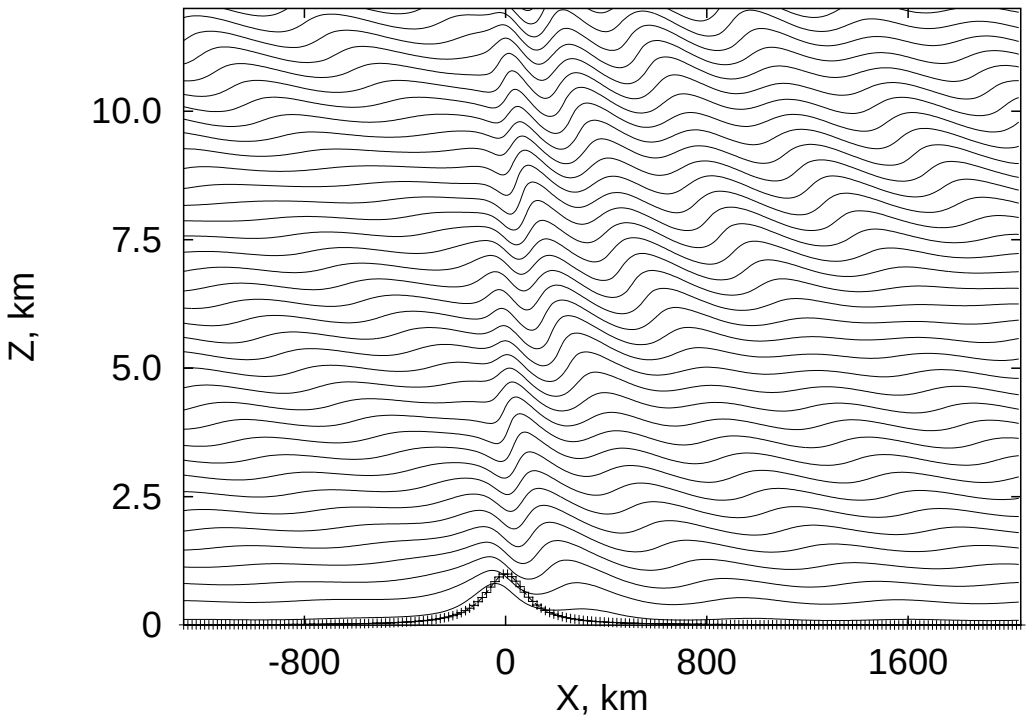

Fig. 4.8b. Same as Fig. 4.8a, except $U = 10$ m/s.

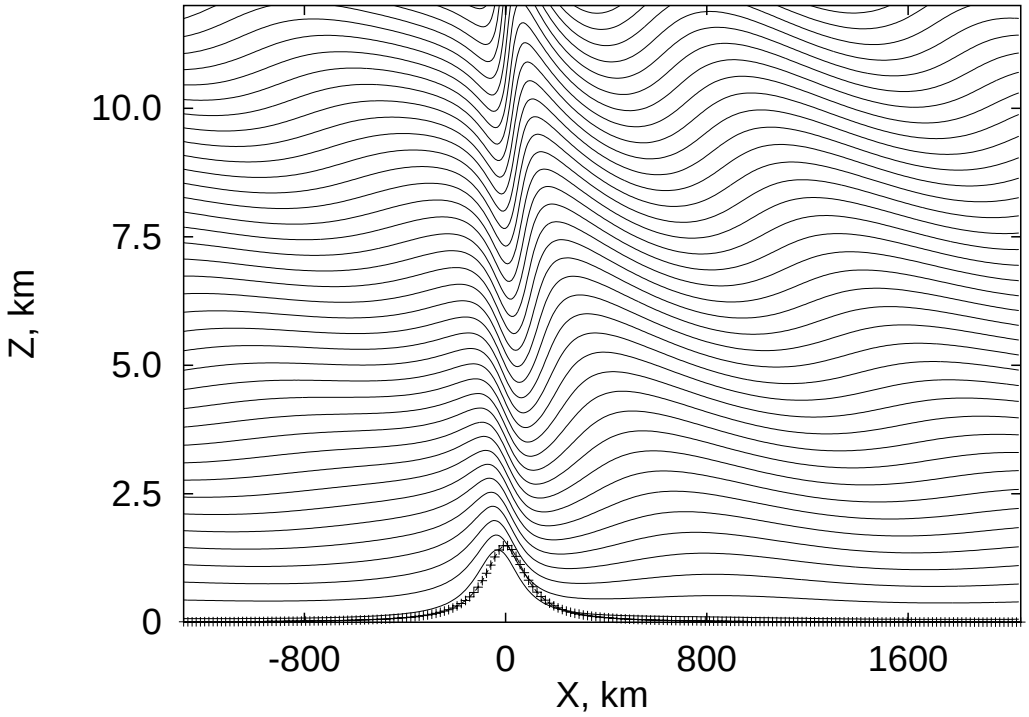

Fig. 4.8c. Same as Fig. 4.8a, except $h_0 = 1.5$ km.

Presented figures demonstrate that there is no difference in compared models in domain 30 km $< l \leq$ 1000 km. Week difference is observable for longest waves ($l = 1000$ km) between the ExM and EFM from one side, and the MPM – HSM from the other, but this difference, caused by different asymptotes of q for different two model groups, is really very small (Fig. 4.6a and 4.6b) and can be disregarded for most applications.

The first real model-branching begins at $l \leq 30$ km and this is the HSM which makes difference. At first differences are recognizable for $l = 30$ km and stronger winds ($U =$ 25 m/s) as demonstrated on Fig. 4.9a and 4.9b, but they grow rapidly with decrease of l and become significant in the upper troposphere for $l \leq 10$ km (Fig. 4.10a), and for the whole depth of the troposphere for $l \leq 3$ km (Fig. 4.11b and 4.13b). The presented examples demonstrate, that the HSM is not (even in the linear case) usable for $l \leq 10$ km.

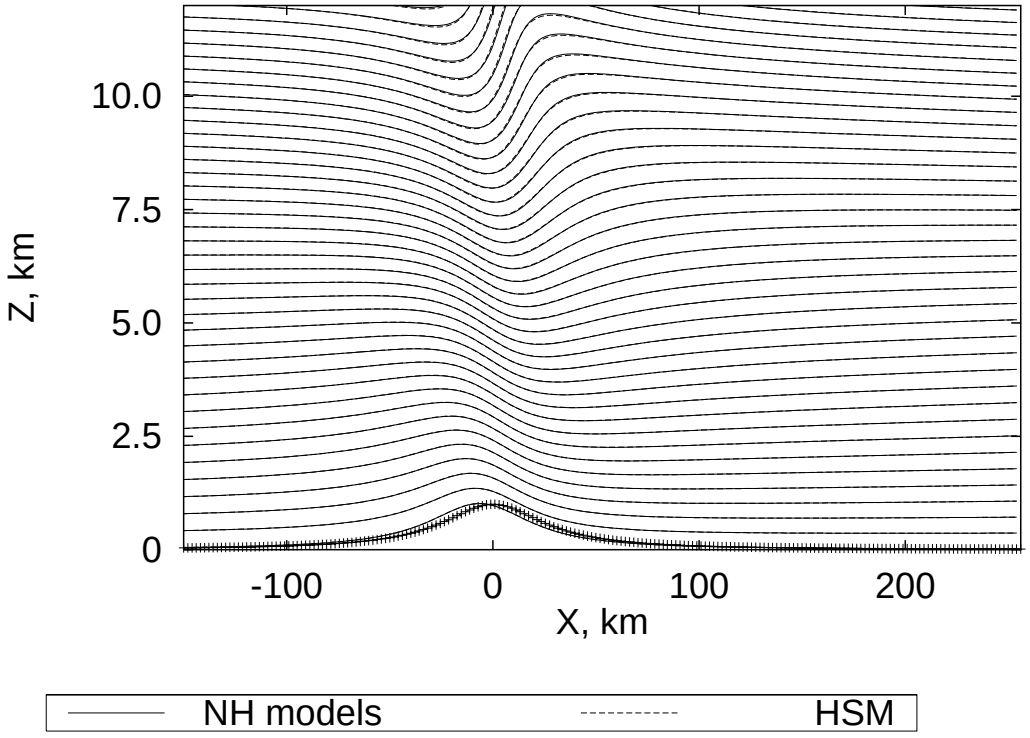

Fig. 4.9a. Comparison of the ExM and HSM. $l = 30$ km, $h_0 = 1$ km, $U = 25$ m/s, $N = 0.01$ 1/s, $\Delta\Theta = 1.0$ K.

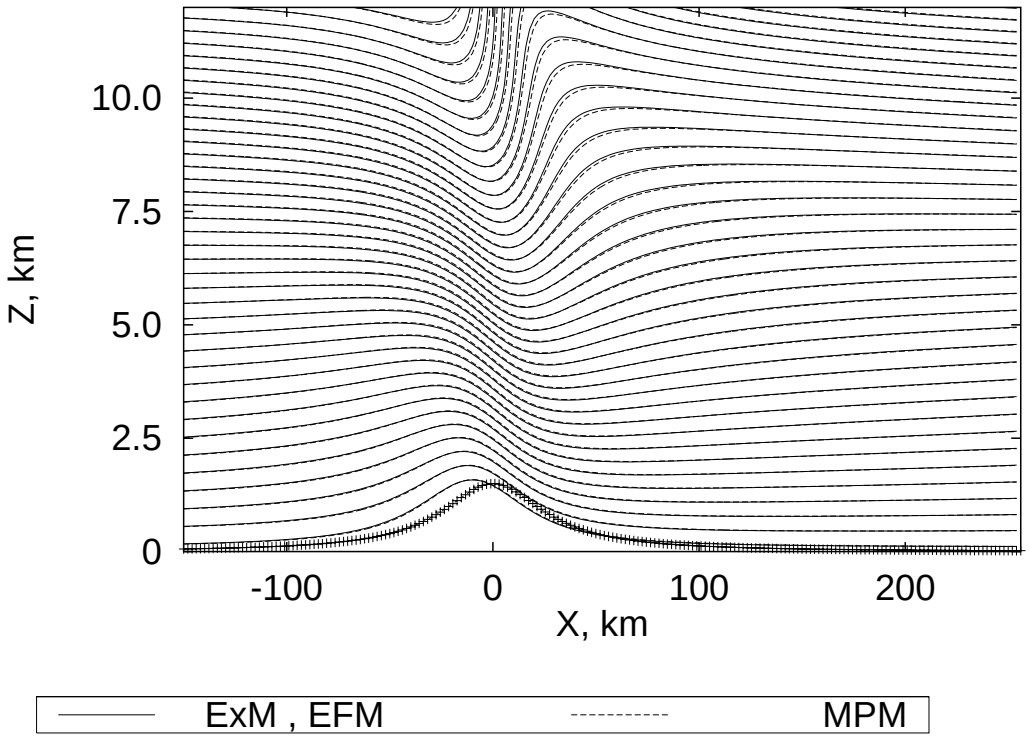

Fig. 4.9b. Different NH models. Parameters are the same as in Fig. 4.9a, except $h_0 = 1.5$ km.

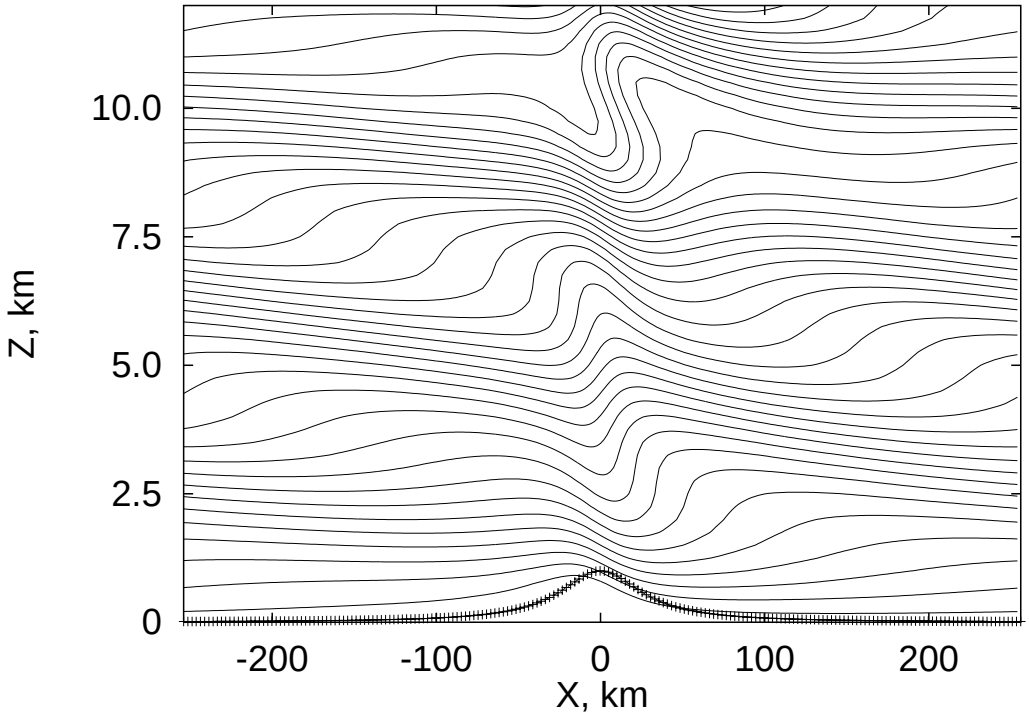

Fig. 4.9c. The same as Fig. 4.9a, except $U = 10$ m/s and $\Delta\Theta = 2.0$ K. All models (incl. the HSM) coincide with high precision.

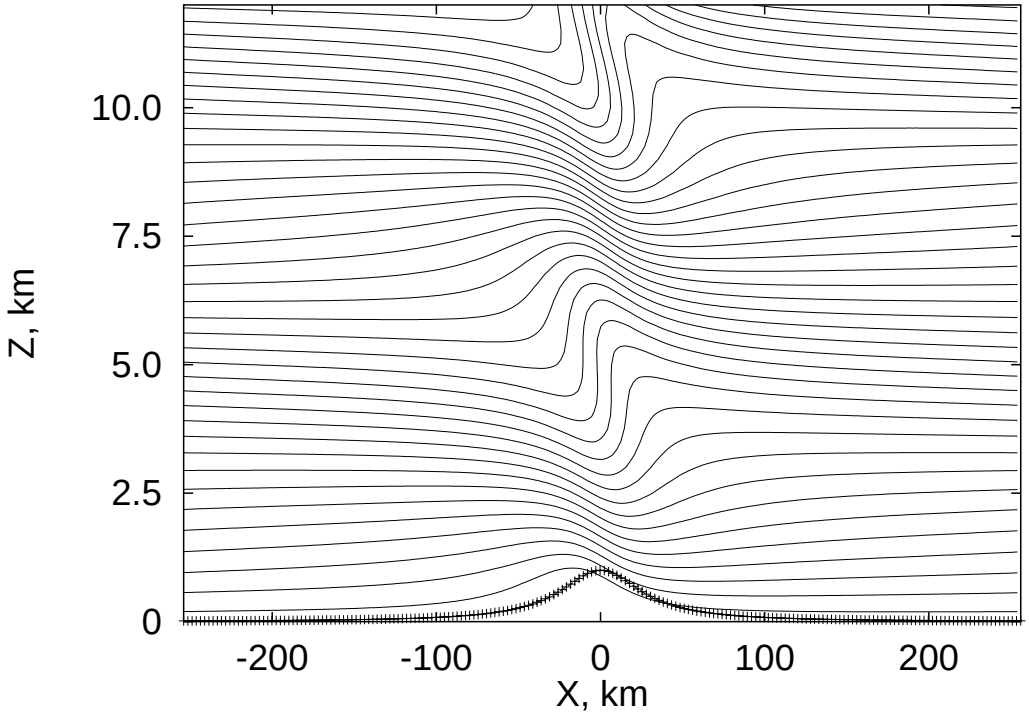

Fig. 4.9d. The same as Fig. 4.9c, except $f = 0$.

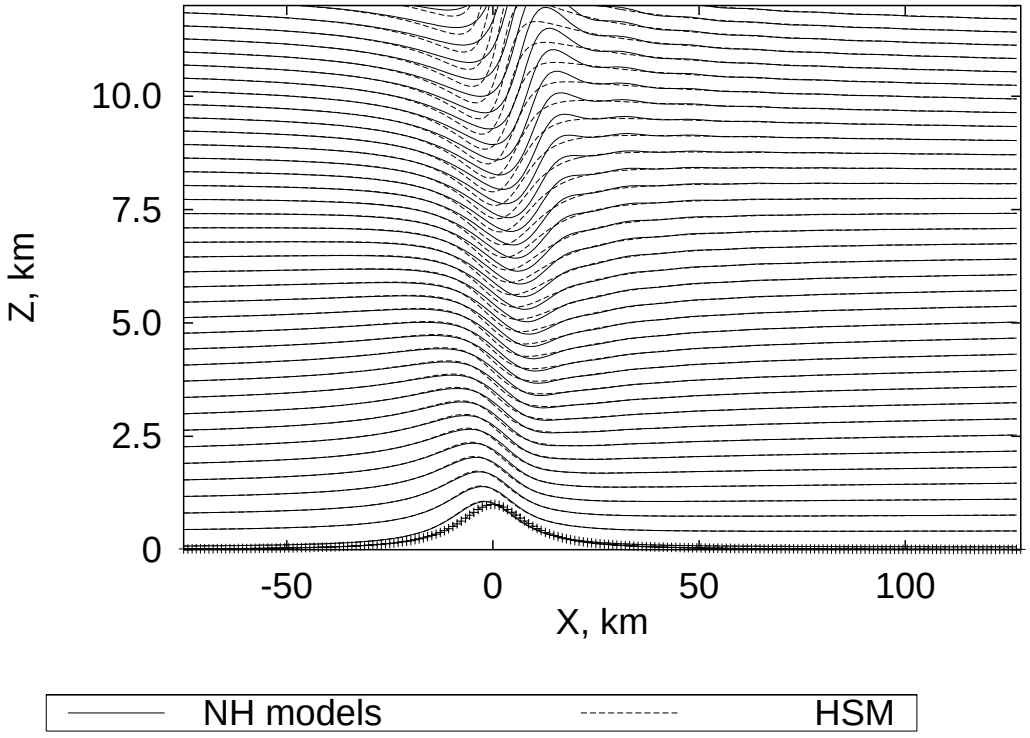

Fig. 4.10a. $l = 10$ km, $h_0 = 1$ km, $U = 25$ m/s, $N = 0.01$ 1/s, $\Delta\Theta = 1.0$ K.

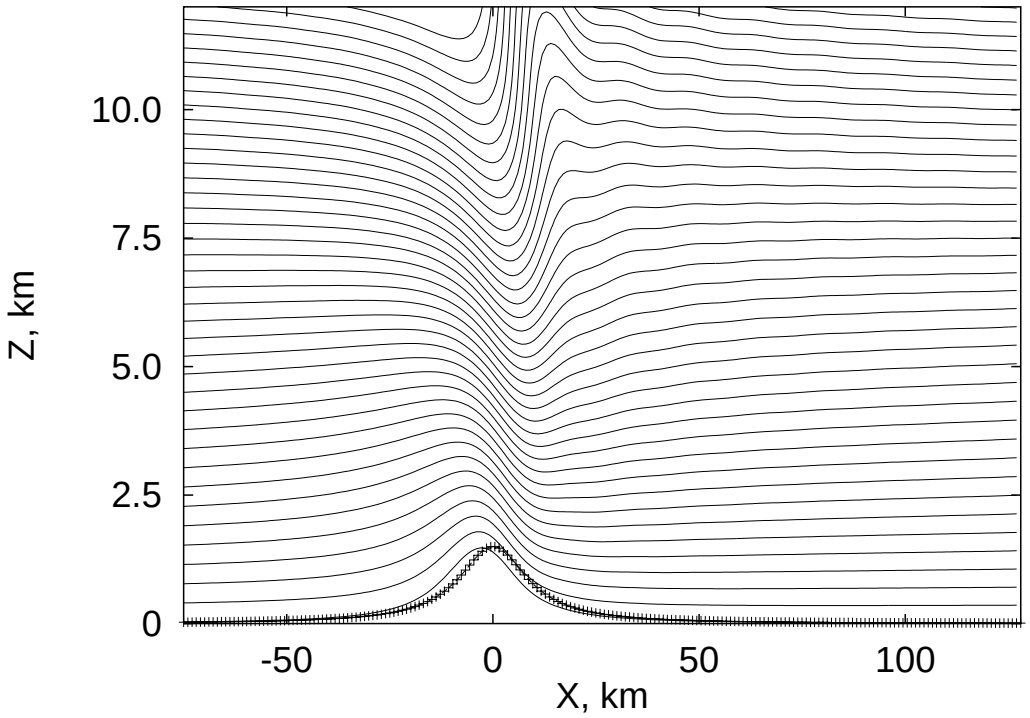

Fig. 4.10b. Exact model. EFM and MPM are very close. $h_0 = 1.5$ km, other parameters as in Fig. 10a.

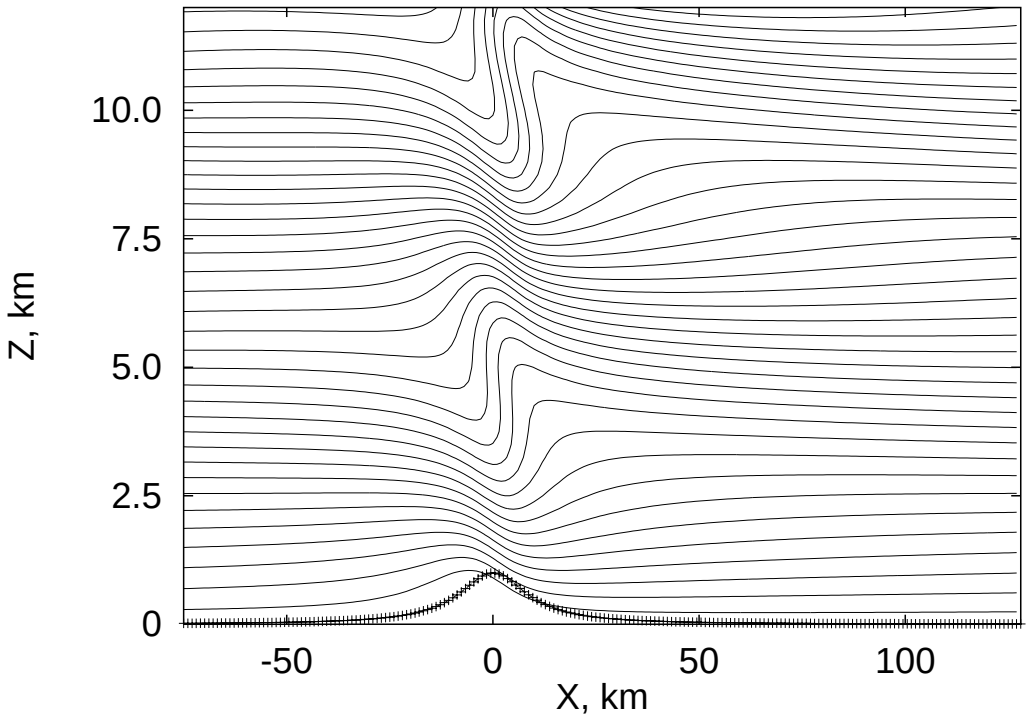

Fig. 4.10c. Exact model. EFM and MPM are very close. $U = 10$ m/s, other parameters as in Fig. 10a.

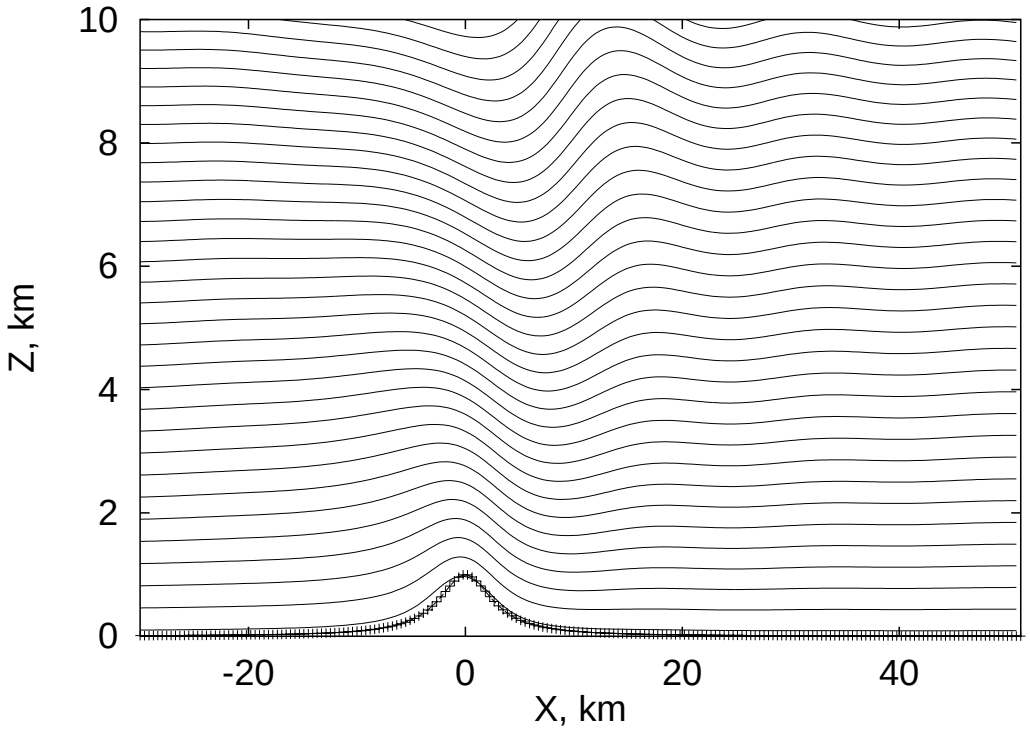

Fig. 4.11a. Model ExM. Other NH models EFM and MPM are very close to it. $l = 3$ km, $h_0 = 1$ km, $U = 25$ m/s, $N = 0.01$ 1/s, $\Delta\Theta = 1.0$ K.

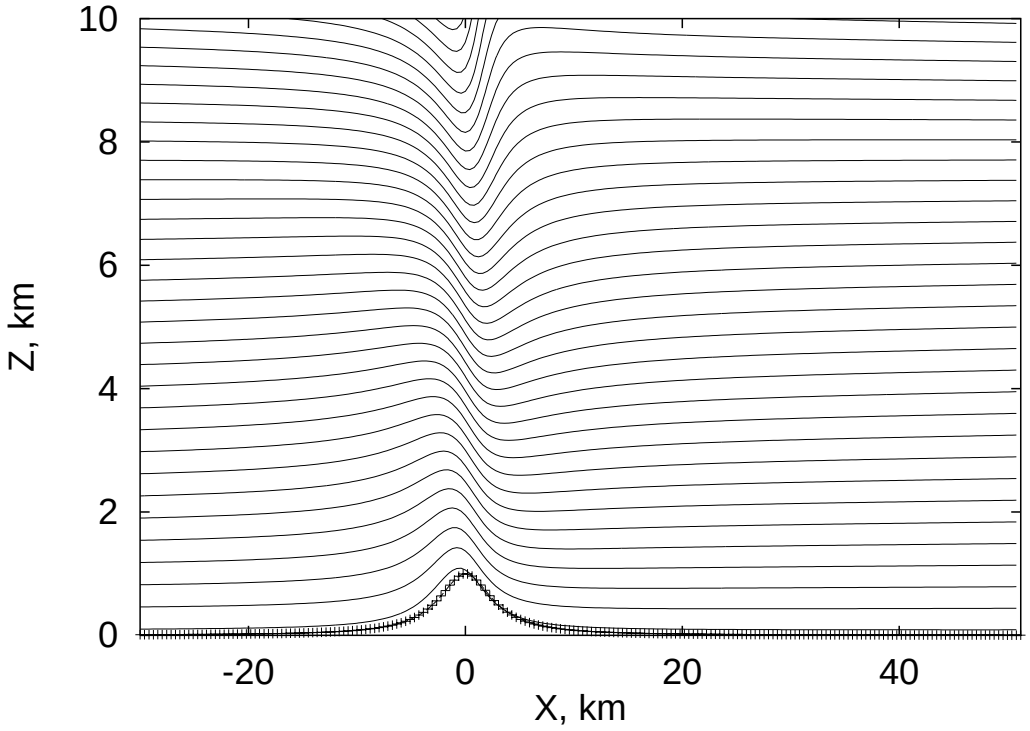

Fig. 4.11b.The model HSM in the same conditions as used in Fig. 4.11a.

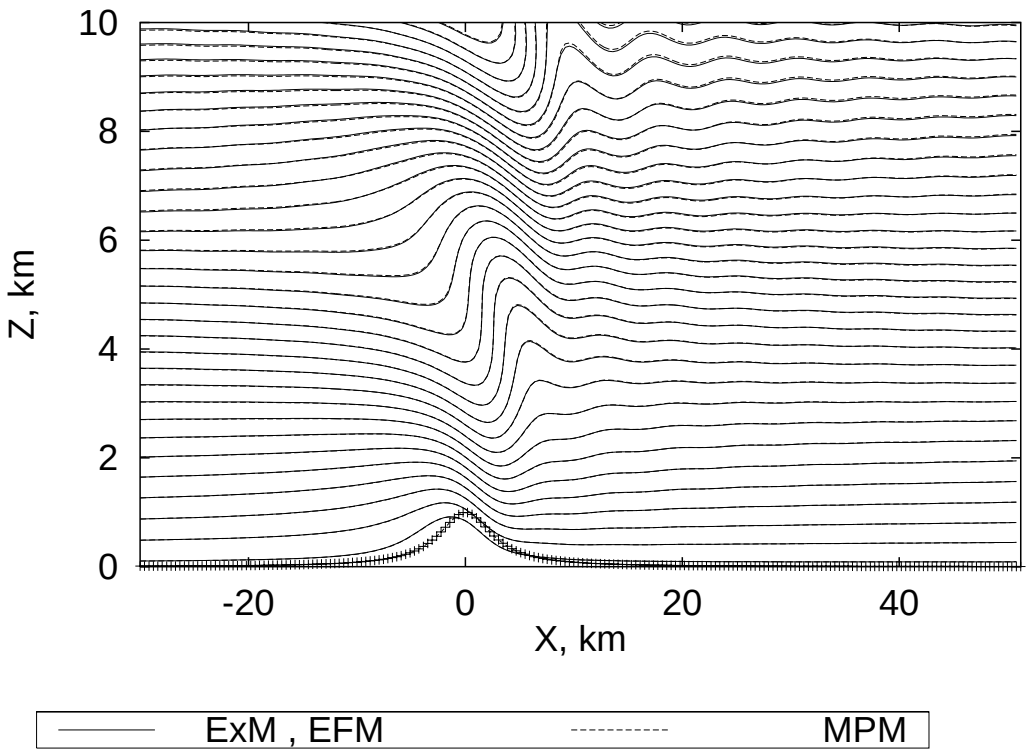

Fig. 4.11c. The same situation as in Fig. 4.11a except that $U = 10$ m/s.

In shorter mesoscale, $l \leq 3$ km, all NH models still remain close to each other (Fig. 4.11a, 11c, 12a, 12b, 13a), until at $l = 300$ m the MPM becomes differ from the ExM and EFM (Fig. 4.14a and 14b). This difference is larger for stronger wind (Fig. 4.14a) and for shorter wave-lengths (Fig. 4.15 and 16). The lower limit, where the MPM can be employed without restrictions is $l \geq 200 - 300$ m. At the half-width $l = 100$ m its difference from the ExM is quite significant, if the wind is strong (Fig. 4.15a), but still moderate for weaker wind (Fig. 4.15b).

Thus, the shorter orographic scale, where the MPM is still relevant, is ~ 100 m. Below that ultimate limit only the EFM remains valid among filtered pressure-space models. In the atmosphere, this is the domain of micro-turbulence. To this domain belong, besides the modelled orographic waves, flows in vicinity of small obstacles like houses, towers, trees, bridges etc., and turbulent processes in the lower 50 - 100 m part of the planetary boundary layer.

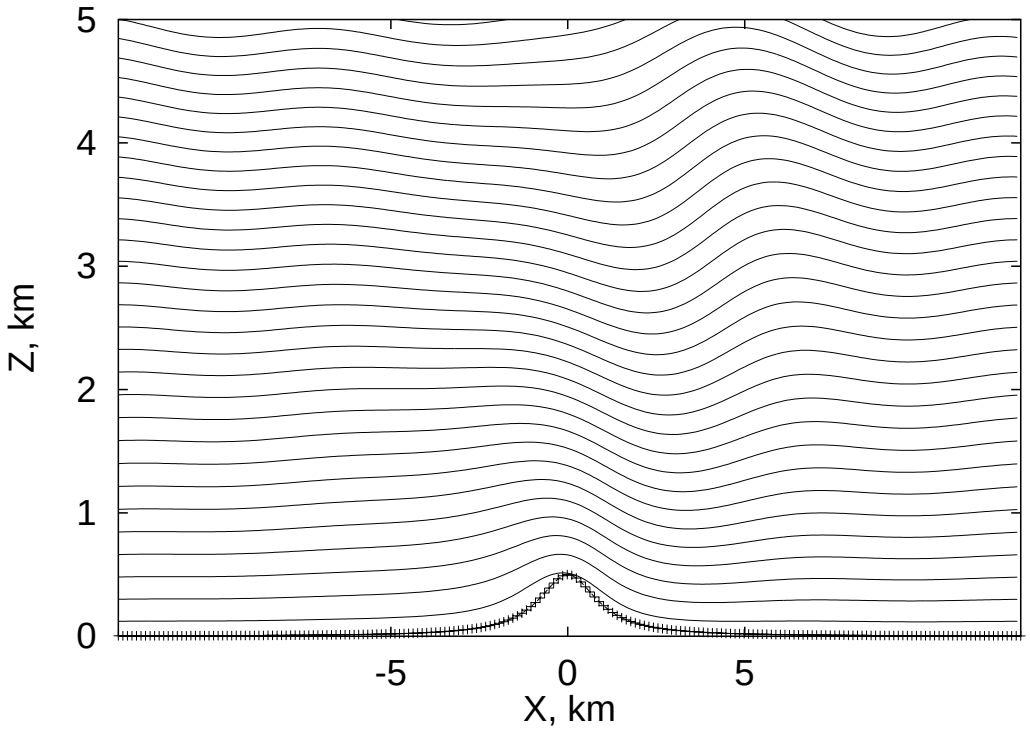

Fig. 4.12a. All NH models. $l = 1$ km, $h_0 = 500$ m, $U = 10$ m/s, $N = 0.01$ 1/s, $\Delta\Theta = 0.5$ K.

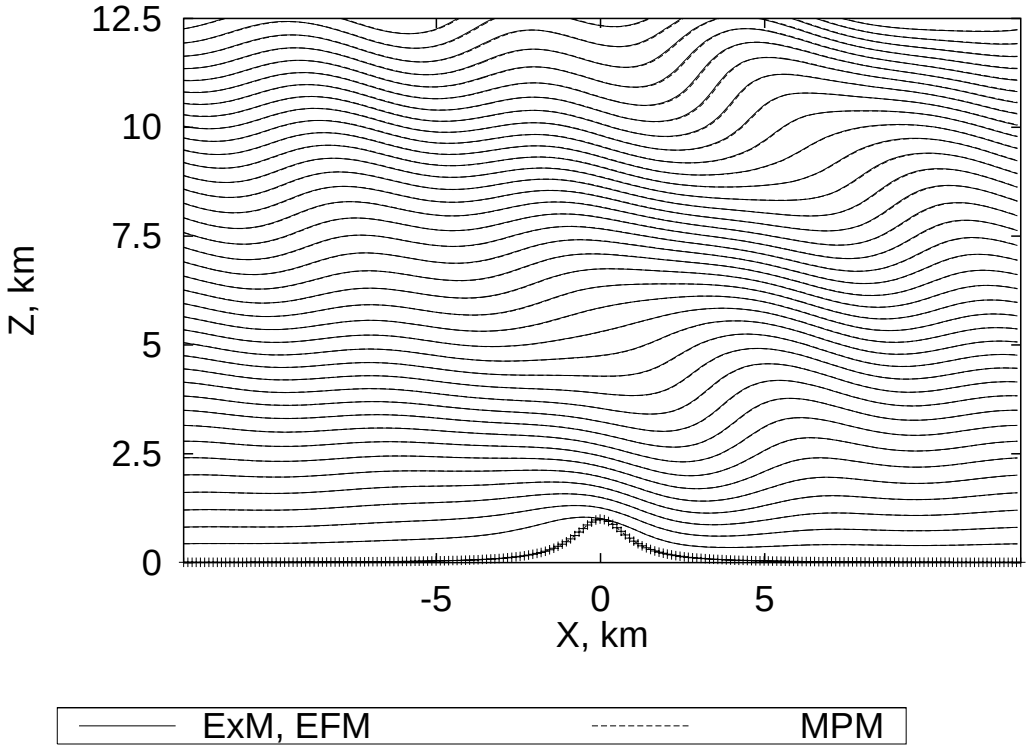

Fig. 4.12b.The same as Fig. 4.12a, except that $h_0 = 1$ km.

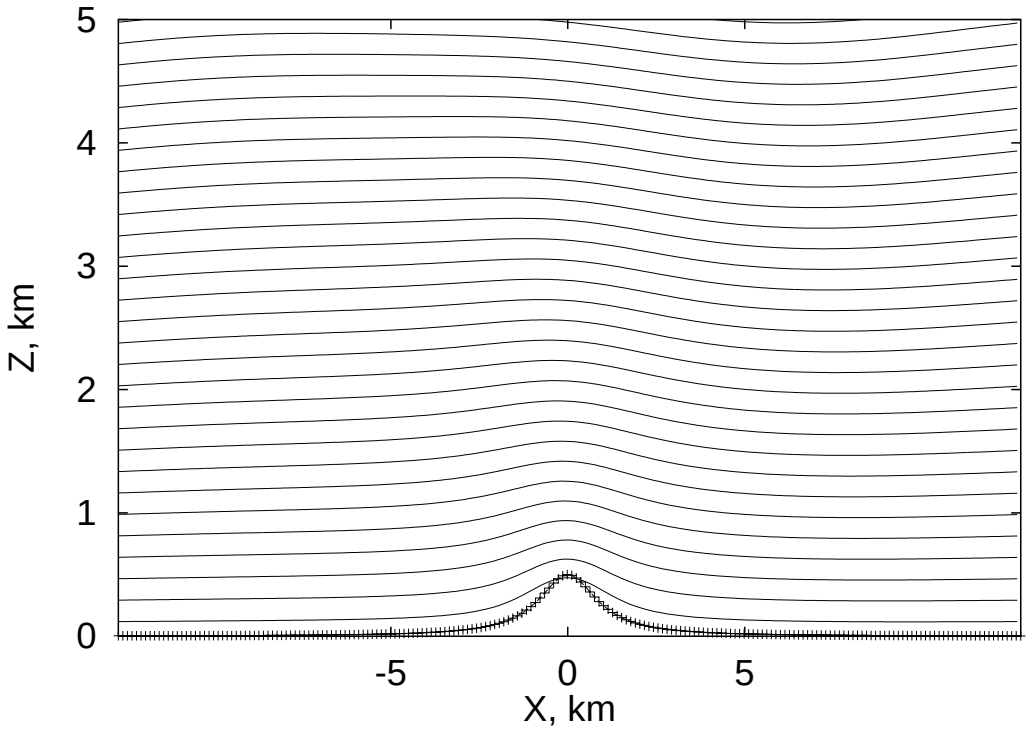

Fig. 4.13a. NH models (EXM, EFM and MPM). $l = 1$ km, $h_0 = 500$ m, $U = 25$ m/s, $N = 0.01$ 1/s, $\Delta\Theta = 0.5$ K.

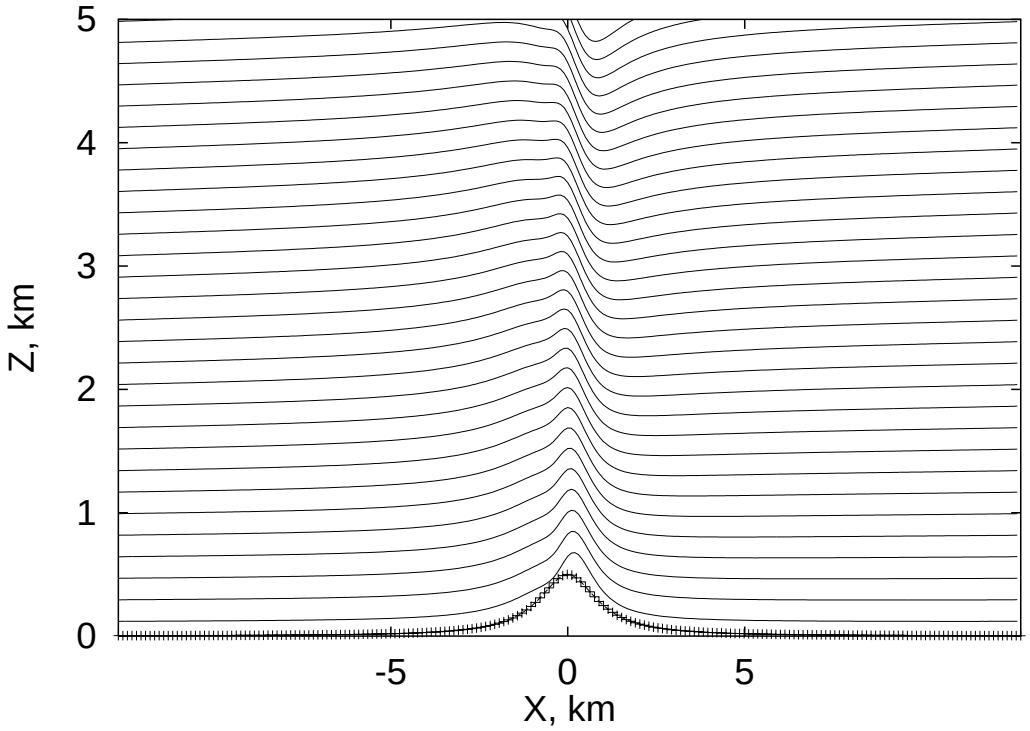

Fig. 4.13b. HSM for the same situation.

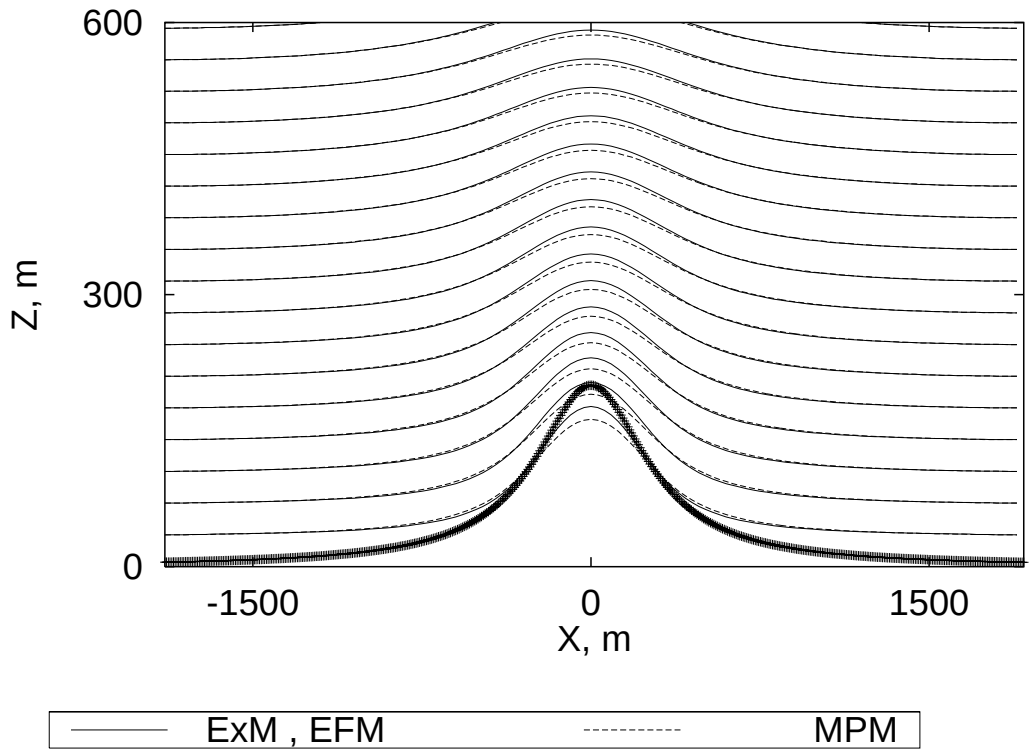

Fig. 4.14a. $l = 300$ m, $h_0 = 200$ m, $U = 25$ m/s, $N = 0.01$ 1/s, $\Delta\Theta = 0.1$ K.

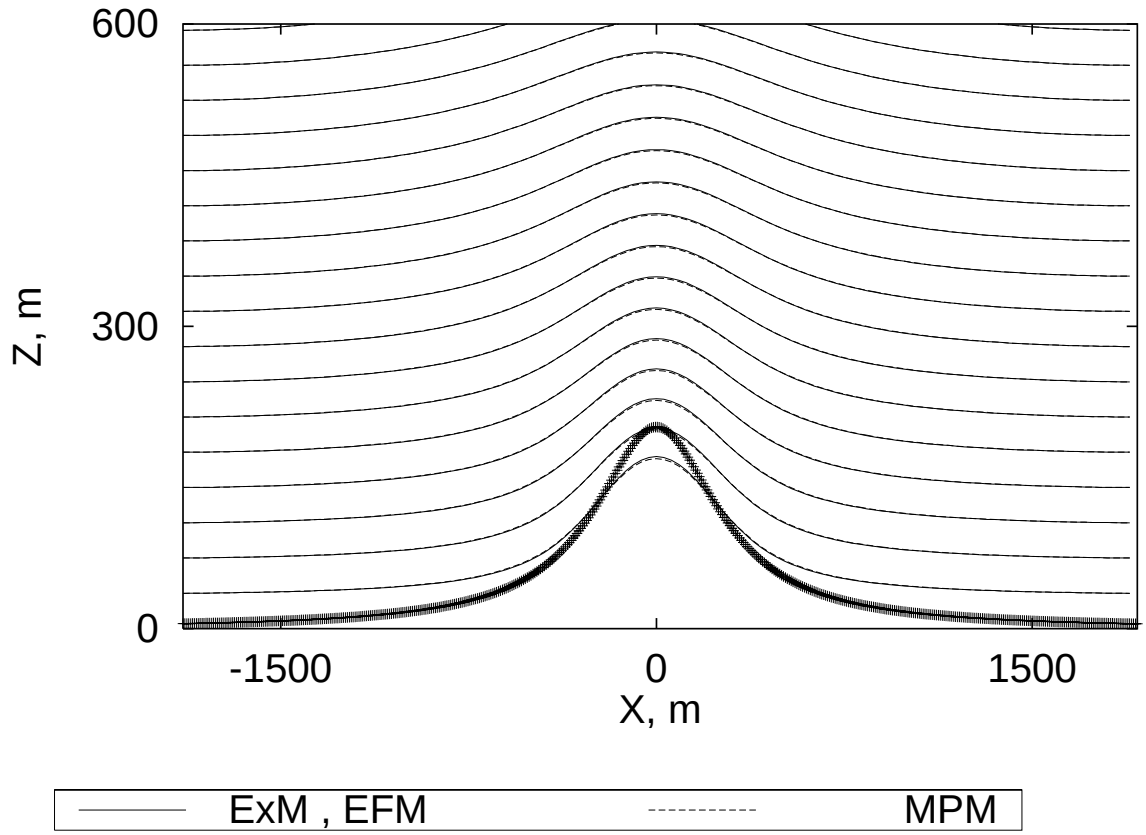

Fig. 4.14b. The same as Fig. 4.14a, except $U = 10$ m/s.

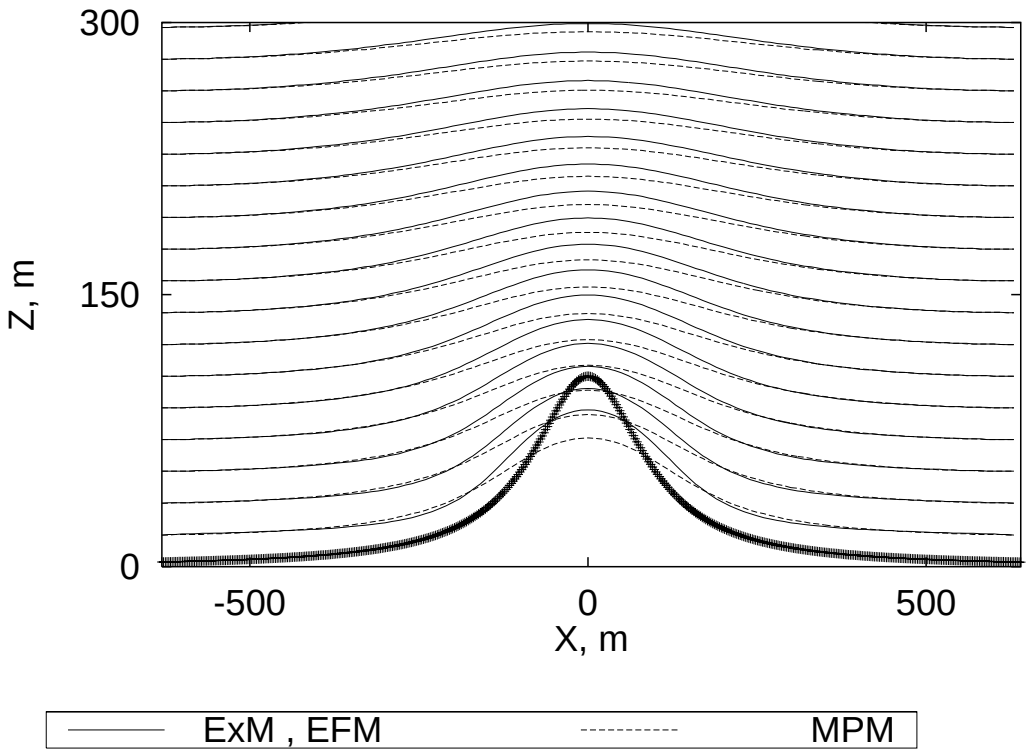

Fig. 4.15a. $l = 100$ m, $h_0 = 100$ m, $U = 25$ m/s, $N = 0.01$ 1/s, $\Delta\Theta = 0.05$ K.

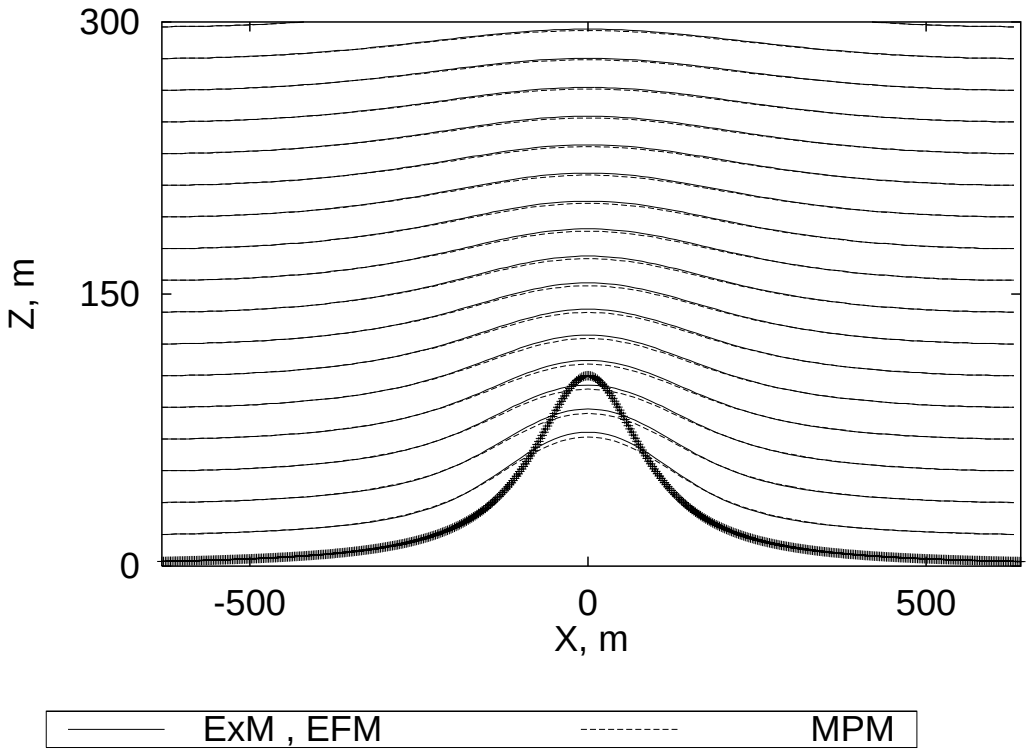

Fig. 4.15b. Same as Fig. 4.15a, except $U = 10$ m/s.

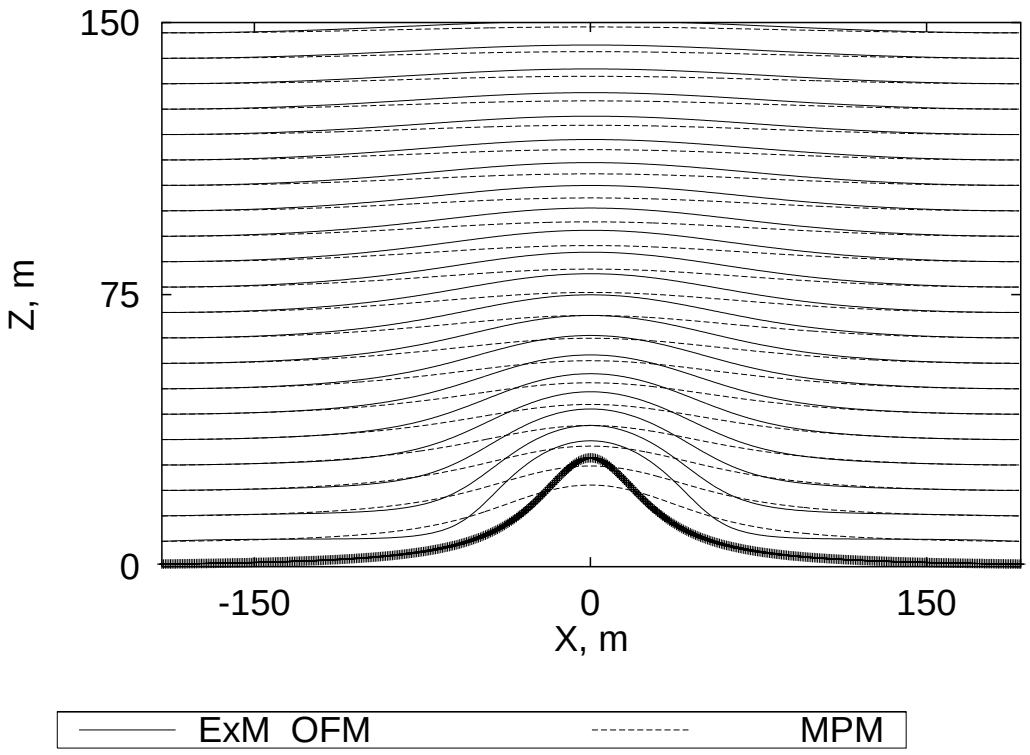

Fig. 4.16a. Domain, where the MPM cannot be employed: $l = 30$ m, $h_0 = 30$ m. $U = 25$ m/s, $N = 0.01$ 1/s, $\Delta\Theta = 0.02$ K.

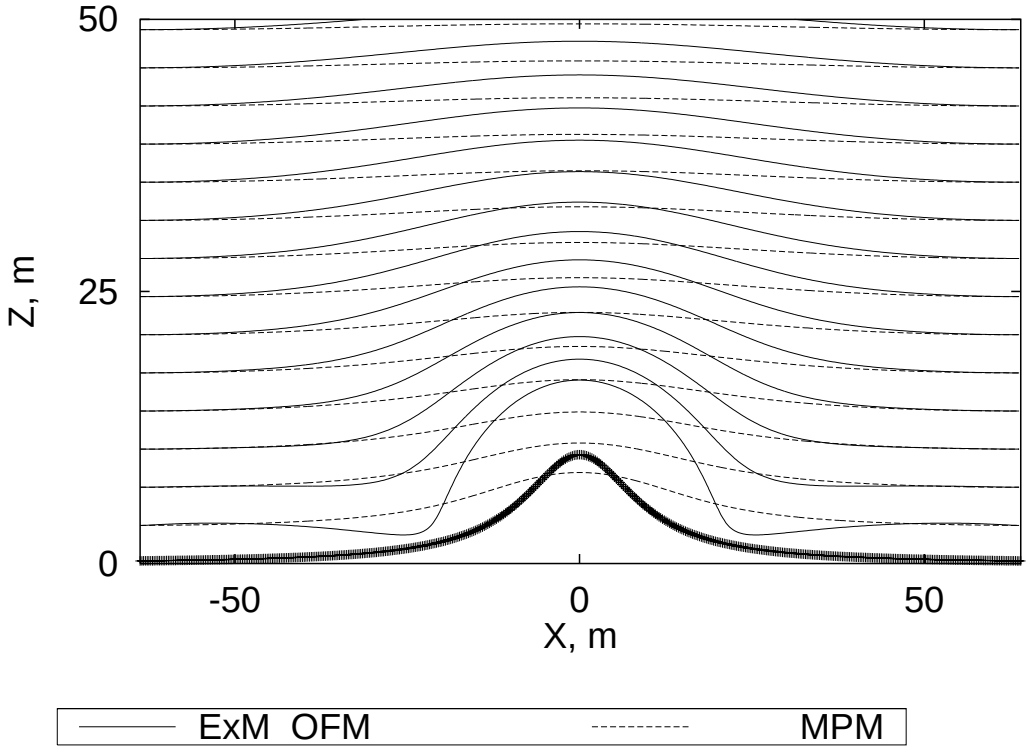

Fig. 4.16b. Domain, where the MPM cannot be employed: $l = 10$ m, $h_0 = 10$ m. ($U = 25$ m/s, $N = 0.01$ 1/s, $\Delta\Theta = 0.01$ K)

CHAPTER FIVE

Nonlinear models in sigma-coordinates

The aim of this chapter is to represent the described in the Chapter 1 different NH, nonlinear, p-space equations in a form, convenient for numerical integration. For that (1), the equations are projected into sigma-coordinate frame (sections 1 – 3), and (2), the Poisson equation for the nonhydrostatic geopotential is deduced (section 4) along with detailed analysis of boundary conditions (section 5) and iterative schemes of solution (section 6).

5.1. General equations in σ–coordinates

The general idea, on which all numerical algorithms ground in the pressure-space, is the use of terrain–following sigma- (or generalized sigma-) coordinates. This representation is used in different forms in all hydrostatic general circulation models (for instance the ECMWF model, see Simmons and Burridge 1981), and limited area models, like the HIRLAM (HIRLAM Documentation Manual 1996). In nonhydrostatic version it is described at first for the MPM by Miller and White, 1984, and used in numerical realization of the MPM by Xue and Thorpe 1991, Miranda 1991, and Miranda and James 1992.

For the exact nonfiltered model the sigma-representation is described first by Rõõm, 1989. In this section the σ-coordinate representation for the general non-filtered model (the ExM) (1.3) is developed. The representation includes the exact equation for the lower boundary evolution in the p–space.

Let us define the sigma–coordinate

$$\sigma \;=\; \frac{p}{p_0}\;, \tag{1}$$

which introduces the (non-dimensional for the convenience) density in the σ–space

$$n_\sigma \;=\; \frac{p_0}{a} n\;, \tag{2}$$

where a is the standard sea-level pressure.

Transformation from p- to σ coordinates performs with the help of formulae (whish are of the same shape disregarding whether the model is hydrostatic or non-hydrostatic one)

$$\frac{\partial}{\partial p} \;=\; \frac{1}{p_0}\frac{\partial}{\partial \sigma}\;, \quad \nabla_p \;=\; \nabla_\sigma \;-\; \frac{\nabla p_0}{p_0}\sigma\frac{\partial}{\partial \sigma}\;. \tag{3a}$$

For compactness of notation it is reasonable to introduce operators in the σ coordinates

$$\hat{S} \;=\; s\frac{\partial}{\partial\sigma}\;, \quad \hat{S}^{+} \;=\; \frac{\partial}{\partial\sigma}s\;, \quad s \;=\; s(\mathbf{x},\;\sigma,\;t) \;=\; \sigma/H\;, \tag{3b}$$

$$\hat{\mathbf{G}} \;=\; \nabla_\sigma \;-\; \frac{\nabla p_0}{p_0}\sigma\frac{\partial}{\partial\sigma}\;, \quad \hat{\mathbf{G}}^{+} \;=\; \nabla_\sigma \;-\; \frac{\nabla p_0}{p_0}\frac{\partial}{\partial\sigma}\sigma\;. \tag{3c}$$

These operators will be used in full extent in filtered models, here we make use of $\hat{\mathbf{G}}$, which coincides with ∇_p in σ-representation.

General equations (1.3) in σ-coordinates are

$$\frac{\mathrm{d}z}{\mathrm{d}t} \;=\; w \tag{4a}$$

$$n\;\frac{\mathrm{d}w}{\mathrm{d}t} \;=\; g(1\;-\;n)\;, \tag{4b}$$

$$n\;\frac{\mathrm{d}\mathbf{v}}{\mathrm{d}t} \;=\; -\,g\hat{\mathbf{G}}z \;-\; nf\hat{\mathbf{z}}\times\mathbf{v}\;, \tag{4c}$$

$$\frac{\mathrm{d}T}{\mathrm{d}t} \;=\; \frac{RT}{c_p}\left(\frac{\dot{\sigma}}{\sigma} \;+\; \frac{\dot{p}_0}{p_0}\right) \;+\; Q\;, \tag{4d}$$

$$\frac{\mathrm{d}n_\sigma}{\mathrm{d}t} \;=\; -\;n_\sigma\left(\nabla_\sigma\cdot\mathbf{v} \;+\; \frac{\partial\dot{\sigma}}{\partial\sigma}\right) \tag{4e}$$

$$n \;=\; -\;\hat{S}z\;. \tag{4f}$$

We have maintained the pressure-space density n (which can be expressed at the need via n_σ) as the primary measure of the compressibility of medium. The continuity equation (4e) is postulated. Sigma-velocity is defined as

$$\dot{\sigma} \;=\; \frac{\mathrm{d}\sigma}{\mathrm{d}t}\;, \tag{5a}$$

and in accordance with this definition the Lagrangian derivative is

$$\frac{\mathrm{d}}{\mathrm{d}t} \;=\; \frac{\partial}{\partial t} \;+\; \mathbf{v}\nabla_\sigma \;+\; \dot{\sigma}\frac{\partial}{\partial\sigma}\;. \tag{5b}.$$

For the right side of temperature equation (4d) the formula

$$\frac{\omega}{p} \;=\; \frac{\dot{\sigma}}{\sigma} \;+\; \frac{\dot{p}_0}{p_0} \tag{5c}$$

is used. $\dot{p}_0$ corresponds to level σ in the sense it represents the rate of change of the ground surface pressure in a point on the ground which moves in horizontal direction with the same speed as the material particle at level σ:

$$\dot{p}_0 \;=\; \left(\frac{\mathrm{d}p_0}{\mathrm{d}t}\right)_\sigma \;=\; \frac{\partial p_0}{\partial t} \;+\; \mathbf{v}|_\sigma\nabla p_0\;.$$

Though the continuity equation (4e) is postulated, it can be deduced from (1.3d) using definition (2), formulae (3a), (5) and identity

$$\frac{\nabla p_0}{p_0} \cdot \frac{\partial \mathbf{v}}{\partial \sigma} \;=\; \frac{1}{p_0} \frac{\partial \dot{p}_0}{\partial \sigma} \;.$$

For determination of $\dot{\sigma}$ and p_0 it is necessary to use the omega-equation (1.6) which in sigma-coordinates reads as

$$\alpha \, \frac{\omega}{p} \;-\; \frac{Q}{T} \;=\; \frac{\sigma}{H} \left(\frac{\partial w}{\partial \sigma} \;-\; \frac{\partial \mathbf{v}}{\partial \sigma} \cdot \hat{\mathbf{G}} z \right) \;-\; \hat{\mathbf{G}} \cdot \mathbf{v} \;. \tag{6}$$

After ω is determined from this relation, (5c) yields with the help of condition

$$\dot{\sigma}|_1 \;=\; 0 \tag{7a}$$

a prognostic equation for p_0:

$$(\dot{p}_0)_1 \;=\; \omega|_1 \;. \tag{7b}$$

Finally, $\dot{p}_0$ at level σ can be determined using

$$\dot{p}_0 \;=\; (\dot{p}_0)_1 \;+\; (\mathbf{v}_\sigma \;-\; \mathbf{v}_1) \, \nabla p_0 \tag{7c}$$

and $\dot{\sigma}$ using (5c).

Equation (7b) along with relation (6) at the lower boundary p_0 is one of the basic dynamical (evolutionary) equations. It rules the evolution of the lower free boundary surface which atmosphere has in the p-space. Slow asymptotes of this equation should be the hydrostatic ground surface pressure equation, postulated in the HSM:

$$\frac{\partial p_0}{\partial t} \;+\; \nabla \cdot \left(p_0 \int_0^1 \mathbf{v} d\sigma \right) \;=\; 0 \;, \tag{8a}$$

and its acoustically filtered analogue

$$\nabla \cdot \left(p_0 \int_0^1 \mathbf{v} d\sigma \right) \;=\; 0 \;. \tag{8b}$$

The detailed and careful study whether and when (7b) transforms to equations (8), presents a special topic of investigation, which is of great interest for synoptic and planetary scale dynamics. In shorter synoptical and mesoscale domains fluctuations of p_0 are very small and have no relevance for dynamics. Thus, in forthcoming study we will disregard p_0 fluctuations and assume that the domain in the p–space is the fixed one.

5.2. MPM in σ-coordinates Most of the MPM equations in σ–coordinates can be deduced straight either from (4) or from (1.12). Combination of (1.12b) and (5c) yields

$$\frac{\tilde{w}}{H} \;=\; -\, \frac{\dot{\sigma}}{\sigma} \;-\; \frac{\dot{p}_0}{p_0} \;. \tag{9a}$$

Equations (1.12c) and (1.12d) transform to

$$\frac{\mathrm{d}\tilde{w}}{\mathrm{d}t} \;=\; g\left(1 \;+\; \hat{S}z\right) \;, \tag{9b}$$

$$\frac{\mathrm{d}\mathbf{v}}{\mathrm{d}t} \;=\; -\,g\hat{\mathbf{G}}z \;-\; f\hat{\mathbf{z}}\times\mathbf{v} \;, \tag{9c}$$

temperature equation (1.12e) does not change at all:

$$\frac{\mathrm{d}T}{\mathrm{d}t} \;=\; -\frac{g}{c_p}\tilde{w} \;+\; Q \;. \tag{9d}$$

Continuity equation (1.12a), which represents diagnostical equation for z, reads as

$$\hat{\mathbf{G}}^{+}\cdot(p_0\mathbf{v}) \;-\; \hat{S}^{+}(p_0\tilde{w}) \;=\; 0 \;, \tag{9e}$$

Most notable changes take place with the ground surface pressure equation. Equation (9a) along with condition (7a) yields

$$(\dot{p}_0)_1 \;=\; -\;\left(\frac{p_0}{H}\tilde{w}\right)_1 \;. \tag{10a}$$

it is reasonable to study separately the slipping and non-slipping ground surface. In the case of non-slipping ground all components of velocity are zero at the surface and (10a) yields

$$(\dot{p}_0)_1 \;=\; \left(\frac{\partial p_0}{\partial t}\right)_1 \;=\; 0 \;. \tag{10b}$$

For slipping boundary only the component of the velocity, orthogonal to the surface, is absent, which yields

$$\tilde{w}|_1 \;=\; \frac{\mathrm{d}h}{\mathrm{d}t}$$

and (10a) becomes

$$(\dot{p}_0)_1 \;=\; -\;\left(\frac{p_0}{H}\right)_1\frac{\mathrm{d}h}{\mathrm{d}t} \;=\; -\;\left(\frac{p_0}{H}\mathbf{v}\right)_1\cdot\nabla h \;. \tag{10c}$$

This is an exact relation, enabling the computation of the ground surface pressure tendency at every instant

$$\frac{\partial p_0}{\partial t} \;=\; -\,\mathbf{v}_1\cdot\nabla p_0 \;-\; \left(\frac{p_0}{H}\mathbf{v}\right)_1\cdot\nabla h \;. \tag{10c$'$}$$

Because the ground surface pressure fluctuations and temperature fluctuations at the ground are always small, H can be approximated in (10c) with high efficiency with H_*:

$$H_*(\mathbf{x},\sigma) \;=\; H_0(p_0\sigma) \;, \tag{11}$$

where $H_0(p)$ is a horizontally homogeneous background height-scale. Then

$$(\dot{p}_0)_1 \;=\; -\left(\frac{p_0}{H_*}\right)_1 \frac{\mathrm{d}h}{\mathrm{d}t}\;. \tag{12a}$$

This equation has a solution

$$p_0 \;=\; a\mathrm{e}^{-\int_0^h \frac{dz}{H_0}}\;, \tag{12b}$$

Which means

$$p_0 \;=\; \overline{p_0}\;, \quad \frac{\partial p_0}{\partial t} \;=\; 0\;. \tag{12c}$$

This approximate definition for the slipping boundary p_0 agrees with the non–slipping condition (10b). It supports the supposition, formulated at the end of the previous section that the domain can be fixed in the p-space for slow processes. We will assume (12c) everywhere except at the referencing of the model of Miranda (1990) in the next section. It does mean that pressure fluctuations at the ground are entirely absent in our models. They are easily expressed via z fluctuations at the level $\overline{p_0}$. What is expressed by (12c) is just the statement that changes in the geometry due to the small replacements of the lower boundary in the p-space are inessential for dynamics.

Evaluation of $\dot{\sigma}$ grounds in general on equations (9a) and (10c). An elimination of pressure tendency from these relations yields

$$\dot{\sigma} \;=\; \sigma\;\left[\left(\frac{\tilde{w}}{H}\right)_1 \;-\; \frac{\tilde{w}}{H} \;+\; (\mathbf{v}_1 \;-\; \mathbf{v}_\sigma)\cdot\frac{\nabla p_0}{p_0}\right]\;. \tag{13}$$

Assuming (12c) and $H_1 \approx H_{*1}$, (13) simplifies to

$$\dot{\sigma} \;=\; \sigma\;\left(-\frac{\tilde{w}}{H_*} \;+\; \mathbf{v}_\sigma\cdot\frac{\nabla h}{H_{*1}}\right)\;. \tag{13'}$$

If this approximation is valid, then continuity equation (9c) can be presented as

$$\nabla_\sigma\cdot(p_0\mathbf{v}) \;+\; \frac{\partial p_0\dot{\sigma}}{\partial\sigma} \;=\; 0\;. \tag{13''}$$

5.3. MPM with mean height-scale

It is possible to simplify the developed in previous section variant of MPM, using further linearization in respect of temperature and geopotential fluctuations. Let the background geopotential

$$z_*(\mathbf{x},\sigma) \;=\; z_0(\overline{p_0}\sigma) \tag{14a}$$

is defined in accordance with the background height-scale H_*:

$$\frac{p}{H_0}\frac{\partial z_0}{\partial p} \;+\; 1 \;=\; 0\;,$$

then

$$\left(\nabla_\sigma \ - \ \sigma\frac{\nabla\overline{p_0}}{\overline{p_0}}\frac{\partial}{\partial\sigma}\right) z_0(\sigma\overline{p_0}) \ = \ \nabla_p z_0(p) \ = \ 0 \ .$$

Let equivalents of operators (3b) and (3c) in background conditions are

$$\overline{\hat{S}} \ = \ s\frac{\partial}{\partial\sigma} \ , \quad \overline{\hat{S}^+} \ = \ \frac{\partial}{\partial\sigma}s \ , \quad s \ = \ s(\mathbf{x},\sigma) \ = \ \sigma/H_* \ , \tag{14b}$$

$$\overline{\hat{\mathbf{G}}} \ = \ \nabla_\sigma \ - \ \frac{\nabla\overline{p_0}}{\overline{p_0}}\sigma\frac{\partial}{\partial\sigma} \ , \quad \overline{\hat{\mathbf{G}}^+} \ = \ \nabla_\sigma \ - \ \frac{\nabla\overline{p_0}}{\overline{p_0}}\frac{\partial}{\partial\sigma}\sigma \ . \tag{14c}$$

then the last relations are

$$\overline{\hat{S}}z_* \ = \ -\,1 \ , \quad \overline{\hat{\mathbf{G}}}z_* \ = \ 0 \ . \tag{14d}$$

Let us define analogically

$$N_* \ = \ N_0[\sigma p_0(\mathbf{x})] \ , \quad T_* \ = \ T_0[\sigma p_0(\mathbf{x})] \ . \tag{14e}$$

Presentation $z = z_* + z'$, $T = T_* + T'$ and linearization of system (9) in z' and T' with maintenance of advection terms yields

$$\frac{\tilde{w}}{H_*} \ = \ -\,\frac{\dot{\sigma}}{\sigma} \ - \ \frac{\dot{\overline{p_0}}}{\overline{p_0}} \ , \tag{15a}$$

$$\frac{\mathrm{d}\tilde{w}}{\mathrm{d}t} \ = \ g\left(\frac{T'}{T_*} \ + \ \overline{\hat{S}}z'\right) \ , \tag{15b}$$

$$\frac{\mathrm{d}\mathbf{v}}{\mathrm{d}t} \ = \ -\,g\overline{\hat{\mathbf{G}}}z' \ - \ f\hat{\mathbf{z}}\times\mathbf{v} \ , \tag{15c}$$

$$\frac{\mathrm{d}T'}{\mathrm{d}t} \ = \ -T_*\frac{N_*^2}{g}\tilde{w} \ + \ Q \ . \tag{15d}$$

$$\overline{\hat{\mathbf{G}}^+}\cdot(\overline{p_0}\mathbf{v}) \ - \ \overline{\hat{S}^+}(\overline{p_0}\tilde{w}) \ = \ 0 \ , \tag{15e}$$

At the derivation of temperature equation (15d), it is useful to carry the T' separation out in pressure coordinates and to transform the obtained equation into the sigma-space after that. Like the nonlinear form of Chapter 3, in partially linearized model (15) the term T_*N_* should be constant for energy conservation.

In the present model it is postulated explicitly that the domain is fixed in the p–space and the lower surface, $\overline{p_0}$ is time independent. This is an internally concordant assumption: if $p_0 = \overline{p_0}$ at initial moment, then $\partial p_0/\partial t = 0$ and $p_0 = \overline{p_0}$ for all successive moments. For the proof of the last statement it is sufficient to note that right side of (10c') turns zero for $H = H_*$ and $p_0 = \overline{p_0}$. In other words, in present model the 3D p–space velocity at the lower boundary, $(\mathbf{v},\omega)_1 = (\mathbf{v}, -\overline{p_0}w/H_*)_1$, is parallel to the boundary, which is described with equation $\overline{p_0}(x,y) \ - \ p \ = \ 0$.

Model (15) is close to original MPM, which is at first described by Miller and Pearce (1974) and used by Xue and Thorpe, 1991, and Miranda, 1990. Main differences still are:

(1) In those models the potential temperature, Θ_*, and potential temperature fluctuation, Θ', are used instead of T_* and T';

(2) The sigma coordinate is defined in a slab $p_0 > p > p_{top} > 0$ rather than in the whole atmosphere:

$$\sigma = \frac{p - p_{top}}{p_0 - p_{top}} , \tag{16a}$$

which yields in equations of motion the effective ground surface pressure p_* instead of $\overline{p_0}$:

$$p_* = p_0 - p_{top} , \tag{16b}$$

and replacement of $s = \sigma/H_*$ in (14b) with

$$s = \frac{p}{p_* H_*} = \frac{\sigma + p_{top}/p_*}{H_*} , \tag{16c}$$

and (14b), (14c) with

$$\hat{S} = s\frac{\partial}{\partial\sigma} , \quad \hat{S}^+ = \frac{\partial}{\partial\sigma}s , \tag{16d}$$

$$\hat{\mathbf{G}} = \nabla_\sigma - \frac{\nabla p_*}{p_*}\sigma\frac{\partial}{\partial\sigma} , \quad \hat{\mathbf{G}}^+ = \nabla_\sigma - \frac{\nabla p_*}{p_*}\frac{\partial}{\partial\sigma}\sigma . \tag{16e}$$

(3). In numerical models by Xue and Thorpe, 1991, and Miranda, 1990, the ground surface pressure p_0 in definition (16b) is treated as dynamical parameter which evolves in accordance with (8a).

Concisely the MPM, employed by Miranda, reads

$$\frac{s\tilde{w}}{\sigma} = -\frac{\dot{\sigma}}{\sigma} - \frac{\dot{p}_*}{p_*} , \tag{17a}$$

$$\frac{\mathrm{d}\tilde{w}}{\mathrm{d}t} = g\left(\frac{\Theta'}{\Theta_*} + \hat{S}z'\right) , \tag{17b}$$

$$\frac{\mathrm{d}\mathbf{v}}{\mathrm{d}t} = -g\hat{\mathbf{G}}\,z' - f\hat{\mathbf{z}}\times\mathbf{v} , \tag{17c}$$

$$\frac{\mathrm{d}\Theta'}{\mathrm{d}t} = -\Theta_*\frac{N_*^2}{g}\tilde{w} + Q , \tag{17d}$$

$$\hat{\mathbf{G}}^+\cdot(p_*\mathbf{v}) - \hat{S}^+(p_*\tilde{w}) = 0 . \tag{17e}$$

Though in the original model by Miranda (1990) it is assumed that the lower boundary surface p_* evolves in accordance with equation (8a), in reality, as it was discussed above, in the partially linearized version of the MPM with linearization in z', the p_*

must be treated as the fixed surface. In this case $\dot{p}_* = \mathbf{v}\cdot\nabla p_*$ and last equation can be alternatively presented with the help of (17a) as

$$\nabla_\sigma \cdot (p_*\mathbf{v}) + \frac{\partial p_*\dot{\sigma}}{\partial\sigma} = 0 \ . \qquad (17e')$$

This relation, as well as (13"), represents a variant of the continuity equation, written with use of $\dot{\sigma}$ (and valid for fixed p_* only). Its integrated form is

$$\dot{\sigma} = -\frac{1}{p_*}\int_0^\sigma \nabla\cdot(p_*\mathbf{v})d\sigma' \ . \qquad (18a)$$

At the lower boundary it yields

$$\int_0^1 \nabla\cdot(p_*\mathbf{v})d\sigma = 0 \ . \qquad (18b)$$

Because the same equation follows from the vertically integrated version of equation (17e), if at the lower boundary kinematical condition $(sw)_1$ = -$(\dot{p}_*/p_*)_1$ holds, (18b)is satisfied automatically and it does not represent an independent relation, which could be used, for instance, for the determination of ground surface pressure fluctuations.

If one disregards with differences in sigma-coordinate definition (assuming for instance $p_{top} = 0$ and $p_* = \overline{p_0}$), then essential difference between models (17) and (15) is in temperature equation. For Θ' from (15d) an equation follows

$$\frac{\mathrm{d}\Theta'}{\mathrm{d}t} = -\left(\Theta_*\frac{N_*^2}{g} - \frac{R}{c_p}\Theta'\right)\tilde{w} + \left(\frac{a}{p_0\sigma}\right)^{R/c_p} Q \ ,$$

which differs from (17d) with additional (second order) term on the right side. In other respect both models are very similar.

Further we will use in nonlinear case model (9) and in partially linearized version – the Miranda formulation (17a) – (17e), whish includes (at least at formal substitution Θ_*, $\Theta' \to T_*$, T') (15) as a special case. The only restriction is that p_* will be treated as a time-independent mean function:

$$p_* = \overline{p_0} - p_{top} \ . \qquad (19)$$

This enables in the most flexible way to treat the Miranda model and our model in the same numerical algorithm in parallel.

For numerical applications it is useful present (17a) – (17e) in the divergent (mass-conserving) form:

$$\frac{s\tilde{w}}{\sigma} = -\frac{\dot{\sigma}}{\sigma} - \frac{\dot{p}_*}{p_*} \ , \qquad (20a)$$

$$\frac{\partial p_*\tilde{w}}{\partial t} + \hat{\mathcal{F}}\tilde{w} = gp_*\left(\frac{\Theta'}{\Theta_*} + \hat{S}z'\right) \ , \qquad (20b)$$

$$\frac{\partial p_*\mathbf{v}}{\partial t} \ + \ \hat{\mathcal{F}}\mathbf{v} \ = \ - \ gp_*\hat{\mathbf{G}}z' \ - \ fp_*\hat{\mathbf{z}}\times\mathbf{v} \ , \tag{20c}$$

$$\frac{\partial p_*\Theta'}{\partial t} \ + \ \hat{\mathcal{F}}\Theta' \ = \ - \ p_*\Theta_*\frac{N_*^2}{g}\tilde{w} \ + \ p_*Q \ , \tag{20d}$$

$$\hat{\mathbf{G}}^+\cdot(p_*\mathbf{v}) \ - \ \hat{S}^+(p_*\tilde{w}) \ = \ 0 \ . \tag{20e}$$

where notation is used

$$\mathcal{F}\varphi \ = \ \frac{\partial}{\partial x}(p_*v_x\varphi) \ + \ \frac{\partial}{\partial y}(p_*v_y\varphi) \ + \ \frac{\partial}{\partial\sigma}(p_*\dot{\sigma}\varphi) \ . \tag{20f}$$

5.4. Diagnostical equation for geopotential height

Let us deduce equation for z in system (9). For that we represent equations (9b), (9c) and (9e) as

$$\frac{\partial\tilde{w}}{\partial t} \ = \ g\hat{S}z \ + \ f_z \ - \hat{A}\tilde{w} \ \equiv \ F_z \ , \tag{21a}$$

$$\frac{\partial\mathbf{v}}{\partial t} \ = \ -g\hat{\mathbf{G}}z \ - \ \mathbf{f}_x \ - \ \hat{A}\mathbf{v} \ \equiv \ \mathbf{F}_x \ , \tag{21b}$$

$$\hat{\mathbf{G}}^+\cdot(p_0\mathbf{v}) \ - \ \hat{S}^+(p_0\tilde{w}) \ = \ 0 \ . \tag{21c}$$

Forces f_z and $\mathbf{f}_x$ are

$$f_z \ = \ g \ + \ f_z^0 \ , \quad \mathbf{f}_x \ = \ f\hat{\mathbf{z}}\times\mathbf{v} \ + \ \mathbf{f}_x^0 \ , \tag{22d}$$

where f_z^0 and $-\mathbf{f}_x^0$ are components of external force (and turbulent friction forces, perhaps). $\hat{A}$ is ordinary advection operator

$$\hat{A} \ = \ \mathbf{v}\cdot\nabla \ + \ \dot{\sigma}\frac{\partial}{\partial\sigma} \ . \tag{22f}$$

The wanted equation follows after differencing of (21c) in time and elimination of velocity tendencies with the help of (21a) and (21b):

$$\hat{\mathbf{G}}^+\cdot p_0\hat{\mathbf{G}}z \ + \ \hat{S}^+p_0\hat{S}z \ = \ - \ \frac{1}{g}\left(\hat{\mathbf{G}}^+\cdot p_0\mathbf{a}_x \ + \ \hat{S}^+p_0a_z \ + \ \frac{\partial\hat{S}^+}{\partial t}p_0\tilde{w}\right) \ , \tag{23a}$$

where

$$a_z \ = \ f_z \ - \ \hat{A}\tilde{w} \ , \quad \mathbf{a}_x \ = \ \mathbf{f}_x \ + \ \hat{A}\mathbf{v} \ . \tag{23b}$$

The obtained relationship represents a Poisson equation for the total NH geopotential height z. Analogical diagnostical equation in model (19) for z' reads

$$\hat{\mathbf{G}}^+\cdot p_*\hat{\mathbf{G}}z' + \hat{S}^+p_*\hat{S}z' \ = \ - \ \frac{1}{g}\hat{\mathbf{G}}^+\left(\mathcal{F}\mathbf{v} \ + \ p_*f\hat{\mathbf{z}}\times\mathbf{v}\right) + \frac{1}{g}\hat{S}^+\left(\mathcal{F}\tilde{w} \ - \ gp_*\frac{\Theta'}{\Theta_*}\right) \ . \tag{24}$$

This equations transforms after use of formula $\hat{\mathbf{G}}^+(p_*\cdot) = (\nabla p_*)\cdot\ + p_*\hat{\mathbf{G}}^+\cdot$ and after multiplication with $1/p_*$ to the corresponding equation Miranda (Miranda, 1990, Eq. (3.21)).

5.5. Boundary conditions for the z equation

As the determination of z (or z') requires solution of an elliptic equation, it is necessary to supply this equation with boundary conditions at all boundary surfaces: at the bottom, at the top and at the lateral boundaries. Note that the boundary value problem for z is specific for filtered models, because it is created by the change of evolutionary equation for z to an diagnostical elliptical equation (23a) or (24).

General idea which enables to formulate required boundary conditions correctly at the bottom and at the lateral boundary, is that these boundary surfaces represent ideal constraints, which generate ideal forces of reaction, which coincide with the normal components of geopotential gradients at boundary.

A similar treatment is applicable at the top, if the top surface is treated as a rigid lid. Still, in reality the top of the atmosphere, $p\ \rightarrow\ 0$, is physically rather equivalent to the free surface. This assumes special treatment, based on the regularity of solution at $p\ =\ 0$ rather than the constraint-method.

5.5.1. Boundary condition at the bottom. Primary condition for z at the bottom is

$$z|_1\ =\ h\ .$$

This represents an ideal constraint. It generates for slipping boundary an kinematical condition for velocity components

$$w|_1\ -\ \mathbf{v}|_1\cdot\nabla h\ =\ 0\ , \tag{25a}$$

which is the orthogonality condition for 3D-velocity $(v_x,\ v_y,\ w)$ and normal vector of the ground, which is represented by the equation $\varphi(\mathbf{x},\ z)\ \equiv\ z\ -\ h(\mathbf{x}) = 0$.

As we approximate the ground in pressurethe p–space by the mean surface $\overline{p_0}$, then condition (25a) is for model (9) equivalent to

$$\left(\frac{w}{H_*}\right)_1\ +\ \frac{\mathbf{v}|_1\nabla\overline{p_0}}{\overline{p_0}}\ =\ 0\ , \tag{25b}$$

and for model (20) to

$$(sw)_1\ +\ \frac{\mathbf{v}|_1\nabla p_*}{p_*}\ =\ 0\ , \tag{25c}$$

which both yield required condition for sigma-velocity at the bottom

$$\dot{\sigma}|_1\ =\ 0\ . \tag{25d}$$

At a very profound treatment the principle of virtual replacements should be applied to get the required expression for the reaction force. We, still, simplify the problem

essentially, noting, that because the underlying surface is fixed, the real replacement coincides with one of virtual replacements. Thus, it is sufficient to differentiate (25b) or (25c) in time (it is indifferent whether the local or material derivative is used – the final result is the same) and eliminate time derivatives with the help of (21a) and (21b):

$$(\hat{S}z)_1 \;=\; -\;\Big(\nabla h\cdot\hat{\mathbf{G}}z\Big)_1 \;-\; \frac{f_z|_1}{g} \;+\; \frac{1}{g}\mathbf{f}_x|_1\cdot\nabla h \;+\; \frac{1}{g}(v_\alpha v_\beta)_1\frac{\partial^2 h}{\partial x_\alpha\partial x_\beta}\;. \qquad (26)$$

This is a Neumann boundary condition for z, with the left side in the role of the reaction force. We note without detailed proof that the same boundary condition can be deduced for the EFM (except that n, though adjusted, is not necessarily equal to 1 exactly).

Boundary condition (26) has the following interpretation. On the left side we have the reaction force of the ground surface, divided by g, on the right hand stay terms, which this force has to balance at every instant to maintain the replacement of air particle parallel to the surface. First term on the right side represents an additional non-classical contribution to the ordinary nonhomogeneous boundary condition. It depends on the horizontal gradient of the unknown function, ie ∇z, and must be determined in the course of solution. One way to do this is to take it into account iteratively. This procedure will be discussed in detail later. Anyway, it is not a part of the ideal reaction force, as it will be demonstrated later. Second and third terms together perform the projection of external force onto the normal direction of ground surface. The last term on the right side is the (divided by g) acceleration due to the curvature of the ground surface. $h_{,\alpha\beta}$ is the curvature tensor of the orography. For a spherical surface, for instance,

$$\frac{\partial^2 h}{\partial x_\alpha\partial x_\beta} \;=\; \delta_{\alpha\beta}\frac{1}{R}\;,$$

where R is the radius of curvature, which is negative for a hill-top and positive for a hollow. Thus, the last term is in this special case $\mathbf{v}^2/(gR)$. It is negative near the hill-top and causes negative contribution to vertical gradient of z, which is proportional to negative pressure fluctuation (see Fig. 1.2). As a consequence, air-flow causes pressure depression in vicinity of a convex – a fact, which is wellknown in hydrodynamics.

Lower boundary condition for model (20) follows from (25c) analogically and reads as

$$\left\{\left[1 \;+\; \left(\frac{\nabla p_*}{sp_*}\right)^2\right]\frac{\partial z'}{\partial\sigma} \;-\; \frac{\nabla p_*\nabla z'}{s^2p_*}\right\}_1 \;=\; -\;\left(\frac{Q_w}{gsp_*} \;+\; \frac{\nabla p_*\cdot\mathbf{Q_v}}{gs^2p_*^2}\right)_1\;, \qquad (27a)$$

where Q–terms are

$$Q_w \;=\; gp_*\frac{\Theta'}{\Theta_*} \;-\; \mathcal{F}w\;,\quad \mathbf{Q_v} \;=\; -\;\mathcal{F}\mathbf{v} \;-\; fp_*\hat{\mathbf{z}}\times\mathbf{v}\;. \qquad (27b)$$

Equation (27a) looks very different from (26), nevertheless they are quite close and (26) can be presented in the form, very similar to (27a), after separation of z' and z_*. Both

forms have special advantages: (26) is better for theoretical discussion, while (27a) is convenient for numerical applications.

Again on the left side an additional term arrived (beside the vertical gradient), which depends on the horizontal gradient of the geopotential fluctuation, $\nabla z'_1$. From the "boundary condition view-point" this term is an unknown quantity.

At the discussion of (26) we pointed without proof that the vertical gradient on the left side of (26) is the force of reaction. Similar problem arrives with boundary condition (27a): it is essential to know (for applications in other models, for energy conservation consideration etc.) which term on the left side of (27a) represents precisely the reaction force of the boundary. We prove now that **the reaction force of the slipping lower boundary is orthogonal to the boundary surface and its vertical component is** (in the case of model (19) and boundary condition (27a))

$$r_z \;=\; g\left(s\frac{\partial z'}{\partial \sigma}\right)_1 \;.$$

To prove the statement we treat the boundary equation in the form

$$\Phi(x,z) \;=\; z \;-\; h(x) \;=\; 0 \;, \tag{28}$$

and assume

$$\nabla h \;=\; -\,\frac{1}{s_1}\frac{\nabla p_*}{p_*} \;\equiv\; \mathbf{K} \;.$$

The normal vector to the surface is

$$\mathbf{N} \;=\; \frac{\hat{\mathbf{z}} \;-\; \mathbf{K}}{\sqrt{1 \;+\; \mathbf{K}^2}} \;.$$

at that kinematical condition (19) is an orthogonality condition

$$(\mathbf{v}, w)_1 \perp \mathbf{N}$$

The ideal reaction force $\mathbf{R} = (\mathbf{r}_x, r_z)$ is a force, which is orthogonal to surface (and thus, being orthogonal to the 3D velocity, it does not carry out any work) and does not let a particle to leave the surface. This yields

$$\mathbf{R} \;=\; r_z(\hat{\mathbf{z}} \;-\; \mathbf{K}) \;.$$

Presenting equations (15b) and (15c) at the boundary in the form

$$\frac{\partial w|_1}{\partial t} \;=\; r_z \quad +\; F'_z \;, \quad \frac{\partial \mathbf{v}|_1}{\partial t} \;=\; -\,r_z\mathbf{K} \;+\; \mathbf{F'}_x \;,$$

we discover that r_z coincides with the normal gradient of z'. Statement (28) is proved.

$z'|_1$ in (27a) is a non-fixed dynamic field. At numerical modeling the second term on the left side of (27a), which is determined by $z'|_1$, is treated as a perturbation and it

is calculated iteratively. If z' is determined, the corresponding ground surface pressure fluctuation can be estimated from the formula (see (1.2))

$$\left(\frac{p'}{p_*}\right)_1 \;=\; \left(\frac{z'}{H_*}\right)_1 \;.$$

For future applications it is convenient solve (27a) in $(\partial z'/\partial\sigma)_1$:

$$\left(\frac{\partial z'}{\partial\sigma}\right)_{\sigma=1} \;=\; \Gamma_1 \;, \tag{29a}$$

where

$$\Gamma_1 \;=\; \left\{\left[1 \;+\; \left(\frac{\nabla p_*}{s p_*}\right)^2\right]^{-1}\left(\frac{\nabla p_*\nabla z'}{s^2 p_*} \;-\; \frac{Q_w}{g s p_*} \;-\; \frac{\nabla p_*\cdot\mathbf{Q_v}}{g s^2 p_*^2}\right)\right\}_{\sigma=1} \;. \tag{29b}$$

5.5.2. Boundary condition at the top.

At first we consider in short the **rigid lid boundary condition** at the top. The rigid lid yields kinematical conditions at the top

$$\dot\sigma|_0 \;=\; 0 \;, \tag{30a}$$

$$w|_0 \;=\; 0 \;. \tag{30b}$$

Last condition at every instant is equivalent to

$$\frac{\mathrm{d}w_0}{\mathrm{d}t} \;=\; \left(\frac{\mathrm{d}w}{\mathrm{d}t}\right)_0 \;=\; 0 \;,$$

which yields with the help of (20b)

$$\left(\frac{\Theta'}{\Theta_*} \;+\; s\frac{\partial z'}{\partial\sigma}\right)_0 \;=\; 0 \;. \tag{30c}$$

The last formula represents the upper boundary condition for z' in the rigid lid model. It coincides with the one used by Miranda (1990).

For practical use in further application it is convenient present (30c) as

$$\left(\frac{\partial z'}{\partial\sigma}\right)_0 \;=\; \Gamma_0 \;\equiv\; -\left(\frac{\Theta'}{s\Theta_*}\right)_{\sigma=0} \;. \tag{30d}$$

The free boundary condition at the top. There is no rigid lid at the top and the only restriction to z' is that it must be finite (or, if the finiteness is not supported, then it should grow near infinity with lowest possible speed). To get the required boundary condition, which is in addition applicable in discrete numerical modeling, we propose a

special "top-shell" method. The essence of this method is the analytical continuation of the solution above some certain level p_m, into the domain $0 < p < p_m$), which is the top-shell. The lower boundary of the top-shell, p_m, is not necessarily equal to p_{top}. The problem is identical for equations (23a) and (24), but for the definiteness we consider equation (24).

Because the top-shell is very thin, coefficients of the equation (23') in this domain, $H_* \approx H_0(p_m) = H_m$ and $p_* \approx \overline{p_*}$ can be treated as constants. As a result, equation (24) simplifies essentially and takes the form

$$H_m^2 \nabla^2 z' + \frac{\partial}{\partial \sigma}\left((\sigma + \sigma_0)^2 \frac{\partial z'}{\partial \sigma}\right) = \frac{H_*^2}{p_*} A \equiv A_0 , \tag{31}$$

where A represents sources on the right side of (24) (Note that on the right side we have maintained actual values of H_* and p_*), and

$$\sigma_0 = p_{top}/p_* \approx p_{top}/\overline{p_*} . \tag{32}$$

We apply to (31) the Fourier transform in horizontal coordinates, ($\mathbf{x} \rightarrow \mathbf{k}$) and in vertical employ an coordinate transformation

$$\zeta - \zeta_m = -\ln\left(\frac{\sigma + \sigma_0}{\sigma_m + \sigma_0}\right) . \tag{33}$$

which yield (for the fixed $\mathbf{k}$)

$$\frac{d^2 z'}{d\zeta^2} - \frac{dz'}{d\zeta} - H_0^2 \mathbf{k}^2 z' = A_0 . \tag{34}$$

This equation can be solved in easy way using the Laplace transform. The solution is

$$z' = z'_1(\zeta) + z'_2(\zeta) , \tag{35a}$$

$$z'_i(\zeta) = \left[(a_i - b_i)\, z'(\zeta_m) + b_i \frac{dz'(\zeta_m)}{d\zeta}\right] \mathrm{e}^{\mu_i(\zeta-\zeta_m)} + b_i \int_{\zeta_m}^{\zeta} \mathrm{e}^{\mu_i(\zeta-\zeta')} A(\zeta') d\zeta' , \tag{35b}$$

$$a_1 = \frac{\mu_1}{\mu_1 - \mu_2} , \quad a_2 = \frac{\mu_2}{\mu_2 - \mu_1} , b_1 = -b_2 = \frac{1}{\mu_1 - \mu_2} , \tag{35c}$$

$$\mu_1 = 1/2 - \sqrt{1/4 + H_0^2 \mathbf{k}^2} , \quad \mu_2 = 1/2 + \sqrt{1/4 + H_0^2 \mathbf{k}^2} . \tag{35d}$$

To avoid the exponential growth of this solution at $\zeta \rightarrow \infty$ (the "regularity requirement") we have to choose

$$(a_2 - b_2) z'(\zeta_m) + b_2 \frac{d(\zeta_m)}{d\zeta} + b_2 \int_{\zeta_m}^{\infty} \mathrm{e}^{\mu_2(\zeta_m - \zeta)} A(\zeta) d\zeta = 0 . \tag{36a}$$

The detailed behaviour of the solution in the top shell has no significance for the further, what we need, is an upper boundary ($\sigma = \sigma_m$) condition for for z' in the lower domain, which yields from (36a):

$$(\sigma_m + \sigma_0)\frac{dz'(\sigma_m)}{d\sigma} - (\mu_2 - 1)z'(\sigma_m) = \int_{-\sigma_0}^{\sigma_m} \left(\frac{\sigma + \sigma_0}{\sigma_m + \sigma_0}\right)^{\mu_2 - 1} A(\sigma)\frac{d\sigma}{\sigma_m + \sigma_0} \ . \quad (36b)$$

This is an exact upper boundary condition at level σ_m supposing the used preconditions are exact. The specific feature of this boundary condition is that it can applied in the Fourier-space only.

Assuming in the top-shell

$$A(\sigma) = A(\sigma_m) + \gamma\sigma \ ,$$

we get from (36b)

$$(\sigma_m + \sigma_0)\frac{dz'(\sigma_m)}{d\sigma} - (\mu_2 - 1)z'(\sigma_m) = \frac{1}{\mu_2}\left(A(\sigma_m) - \gamma\frac{\sigma_0 - \mu_2\sigma_m}{\mu_2 + 1}\right) \ . \quad (36c)$$

In special case $\sigma_m = 0$ and $A|_{\sigma=-\sigma_0} = 0$:

$$\sigma_0\left(\frac{dz'(\sigma)}{d\sigma}\right)_0 - (\mu_2 - 1)z'(0) = \frac{A(0)}{\mu_2 + 1} \ . \quad (36c')$$

For further discussion it is useful to represent (36b) and (36c') in a symbolic way

$$\hat{L}z' = \hat{G}A \ , \quad (36d)$$

where $\hat{L}$ and $\hat{G}$ projection operators defined via (36b) – (36c').

If the described free boundary condition is applied, then there is no restriction for vertical velocity w at the upper boundary.

5.5.3. Lateral boundary conditions.

If the momentum flow through the lateral boundary is given at every instant, then the momentum equations yield a condition for the normal derivative $\partial z'/\partial n$, at which this flow will be maintained:

$$\left(\frac{\partial z'}{\partial n}\right)_\Sigma = \Gamma_L \ . \quad (37a)$$

This is a Neumann condition, derivative is evaluated along the external normal at every point and Γ is (for equation 15a')

$$\Gamma_L = -\left[\frac{1}{gp_*}\mathbf{n}\cdot\left(\frac{\partial p_*\mathbf{v}}{\partial t} + \hat{\mathcal{F}}\mathbf{v} - g\nabla p_*\sigma\frac{\partial z'}{\partial\sigma} + fp_*\hat{\mathbf{z}}\times\mathbf{v}\right)\right]_\Sigma \ . \quad (37b)$$

The velocity tendency is an external (given) field. The only restriction to $\partial \mathbf{v}/\partial t|_\Sigma$ is that it must be mass-balanced: the total mass flow through Σ must be equal to zero. This condition, representing a consequence of the incompressibility of medium in the p-space, is absolute for the rigid lid upper boundary condition. For the free upper boundary model this condition is not so absolute in kinematical sense, but in reality it is valid high precision.

Boundary condition is, analogically to the rigid lid condition, an absolute rigid lateral boundary condition (condition (37) corresponds to a rigid lateral boundary, which replaces at every instant in its normal direction with the fixed speed). This rigidness is a potential source of nonphysical phenomena, like reflection on Σ of wave-like disturbances, which move with the speed, different from $\mathbf{v}$. In reality, where there is no rigid lateral surface, these waves leave (or enter) the integration domain without reflections.

There exist two wellknown methods to turn the lateral boundary transparent not altering at that boundary condition (37a). The first one, which is simpler but more time-consuming at numerical realization, is the "sponge layer" method. In this approach an absorbing layer is introduced near the lateral boundary, in which the horizontal velocity evolution is ruled by the Rayleigh relaxation mechanism

$$\frac{\partial}{\partial t}(\mathbf{v} - \mathbf{v}_b) \sim -\kappa\,(\mathbf{v} - \mathbf{v}_b)\,. \tag{38}$$

$\mathbf{v}_b$ represents the external velocity field which is determined in the whole sponge layer, and κ is the relaxation coefficient (Rayleigh friction coefficient), with smooth monotone grow from zero at the internal boundary of the sponge layer to its maximum value at Σ. The sponge layer model is used, for instance, in the HIRLAM (HIRLAM Doc Manual, 1996).

Other method is known as the "radiative" boundary condition. In this method, the lateral boundary is turned transparent to quick waves with the special choice of $\partial \mathbf{v}/\partial t$ in (37b). This method is proposed by Orlanski (1976) extended by Raymond and Kuo (1984) and modified and in detail discussed by Miranda (1990). Further, in numerical realization we will use Miranda algorithm without modifications.

Summarising, we have (and will use in numerical model) two kind of boundary conditions for elliptic equations (23a), (24):

– the rigid lid model, Neumann boundary condition is applied at all boundary.

– the free surface model,where the Neumann boundary condition is applied at the bottom and at the lateral boundary, but at the top the mixed Neumann–Dirichlet boundary condition (36) is used.

5.6. Solution of the elliptic equation for z'

In this section the iterative solution procedure for (24) will be discussed in details. Equation (23a) can be solved in the same way. In general lines, the solution algorithm follows the Miranda scheme (1990), the detailed revision is needed because both the geometry and boundary conditions are different from those applied in the Miranda scheme.

The Miranda method consists of division of the elliptical operator on the left side of (24) to the main, horizontally homogeneous component, and horizontally inhomogeneous perturbation operator. An additional specific and very powerful method employed by Miranda is the use of the Williams transformation (Williams, 1969), which transforms the initial nonhomogeneous boundary value problem to the homogeneous one and makes applicable the fast Fourier transform (FFT). The specific method, which we add to the scheme of Miranda, is the iterative approximation of boundary condition at the lower boundary (first terms on the right side of (26) and (29b) are estimated from previous iteration) and in the free boundary model at the top (source function A in (36) is calculated from previous iteration).

For expansion of the elliptical operator in (24) we present

$$s \;=\; \overline{s}(\sigma) \;+\; s'(\mathbf{x},\;\sigma)\;, \quad \overline{s'} \;=\; 0\;,$$

where overline means horizontal mean. With the help of this expansion equation (24) can be presented (after some "algebra" and division by p_*) as

$$\mathcal{L}z' \;+\; \mathcal{M}z' \;=\; A\;, \tag{39a}$$

where $\mathcal{L}$ and $\mathcal{M}$ are the horizontally homogeneous main operator and the nonhomogeneous perturbation operator consequently:

$$\mathcal{L} \;=\; \nabla^2 \;+\; \frac{\partial}{\partial\sigma}\overline{s}^2\frac{\partial}{\partial\sigma} \tag{39b}$$

$$\mathcal{M} \;=\; \frac{\partial}{\partial\sigma}\left[\sigma^2\left(\frac{\nabla p_*}{p_*}\right)^2 \;+\; s'^2\right]\frac{\partial}{\partial\sigma} \;-\; \frac{\nabla^2 p_*}{p_*}\sigma\frac{\partial}{\partial\sigma} \;-\; 2\frac{\nabla p_*}{p_*}\cdot\nabla\sigma\frac{\partial}{\partial\sigma}\;, \tag{39c}$$

and A is the divided by p_* right side term of (24). Operator ∇ represents the gradient on the constant sigma surface.

Perturbation operator $\mathcal{M}$ depends on the surface orography only and makes zero for the flat underlying surface. As orography (except very artifical model situations) is allays low and in most cases smooth, the perturbation term is small in comparison with the main operator $\mathcal{L}$, which justifies the iteration technique.

It is convenient at qualitative discussion to present the boundary condition as a linear projector $\mathcal{P}$: $R^3 \;\rightarrow\; \Sigma$:

$$\mathcal{P}z' \;=\; \Gamma(z')\;. \tag{40}$$

In the rigid lid model

$$\mathcal{P}z' \;=\; \left(\frac{\partial z'}{\partial n}\right)_\Sigma$$

at all boundary, and (40) is explicitly as

$$\left(\frac{\partial z'}{\partial\sigma}\right)_{\sigma=1} \;=\; \Gamma_1(z')\;, \qquad \left(\frac{\partial z'}{\partial n}\right)_{\Sigma_L} \;=\; \Gamma_L\;, \qquad \left(\frac{\partial z'}{\partial\sigma}\right)_{\sigma=0} \;=\; \Gamma_0\;, \tag{41}$$

where Γ_1, defined by (29b), includes z' as perturbation. Γ_L is defined by (37b) and Γ_0 is defined by (30d).

For the free boundary model the conditions are the same at the bottom and lateral boundary, but at the top, according to (36d), we have a different situation:

$$\left(\frac{\partial z'}{\partial \sigma}\right)_{\sigma=1} = \Gamma_1(z') \ , \quad \left(\frac{\partial z'}{\partial n}\right)_{\Sigma_L} = \Gamma_L \ , \quad \hat{L}z' = \hat{G}(A - \mathcal{M}z') \ . \tag{42}$$

It is an essential feature of the algorithm, that the projective operator $\hat{G}$ corresponds to the undisturbed main elliptical operator $\mathcal{L}$, therefore in (42) operator $\hat{G}$ acts both on the source function and perturbation operator.

The solution is looked for iteratively, for which equation (39a) is presented as

$$\mathcal{L}z^{(i)} = A - \mathcal{M}z^{(i-1)} \ . \tag{43a}$$

Here $z^{(i)}$ represents the ith iterative (approximate) solution of the problem. Consequently, boundary conditions for (43a) are

$$\mathcal{P}z^{(i)} = \Gamma(z^{(i-1)}) \ . \tag{43b}$$

The required solution will be presented as a sum of two functions,

$$z' = z'_h + z'_b \ , \tag{44a}$$

and consequently, iterative approximations as

$$z^{(i)} = z_h^{(i)} + z_b^{(i)} \ , \tag{44b}$$

where z'_b (or $z_b^{(i)}$) is a known function, which satisfies the nonhomogeneous boundary condition on the (part of) boundary, and z'_h ($z_h^{(i)}$) is the new unknown function, which obviously satisfies on the consequent part of the boundary the homogeneous boundary condition. The choice of z_b is in certain degree arbitrary. In the discrete model it is straightforward to choice this reference function equal to zero at internal points and non-zero at the consequent boundary points. The main purpose of the expansion (44) is to get homogeneous boundary condition for the new unknown z_h at lateral boundaries, which makes possible an employment of the FFT in horizontal coordinates. Therefore, it is not absolutely necessary to use the described homogenisation at the top and bottom.

Miranda (1990) employs homogenisation at all boundary. This is straightforward, if the right side of (40) does not depend on z' (and in Miranda model this condition holds). In short, the Miranda algorithm is in our notation as follows.

$$z^{(0)} = z_b \ , \quad z^{(i)} = z_h^{(i)} + z_b \quad (i > 0) : \tag{45a}$$

$$\left(\frac{\partial z_b}{\partial \sigma}\right)_{\sigma=1} = \Gamma_1 , \quad \left(\frac{\partial z_b}{\partial n}\right)_{\Sigma_L} = \Gamma_L , \quad \left(\frac{\partial z_b}{\partial \sigma}\right)_{\sigma=0} = \Gamma_0 , \tag{45b}$$

(Γ_1 does not depend on z'–st in this case)

$$\left(\frac{\partial z_h^{(i)}}{\partial \sigma}\right)_{\sigma=1} = 0 , \quad \left(\frac{\partial z_h^{(i)}}{\partial n}\right)_{\Sigma_L} = 0 , \quad \left(\frac{\partial z_h^{(i)}}{\partial \sigma}\right)_{\sigma=0} = 0 , \tag{45c}$$

$$\mathcal{L} z_h^{(i)} = A - \mathcal{L} z_b - \mathcal{M} z^{(i-1)} . \tag{45d}$$

Iteration starts with an initial approximation (see(45a)) $z_h^{(0)} = 0$, $z^{(0)} = z_b^{(0)}$.

A simple elegant numerical algorithm can be obtained, if the iteration correction function

$$\varphi^{(i)} = z_h^{(i)} - z_h^{(i-1)} \tag{46}$$

is used instead of $z_h^{(i)}$:

$$z^{(0)} = z_b , \quad z^{(i)} = z^{(i-1)} + \varphi^{(i)} \quad (i > 0) : \tag{47a}$$

$$\left(\frac{\partial z_b}{\partial \sigma}\right)_{\sigma=1} = \Gamma_1 , \quad \left(\frac{\partial z_b}{\partial n}\right)_{\Sigma_L} = \Gamma_L , \quad \left(\frac{\partial z_b}{\partial \sigma}\right)_{\sigma=0} = \Gamma_0 , \tag{47b}$$

$$\left(\frac{\partial \varphi^{(i)}}{\partial \sigma}\right)_{\sigma=1} = 0 , \quad \left(\frac{\partial \varphi^{(i)}}{\partial n}\right)_{\Sigma_L} = 0 , \quad \left(\frac{\partial \varphi^{(i)}}{\partial \sigma}\right)_{\sigma=0} = 0 , \tag{47c}$$

$$\mathcal{L} \varphi^{(i)} = A - (\mathcal{L} + \mathcal{M}) z^{(i-1)} . \tag{47d}$$

Iteration process begins with $z^0 = z_b$. At every successive step the correction $\varphi^{(i)}$ will be find solving elliptical equation (47d) and the result will be added to the previous value $z^{(i-1)}$ to get the new one, $z^{(i)}$.

The described original algorithm of Miranda can be successfully applied in the rigid-lid model, though in the lower boundary condition Γ_1 is dependent on z'. This is achieved in this way that after each iteration the iterated solution is extrapolated from internal point to the boundary according to the rule

$$z^{(i)}_{Boundary} = z^{(i)}_{Boundary-1} + \Gamma_1(z^{(i-1)}) \cdot \Delta\sigma . \tag{47e}$$

In the case of the free boundary model it is possible to develop an algorithm, which is very close to the Miranda algorithm, just described. For that it is necessary to take for z_b a function which satisfies on lateral boundary nonhomogeneous boundary condition, but at the bottom and at the top – homogeneous one. Consequently, for z_h an opposite boundary condition holds. The whole algorithm reads as

$$z^{(0)} = z_b , \quad z^{(i)} = z_h^{(i)} + z_b \quad (i \geq 1) : \tag{48a}$$

$$\left(\frac{\partial z_b}{\partial \sigma}\right)_{\sigma=1} = 0\ , \quad \left(\frac{\partial z_b}{\partial n}\right)_{\Sigma_L} = \Gamma_L\ , \quad (z_b)_{\sigma=0} = 0\ , \tag{48b}$$

$$\left(\frac{\partial z_h^{(i)}}{\partial \sigma}\right)_{\sigma=1} = \Gamma_1(z^{(i-1)})\ , \quad \left(\frac{\partial z_h^{(i)}}{\partial n}\right)_{\Sigma_L} = 0\ , \quad \hat{L} z_h^{(i)} = \hat{G}(A - \mathcal{M} z^{(i-1)}) \tag{48c}$$

$$\mathcal{L} z_h^{(i)} = A - \mathcal{L} z_b - \mathcal{M} z^{(i-1)}\ . \tag{48d}$$

Note that in this model z_b is in discrete case zero everywhere except the lateral boundary (i.e., it is zero in addition to the internal points, at the bottom and top).

The used initialization $z^{(0)} = z_b$ does not satisfy boundary conditions at the top and bottom, still boundary conditions will be satisfied completely beginning with $i = 1$. The advantage of the proposed initial approximation is similarity of the iteration process for all steps beginning with $i = 1$.

For the iteration correction function (46) algorithm (48) becomes

$$z^{(0)} = z_b\ , \quad z^{(i)} = z^{(i-1)} + \varphi^{(i)}, \quad (i \geq 1)\,: \tag{49a}$$

$$\left(\frac{\partial z_b}{\partial \sigma}\right)_{\sigma=1} = 0\ , \quad \left(\frac{\partial z_b}{\partial n}\right)_{\Sigma_L} = \Gamma_L\ , \quad (z_b)_{\sigma=0} = 0\ , \tag{49b}$$

$$\left(\frac{\partial \varphi^{(i)}}{\partial \sigma}\right)_{\sigma=1} = \Gamma_1(z^{(i-1)}) - \Gamma_1(z^{(i-2)})\ , \quad \left(\frac{\partial \varphi^{(i)}}{\partial n}\right)_{\Sigma_L} = 0\ , \tag{49c}$$

$$\hat{L}\varphi^{(i)} = \hat{G}[A - (\mathcal{L} + \mathcal{M})\, z^{(i-1)}]\ , \tag{49d}$$

$$\mathcal{L}\varphi^{(i)} = A - (\mathcal{L} + \mathcal{M})\, z^{(i-1)}\ . \tag{49e}$$

The boundary condition at the top, (49d), has been taken in accordance with the right side of (49e). A direct deduction from (48c) yields the upper boundary condition in the form

$$\varphi^{(i)}|_{\sigma=0} = -\hat{G} M \varphi^{(i-1)}\ .$$

It is easy to prove that this condition is equivalent to (49d). In addition, it is possible to change the quite inconvenient lower boundary condition (49c) to a more simple one,

$$\left(\frac{\partial \varphi^{(i)}}{\partial \sigma}\right)_{\sigma=1} = 0\ , \tag{49f}$$

if one uses the extrapolation algorithm (47e) at the lower boundary.

CHAPTER SIX

Numerical Scheme NHAD

In this chapter a short description of the numerical algorithm NHAD is presented, which realizes ideas of previous sections. Discussion is illustrated with modeling examples.

Model NHAD (= **N**on**H**ydrostatic **A**djusted **D**ynamics) is a modification and generalization of the model NH3D of Miranda (1990). It includes the NH3D as a sub-case, which can be switched on with a logical key ADJUST. With ADJUST=.F. the algorithm works as the NH3D, with ADJUST=.T. the modified version is launched.

6.1. General characteristics

NHAD is a sigma coordinate model.

Integration (modeling) domain is a rectangular area in the sigma-space with dimensions $N_x \cdot \Delta x \times N_y \cdot \Delta y \times N_\sigma \cdot \Delta\sigma$.

The grid used is a staggered grid (Winninghoff, 1968, Williams, 1969), known in atmospheric dynamics as the Arakawa C-grid (Arakawa and Lamb, 1977, Cullen, 1991), see Fig. 6.1. At this grid the rectangle domain is divided into small cubes. Scalar fields, like z, Φ, T, $\nabla\cdot\mathbf{v}$, are given at central points of each cube and represent the mean value of any field inside that cube. Components of vector fields, like $\mathbf{v}$, $\nabla\varphi$ etc, are treated as normal flux components at cube boundary, and are given at central points of cube sides, as shown in Fig. 6.1c. Central points of cubes are treated as the primary grid, and scalar fields are defined on the primary grid. Central points of cube sides represent the grid-points of secondary grid. Components of vector fields are defined on the secondary grid. The specific feature of the staggered grid is, that different components of a vector are determined at different grid-points.

The main advantage of the staggered grid is mutual symmetry of gradient and divergence operations. Any gradient, defined with the help of difference formula

$$(\nabla\varphi)_{ijk} \;=\; \hat{\sigma}\frac{\varphi_{i+1jk}-\varphi_{ijk}}{\Delta\sigma} \;+\; \hat{\mathbf{x}}\frac{\varphi_{ij+1k}-\varphi_{ijk}}{\Delta x} \;+\; \hat{\mathbf{y}}\frac{\varphi_{ijk+1}-\varphi_{ijk}}{\Delta y}$$

in an object of secondary grid. Vice versa, the finite-difference divergence

$$(\nabla\cdot\mathbf{a})_{ijk} \;=\; \frac{a^\sigma_{ijk}-a^\sigma_{i-1jk}}{\Delta\sigma} \;+\; \frac{a^x_{ijk}-a^x_{ij-1k}}{\Delta x} \;+\; \frac{a^y_{ijk}-a^y_{ijk-1}}{\Delta y}$$

is a scalar field on primary grid. This symmetry allows to maintain almost automatically the basic conservation laws, supposing the equations of motion are written in divergent form before discretization (Haltiner and Williams 1980, Cullen 1991).

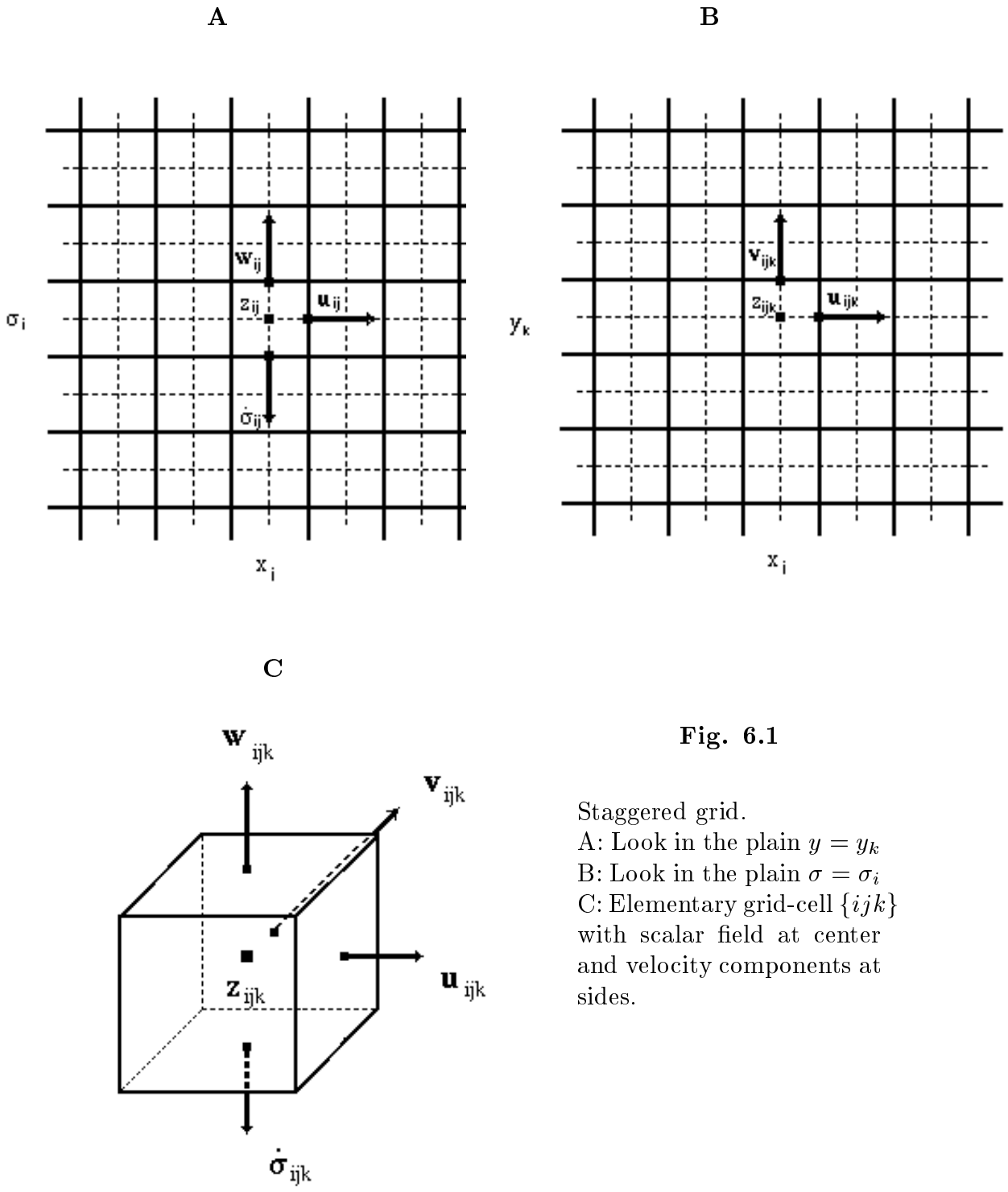

Fig. 6.1

Staggered grid.
A: Look in the plain $y = y_k$
B: Look in the plain $\sigma = \sigma_i$
C: Elementary grid-cell $\{ijk\}$ with scalar field at center and velocity components at sides.

Equations used are those of Miranda, ie. model equations (5.12").

Time integration scheme is an explicit leap-frog algorithm. Differently from hydrostatic models, where intensive buoyancy wave generation (by an explicit scheme) determines the need in quite sophisticated semi-implicit leapfrog schemes (Hoskins and Simmons, 1975), the NH models are stable with the simple explicit one. For temporal smoothing and for suppressing of the decoupling tendency, inherent to leapfrog schemes, an Asselin filtering technique (Robert, 1966, Asselin, 1972) is applied with the smoothing parameter $\gamma_{Asselin} = 0.05$.

Spatial filtering. Two spacial filtering mechanisms are employed. The fourth oder filter is used to suppress short-scale instabilities with wavelengths $\leq$ two grid-length. This is the one used initially by Durran and Klemp (1983) and generalized by Miranda (1990) to the 3D case.

Another filtering (optional) is the Rayleigh filtering at the top of the atmosphere. Its aim is to avoid instabilities due to excessively large amplitudes of gravity waves. In the original NH3D version Miranda employs the Rayleigh filtering to suppress the gravity-wave reflection at the top (the sponge-layer idea). In models with an free upper boundary there is no wave-reflection and the only aim of Rayleigh filtering is stability maintenance.

6.2. Geometry of the domain of integration in the p–space

The domain is fixed in the pressure space, and the effective ground surface pressure p_* is treated in accordance with (5.18) time-independent. As it was pointed in Section 5.3, this assumption is self-concordant in the framework of MPM with mean H_* in the sense that replacements of air particles at lower boundary are allays parallel to lower boundary the in p-space and thus, do not change the configuration of the domain. This quality is mathematically expressed as

$$\frac{\partial p_*}{\partial t} \;=\; \frac{\partial \overline{p_*}}{\partial t} \;=\; 0 \;,$$

and corresponds in the NH case to the usual vertically integrated mass balance condition of hydrostatic models (see (5.8))

$$\nabla \cdot \left(\overline{p_*} \int_0^1 \mathbf{v} d\sigma \right) \;=\; 0 \;.$$

In our NH model the last condition is satisfied automatically, if it is fulfilled at initial moment (see (5.18b) an discussion to it). The ground surface pressure fluctuations are nevertheless different from zero. Like in the hydrostatic models they can be evaluated from z fluctuations at $\sigma = 1$ (See appendix 1)

$$\frac{p_0'}{\overline{p_0}} \;=\; \left(\frac{z'}{H_*} \right)_{\sigma=1} \;. \tag{1}$$

6.3. Numerical solution of the z'–equation

Central task at every time-step is solution of the diagnostical equation for z'. This is done as described in section 5.6, with discrete versions of operators $\mathcal{L}$ and $\mathcal{M}$ and source A. The model supports two kinds of boundary conditions for z': the rigid lid upper boundary condition (starts with logical parameter RIGLID=.T.) and the free upper boundary condition (RIGLID=.F.). The consequent problem formulations are given by formulae (5.47) and (5.49). Equations (5.47d) and (5.49e), which are of the same form and differ in essence by the upper boundary condition only, are solved in $\varphi^{(i)}$ with the help of fast cosinus-Fourier transform (FCFT). The FCFT is suitable because functions $\varphi^{(i)}$ have zero normal gradients at lateral boundaries. The solution algorithm

is different from that of Miranda. Equations (5.47d) and (5.49e) take after application of the FCFT at every horizontal wave vector $\mathbf{k}_{i,j}$ form (subscripts $i,\ j$ are omitted)

$$A_1(l)\varphi_{l-1} \ + \ A_2(l)\varphi_l \ + \ A_3(l)\varphi_{l+1} \ = \ B_k \ , \tag{2}$$

where indices l correspond to discrete σ-levels and B_l represents the FCF-transformed right hand side of equations. Equation (2) represents the finite-difference analogue of equation (compare with (5.39b))

$$\frac{\partial}{\partial\sigma}\left(\overline{s}^2\frac{\partial\varphi}{\partial\sigma}\right) \ - \ \mathbf{k}^2\varphi \ = \ B(\sigma) \ . \tag{2'}$$

Difference equation (2) is treated as ordinary recurrence formula enabling to determine φ_{l-1} for known φ_l and φ_{l+1}. The recursion is started at the lower boundary $l = N_s$. For initialization of the recurrence values of φ_{Ns} and φ_{Ns-1} are needed. In both cases (rigid lid and free upper boundary) we are interested in solutions which satisfy the homogeneous Neumann condition at the bottom, which in finite-difference formulation reads as

$$\varphi_{Ns} \ = \ \varphi_{Ns-1} \ . \tag{3}$$

There exist two special solutions, which are independent and satisfy the homogeneous Neumann condition at the lower boundary, which we denote as ϕ^I and ϕ^{II}:

$$\phi^I : \quad B_l \ \neq \ 0 \ , \quad \phi^I_{Ns} \ = \ \phi^I_{Ns-1} \ = \ 0 \ , \tag{4a}$$

$$\phi^{II} : \quad B_l \ = \ 0 \ , \quad \phi^{II}_{Ns} \ = \ \phi^{II}_{Ns-1} \ = \ 1 \ . \tag{4b}$$

The first special solution is calculated for actual source, B, and it is zero along with the first derivative at the lower boundary. The second solution is calculated for homogeneous recurrence (ie. $B = 0$), and it has the unit value and zero first derivative at the lower boundary.

Any solution

$$\varphi \ = \ \phi^I \ + \ \beta\phi^{II} \tag{5}$$

will satisfy the nonhomogeneous recursion (2) with boundary condition (3). Parameter β can be used for satisfaction of the remaining boundary condition. Here is difference for $\mathbf{k} = 0$ and $\mathbf{k} \neq 0$. Let us consider at first $\mathbf{k} \neq 0$. In the case the upper boundary condition can be used for β determination. For the rigid lid model this condition is the homogeneous Neumann at the top:

$$\varphi_0 \ = \ \varphi_1 \ ,$$

and it yields

$$\beta \ = \ -\frac{\phi^I_1 - \phi^I_0}{\phi^{II}_1 - \phi^{II}_0} \ . \tag{6a}$$

In the case of the free-boundary condition (5.49d) should be used for the determination of β. In explicit representation for φ (superscript (i) is omitted for simplicity) it reads (see (5.36c')

$$\sigma_0 \left(\frac{d\varphi(\sigma)}{d\sigma} \right)_0 \; - \; (\mu_2 - \; 1)\varphi(0) \; = \; \frac{A(0)}{\mu_2 + 1} \; , \tag{7}$$

where $A(0)$ represents the right side of (5.49d) for current iteration. As $\sigma = 0$ represents in staggered grid the half-(or "gradient"-)level, $\varphi(0)$ and $A(0)$ must be interpolated from levels $l = 0$ and $l = 1$. The choice of A(0) is (for the real atmosphere conditions) determined with sub-grid processes in the upper stratosphere and thus, represents a subject for physical parametrization rather than of mathematical extrapolation from the lower atmosphere. The right hand term in (7) corresponds to the situation, where source A decays linearly from level $\sigma \; = \; 0$ to zero at the infinity. As a result, its interpolated value in discrete model is $(A_0 + A_1)/2 = A_1/2$ and the finite-difference analogue of (7) reads

$$b_0 \varphi_0 \; + \; b_1 \varphi_1 \; = \; b_* \; , \tag{8a}$$

where

$$b_0 \; = \; \mu_2 - 1 + 2\sigma_0/\Delta\sigma \; , \quad b_1 \; = \; \mu_2 - 1 - 2\sigma_0/\Delta\sigma \; , \tag{8b}$$

$$b_* \; = \; A_1/(\mu_2 + 1) \; . \tag{8c}$$

With the help of this boundary condition we get for β

$$\beta \; = \; - \; \frac{b_0 \phi_0^I \; + \; b_1 \phi_1^I \; + \; b_*}{b_0 \phi_0^{II} \; + \; b_1 \phi_1^{II}} \; . \tag{9}$$

Another possibility is to choose A zero at the level $\sigma \; = \; 0$ already, which yields

$$b_* \; = \; 0 \; . \tag{8c'}$$

As numeric modeling demonstrates, approximations (8c) and (8c') yield very close results in real conditions.

Thus, (5) and (6a) determine the solution of rigid-lid problem, (5.47), and (5) and (9) determine the solution of free-boundary problem, (5.49), in the Fourier-space. Still, they do this with one exception: $\mathbf{k}$ must differ from zero. For zero wave-number, $\mathbf{k} \; = \; 0$, described solutions does not exist. The reason for such peculiarity is that for special case $\mathbf{k} \; = \; 0$ values of the first derivative $\partial\varphi/\partial\sigma$ are not independent at the ends of integration domain. This is easy verify, integrating (2') once at $\mathbf{k} = 0$:

$$\frac{\partial\varphi}{\partial\sigma} \; = \; \frac{1}{\overline{s}^2} \left(C \; - \; \int_\sigma^1 B \; d\sigma' \right) \; ,$$

where C is the constant of integration. This constant determines the first derivative of φ everywhere uniquely. Choosing $(\partial\varphi/\partial\sigma)_1 \; = \; 0$, i.e. $C = 0$, we cannot insist on the predetermined value of vertical derivative at the upper boundary anymore. At the same time both models, if applied at $\mathbf{k} = 0$, would require predetermined value for

the first derivative at the upper boundary: $\partial\varphi/\partial\sigma = 0$ for the rigid-lid and $\partial\varphi/\partial\sigma = A(0)/\sigma_0/(\mu_2+1)$ (because $\mu_2 - 1 = 0$ in (7) for $\mathbf{k} = 0$) for the free-boundary model.

For this reason in the zero wave-vector case the homogeneous Dirichlet condition at the bottom is taken for the remaining boundary condition:

$$\mathbf{k} = 0 : \quad \varphi|_1 = 0 , \quad \left(\frac{\partial\varphi}{\partial\sigma}\right)_1 = 0 ,$$

which for discrete solution (5) implies

$$\mathbf{k} = 0 : \quad \beta = 0 . \tag{10}$$

6.4. Initialization

At the initial moment $t = 0$ the rigid lid condition (5.30c) is assumed for horizontal velocity $\mathbf{v}$ in both upper boundary models. This condition is not absolutely necessary for the free upper boundary, but even quite moderate deviation from the exact balance can cause violent buoyancy oscillations of the model atmosphere.

If an optional initial field $\mathbf{v}_{in}$ does not satisfy (5.30c), it is projected into the linear space of vertically non-divergent vectors:

$$\mathbf{v}_{in} \Rightarrow \mathbf{v}_f : \quad \nabla\cdot\left(p_*\int_0^1 \mathbf{v}_f d\sigma\right) = 0,$$

by making a simplest assumption

$$\mathbf{v}_{in} = \mathbf{v}_f + \frac{1}{p_*}\nabla\Phi ,$$

where $\Phi = \Phi(x,y)$ is a height-independent potential which can be determined from equation

$$\nabla^2\Phi = \nabla\cdot\left(p_*\int_0^1 \mathbf{v}_{in} d\sigma\right) .$$

The same projection procedure is used in the rigid-lid model periodically at every nth time step.

6.5. Diagnostical evaluation of vertical velocity.

If initial vertical velocity fields satisfy conditions (5.18a), (5.18b) and (5.17a), the same relations will hold (due to the choice of z') for all successive moments. That means, instead of the use of the evolutionary equation for w, (5.17b), one can use successively relations (5.18a) and (5.17a). Of course, do to the small computational errors the vertical sigma-velocity at the ground, $\dot\sigma_1$, can become different from zero, and a correction is needed. In NHAD the correction algorithm, employed at every step, is as follows

$$\dot\sigma_{fin} = \dot\sigma_{in} - \sigma\cdot(\dot\sigma_{in})_1 , \quad \dot\sigma_{in} = -\frac{1}{p_*}\int_0^\sigma \nabla\cdot(p_*\mathbf{v})d\sigma' .$$

6.6. Numerical tests with the rigid-lid model

In Fig. 6.2 results of mountain wave simulations with the rigid-lid version of the NHAD are presented. Modelling is performed for an isolated bell-shape mountain with $h_0 = 1$ km and $l_x = 30$ km, $l_y = \infty$. Upstream incident flow is an uniform wind with $U = 25$ m/s, and $N = 10^{-2}$ s^{-1}. Grid-size is $\Delta x = \Delta y = 10$ km and time step is 10 s. The rigid lid is replaced at the level $p_{top} = 50$ mb. Model includes a Rayleigh absorption layer between 12 km and top levels with maximum characteristic e-fold relaxation period τ_{top} = 300 s at the top. Figures represent isolines of the total potential temperature with the interval $\Delta\Theta = 1$K.

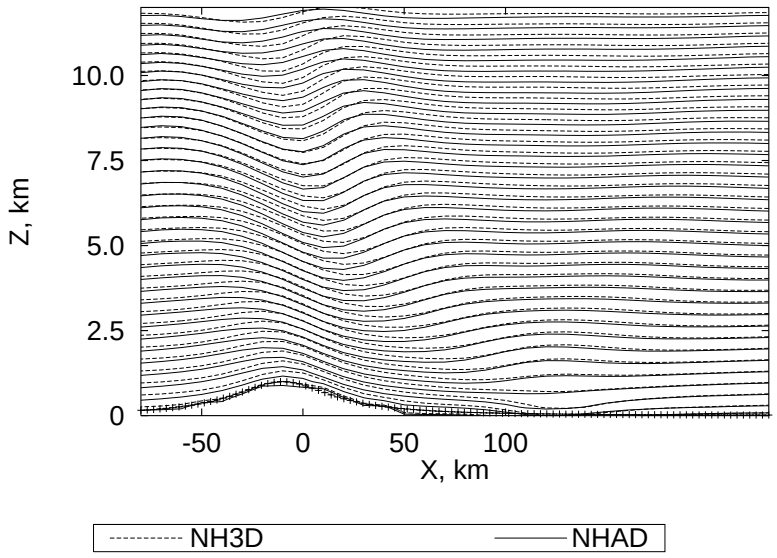

Fig. 6.2a

Comparison of models NH3D and NHAD.

Potential temperature isolines with interval 1 K. Integration period: 5000 s.

Because the flow is slipping, non-viscous and effectively two-dimensional (though the integration domain is three-dimensional with the ground area 320×160 km), the isolines of potential temperature coincide in this particular situation with streamlines.

Integration is started with an initial flow, which is obtained from the uniform flow $(u,\ v,\ w) = (U,\ 0,\ 0)$ with the help of the initialization procedure, described in section 6.4, and it is carried on until the approximate stationary state is established.

In Fig. 6.2a model calculation results for original version by Miranda, NH3D, and the rigid-lid version of NHAD are compared for identical conditions. As this figure demonstrates, the NH3D is effectively a rigid-lid model.

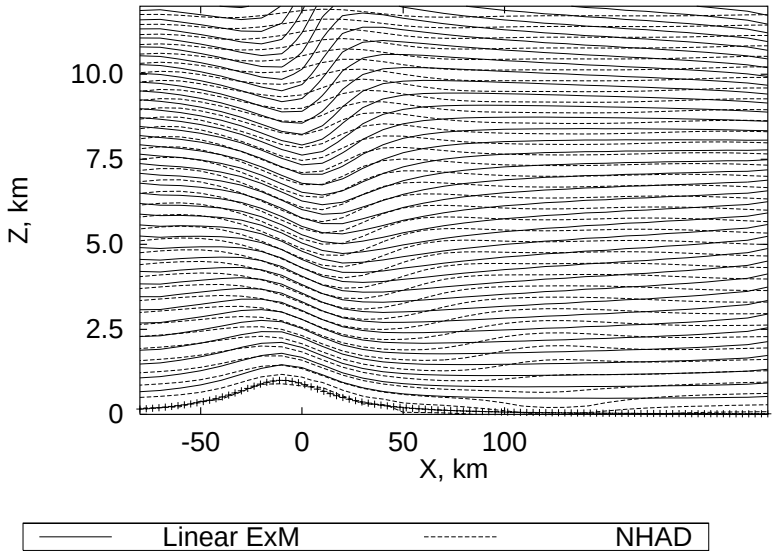

Fig. 6.2b

Comparison of the linear stationary exact model and NHAD. Potential temperature isolines as in Fig. 6.1a Integration period for NHAD: 5000 s.

As demonstrates Fig. 6.2b, the rigid-lid model is quite different from the exact linear stationary solution, especially in the upper atmosphere, where the rigid-lid constriction suppresses vertical wave-replacements very effectively. Because for the given parameters the linear stationary solution is very close to the nonlinear exact solution, we can conclude, that the rigid-lid approximation is applicable, if the modelling of lower troposphere is only required and even in this case the upper boundary should be lifted to high elevations.

The rigid-lid model represents a quite stable integration scheme and allows relatively large time steps. In Fig. 6.1c the results for model with time step 50 s are compared to a model with time-step 10 s. (the same as in Fig. 6.1a and b). In addition the Rayleigh dumping is switched out for the model with large time-step. This causes slightly larger waves in the upper atmosphere, but does not involve numerical instability.

It should be pointed also, that the relaxation period, during which the initial flow transforms to the stationary, is at the rigid-lid case approximately twice shorter as for the free-boundary model.

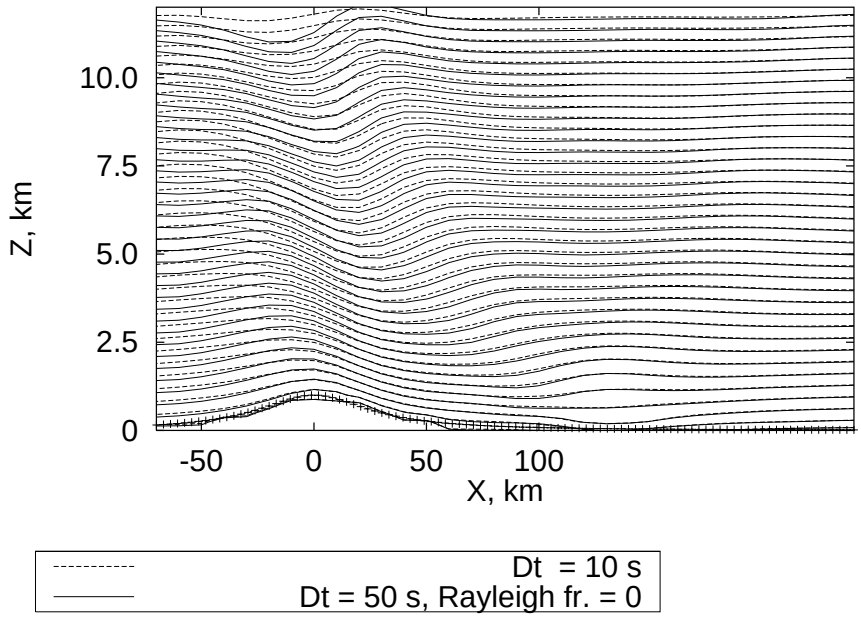

Fig. 6.2c

NHAD: Rig-lid models with different time steps. Θ isolines as in Fig. 6.1b. Integration period: 5000 s .

At the same time, the stability of a stationary flow over an isolated mountain depends (even for exact solutions) on the upper boundary condition. There can exist flows, which are stable (at the same background conditions) for free upper boundary but become unstable for the rigid-lid one. An example represents flow with parameters U = 20 m/s, $N = 10^{-2}$ s^{-1}, h_0 = 1 km, l_x = 10 km. This model is known as a stable (Baines, 1995) for free-boundary condition but it makes turbulent after approximately on hour evolution, if the rigid-lid condition is applied.

6.7. Numerical tests with the free-boundary model

Computation results with free-boundary models are represented in Fig. 6.3. Model parameters are the same as in Fig. 6.2a, except the integration time step, which is 60 s, and the Rayleigh top relaxation time, τ_{top} = 500 s.

In Fig. 6.3a the potential temperature isolines for the free-boundary NHAD model and for the linear ExM are presented. As seen, the coincidence of models is good in the lower and medium-level atmosphere, up to height 8 – 10 km. Deviations above that level are caused by nonlinear effects, which become significant, if the wave amplitude increases, and which are omitted by the linear model. Thus, the free-boundary NHAD model is here the most representative one.

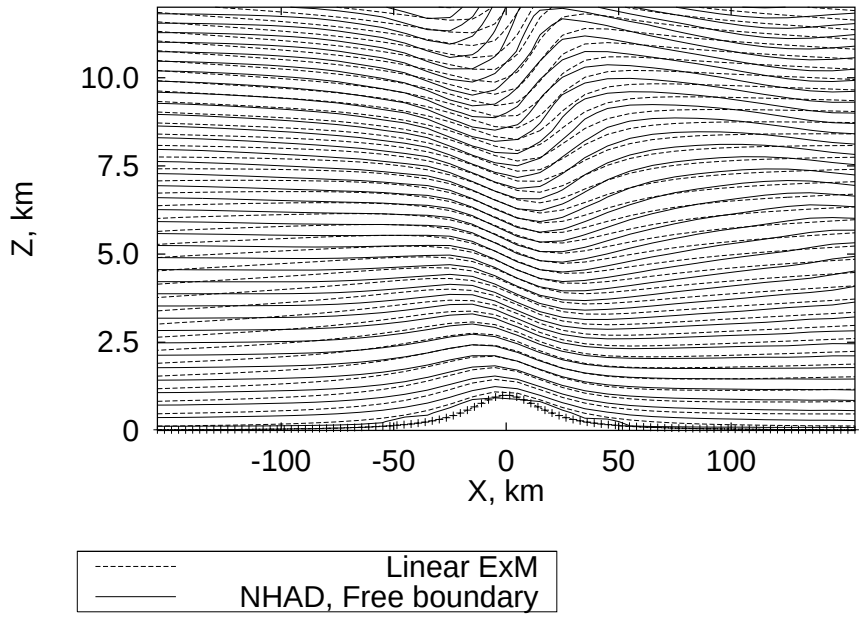

Fig. 6.3a

Potential temperature isolines of the free-boundary NHAD. Comparison with the exact linear stationary solution. Integration period is 12 000 s .

The presented in Fig. 6.3a NHAD solution corresponds to upper boundary condition (8a) with the "exact" right hand term, (8c). Effect on this term in the upper boundary condition on the solution is demonstrated in the next Figure, where modeling results for (8c) and (8c') are compared for the same model conditions as in Fig. 6.3a.

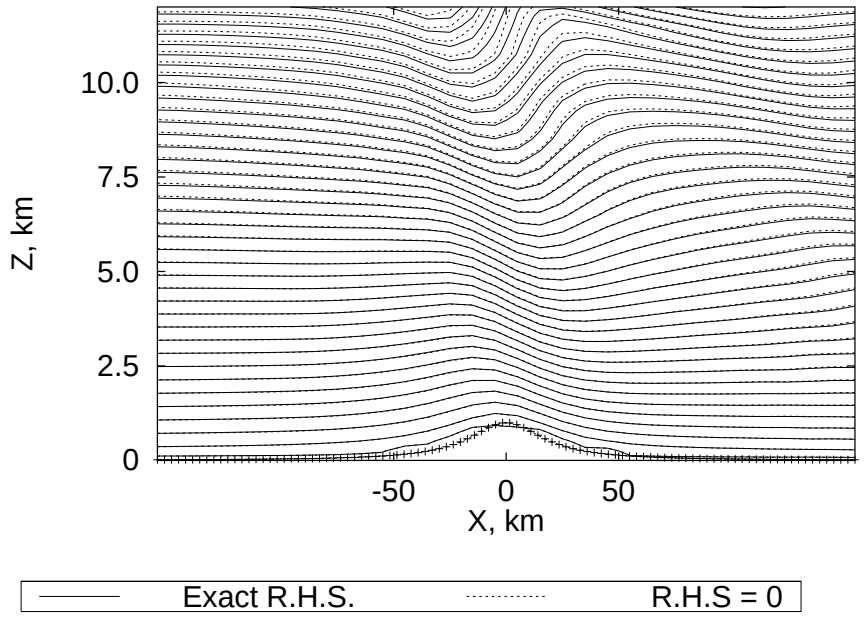

Fig. 6.3b

Free-boundary NHAD. A comparison of the effect of term b_*, in (8a), on the solution. Integration period: 12 000 s .

The conclusion from this example is, that the nonhomogeneous (5.36c') can be replaced without any loss of precision with the homogeneous one.

In Fig. 6.4a and 6.4b modeling results with shorter orography, $l_x = 10$ km, are presented. The incident wind speed is $U = 25$ m/s in Fig. 6.4a, and 10 m/s in Fig. 6.4b. Other parameters are:
$h_0 = 1$ km, $l_y = \infty$, $N = 10^{-2}$ s^{-1}, $\Delta x = \Delta y = 5$ km, and time step is 30 s. Upper boundary is at the level $p_{top} = 25$ mb. Model includes a Rayleigh absorption layer between 12 km and top level, $\tau_{top} = 500$ s.

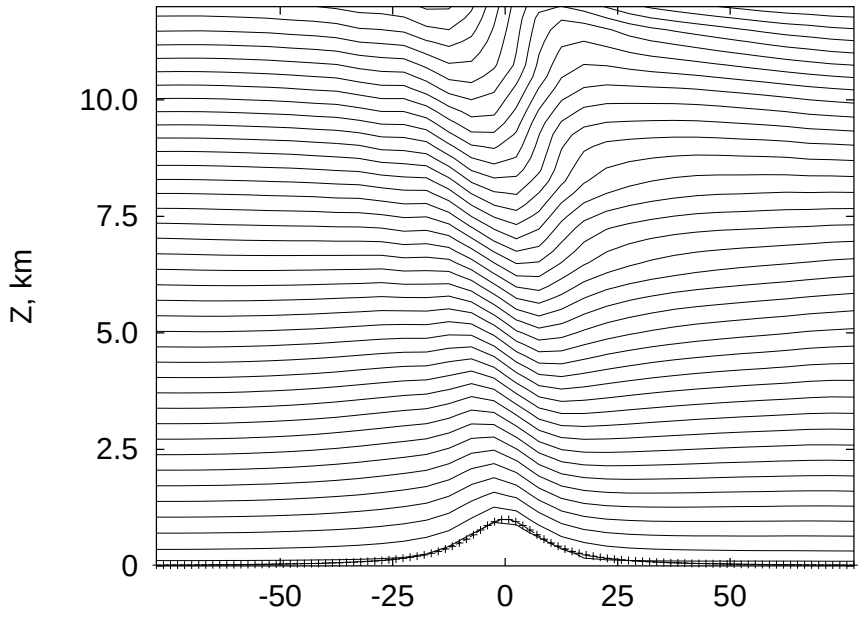

Fig. 6.4a

Potential temperature waves for $U = 25$ m/s over a mountain with $l_x = 10$ km. Integration period: 9000 s.

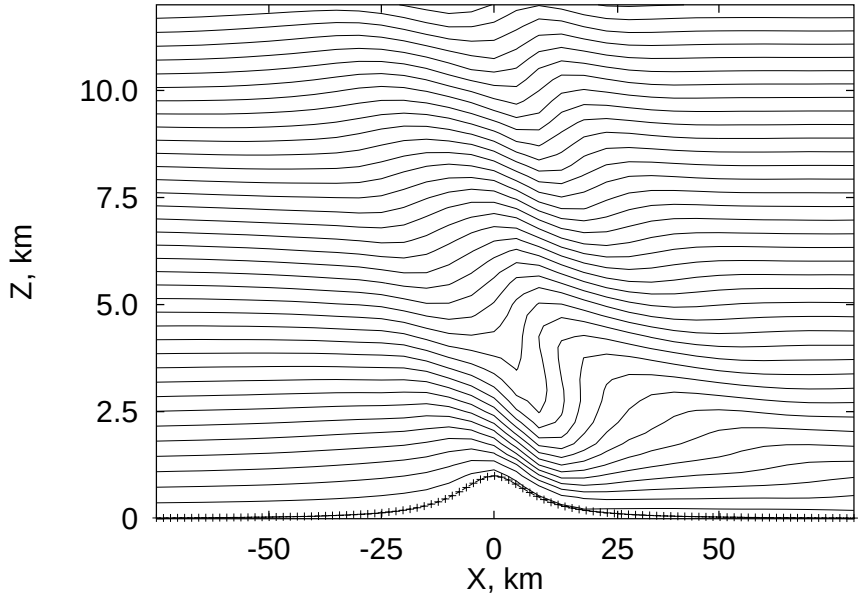

Fig. 6.4b

Potential temperature waves for $U = 10$ m/s. Other parameters as in Fig. 6.4a.

Conclusions from the modeling are:

Free-boundary NHAD yields results, which are in good accordance with exact analytical solutions in situations where the last ones are available.

Free-boundary model is more stable (in comparison with the rigid lid model) numerically and permits slightly (up to 20 %) larger time steps.

Transition from initial profile to the stationary regime is not so rapid as for the rigid-lid model and is, obviously, in a better agreement with the reality.

The general conclusion is that the free-boundary variant of the NHAD is most relevant for modeling of slow dynamical processes in mesoscale and shorter synoptic scale and it can be used, after updating with necessary physical paramterizations, for modeling of real processes in the atmosphere.

APPENDIX 1

Expansion of the geopotential height in σ–coordinate framework

Geopotential height (1.1) can be presented as

$$z(\mathbf{x},\ \sigma,\ t)\ =\ h(\mathbf{x})\ +\ \int_{\sigma}^{1}\frac{H(\mathbf{x},\ \sigma',\ t)}{\sigma'}\mathrm{d}\sigma'\ +\ \mathrm{z_n}(\mathbf{x},\ \sigma,\ \mathrm{t})$$

where the last term represents the non-static correction, which corresponds to density fluctuation n', and the remaining terms correspond to static contribution. From this expansion a lower boundary condition follows

$$z_n|_1\ =\ 0\ .$$

Presenting the temperature as a sum of the background value and fluctuative contribution,

$$T(\mathbf{x},\ \sigma,\ t)\ =\ T_0[\sigma * p_S(\mathbf{x},\ t)]\ +\ T'(\mathbf{x},\ \sigma,\ t)$$

where background temperature $T_0(p)$ generates the corresponding height-scale

$$H(\mathbf{x},\ \sigma,\ t)\ =\ H_0[\sigma * p_0(\mathbf{x},\ t)]\ +\ H'(\mathbf{x},\ \sigma,\ t)$$

we obtain without any approximation

$$z(\mathbf{x},\ \sigma,\ t)\ =\ z_*(\mathbf{x},\ \sigma,\ t)\ \ +\ z'(\mathbf{x},\ \sigma,\ t) \qquad (A.1a)$$

where z_* represents the background height, which can be expressed as a function of z_0:

$$z_*(\mathbf{x},\ \sigma,\ t)\ =\ z_0[\sigma * \overline{p_0}(\mathbf{x},\ t)]\ . \qquad (A.1b)$$

$z_0(p)$ depends on the mean temperature $T_0(p)$ (assuming that $\overline{p_0}$ corresponds to the same mean temperature distribution):

$$z_0(p)\ =\ h(\mathbf{x})\ +\ \int_{p}^{\overline{p_0}(\mathbf{x})}\frac{H_0(p')dp'}{p'}\ =\ \int_{p}^{a}\frac{H_0(p')dp'}{p'}\ .$$

z' presents as

$$z'(\mathbf{x},\ \sigma,\ t)\ =\ z_b(\mathbf{x},\ t)\ +\ \int_{\sigma}^{1}\frac{H'(\mathbf{x},\ \sigma,\ t)}{\sigma'}\mathrm{d}\sigma'\ +\ \mathrm{z_n}(\mathbf{x},\ \sigma,\ \mathrm{t})\ , \qquad (A.1c)$$

and z_b is the baric component, independent of σ:

$$z_b(\mathbf{x},\ t)\ =\ \int_{\overline{p_0}(\mathbf{x})}^{p_0(\mathbf{x},t)}\frac{H_0(p)}{p}\mathrm{dp} \qquad (A.1d)$$

Following fundamental features hold:

$$\nabla_\sigma\ z_*\ -\ \frac{\sigma}{p_0}\frac{\partial z_*}{\partial\sigma}\nabla p_0\ =\ 0 \qquad (A.2a)$$

$$z'|_{\sigma=1}\ =\ z_b\ ,\ \ z_*|_{\sigma=1}\ =\ h\ -\ z_b \qquad (A.2b)$$

$$\nabla z_b\ =\ \left(\frac{H_0}{p}\right)_{p_0}\nabla p_0\ -\ \left(\frac{H_0}{p}\right)_{\overline{p_0}}\nabla\overline{p_0}\ \approx\ \left(\frac{H_0}{p}\right)_{\overline{p_0}}\nabla p_0' \qquad (A.2c)$$

REFERENCES

Alaka,M. A., Ed., 1960: *The Airflow over Mountains.* WMO Tech. Rep. 34, 135 pp.

Arakawa, A., V. R. Lamb, 1977: Computational design of the basic dynamical processes of the UCLA general circulation model. *Methods in Compt. Physics*, **17**, Academic Press, 174 - 265, 337 pp.

Asselin, R., 1972: Frequency filter for time integration. *Mon. Weather Rev.*, **100,** 487 – 490.

Bacmeister, J. T., 1987: Nonlinearity in transient, two-dimensional flow over topography. PhD. thesis, Princeton University, 187 pp.

Baines, P. G., 1995: *Topographic Effects in Stratified Flows.* Cambridge Univ. Press, 482 pp.

Cote, J., S. Gravel, A. Staniforth, 1995: A generalized family of schemes that eliminate the spurious resonant response of semi–Lagrangian schemes to orographic forcing. *Mon. Weather Rev.*, **123,** 3605 – 3613.

Cullen M. J. P., 1991: Finite difference methods. In: Numerical Methods in Atmospheric Models, Vol. I, ECMWF, Reading, U.K., 87 – 102, 290 pp.

Davies, H. C., 1976: A lateral boundary formulation for multi–level prediction models. *Quart. J. Roy. Meteor. Soc.***102**, 405 – 418.

Dudhia, J., 1993: A nonhydrostatic version of the Penn State-NCAR mesoscale model: Validation tests and simulation of an Atlantic cyclone and cold front. *Mon. Weather Rev.*, **121,** 1493 – 1513.

Durran, D. R., 1989: Improving the anelastic approximation. *J. Atmos. Sci.*, **43,**1453 – 1461.

Durran, D. R., 1990: Mountain waves and downslope winds. In: W. Blumen (ed.), *Atmospheric Processes Over Complex Terrain*, American Meteorol. Soc., 59 – 82.

Durran, D. R., and J. B. Klemp, 1983: A compressible model for the simulation of moist mountain waves. *Mon. Weather Rev.*, **111,** 2341 – 2361.

Dutton, J. A. and G. H. Fichtl, 1969: Approximate equations of motion for gases and liquids. *J. Atm. Sci.*, **26**, 241 – 254.

Eliassen, A. 1949: The quasi-static equations of motion with pressure as independent variable. *Geofys. Publikasjoner (Oslo)*, **17**, # 3, 44 p.

Eliassen A. E., and E. Palm, 1960: On the transfer of energy in stationary mountain waves. *Geofys. Publikasjoner (Oslo)*, **21**, 1 – 33.

Gill, A. E. 1982: *Atmosphere-Ocean Dynamics.* Academic Press, New York, 662 pp.

Gustafsson, N. and A. McDonald, 1996: A comparison of the HIRLAM gridpoint and spectral semi–Lagrangian models. *Mon. Weather Rev.*, **124,** 2008 – 2022.

Haltiner, G. J., and R. T. Williams 1980: *Numerical Prediction and Dynamic Meteorology.* John Wiley & Sons, New York.

Hereil, , Ph. R. Laprise, 1996: Sensitivity of internal gravity waves solutions to the time step of a semi-implicit semi-Lagrangian nonhydrostatic model. *Mon. Weather Rev.*, **124,** 972 – 999.

Herivel, J. W., 1955: The derivation of the equations of motion of an ideal fluid by Hamilton's principle*Proc. Cambridge Phil. Soc.,* **51**, 344 – 349.

HIRLAM Documentation Manual, 1996: Ed. by E. Klln, 250 pp.

Hoinka, K. P., 1985: A comparison of numerical simulations of hydrostatic flow over mountain and observations. *Mon. Weather Rev.*, **113,** 719 – 735.

Holton, J. R. 1992: *An Introduction to Dynamic Meteorology.* Third Edition. Academic Press, New York. 511 pp.

Hoskins, B. J., A. J. Simmons, 1975: A multi–layer spectral model and the semi–implicit method. *Q. J. R. Meteorol. Soc.*, **101**, 637 – 655.

Hupert, H. E., and J. W. Miles, 1969: Lee waves in a stratified flow. Part 3. Semi-elliptical obstacle.*J. Fluid Mech.*, **35**, 481 – 496.

Jones, W. L., 1967: Propagation of internal gravity waves in fluids with shear flow and rotation. *J. Fluid Mech.*, **30**, 439 – 488.

Klemp, J. B., and D. K. Lilly, 1978: Numerical simulation of hydrostatic mountain waves. *J. Atmos. Sci.*, **35,**78 – 107.

Klemp, J. B., R. B. Wilhelmson, 1978: The simulation of three-dimensional convective storm dynamics. *J. Atm. Sci.*, **35**, 1070 – 1096.

Landau, L. D., E. M. Lifchitz, 1987: *The classical theory of fields.* Oxford: Pergamon, 402 p.

Laprise, R., 1992: The Euler equations of motion with hydrostatic pressure as an independent variable. *Mon. Weather Rev.*, **120,** 197 – 207.

Laprise R., and W. R. Peltier, 1989: On the structural characteristics of steady finite–amplitude mountain waves over bell–shaped topography. *J. Atmos. Sci.*, **46,** 586 – 595.

Lin, Y.-L., and T.-A. Wang, 1996: Flow regimes and transient dynamics of two-dimensional stratified flow over an isolated mountain ridge. *J. Atmos. Sci.*, **53,** 139 – 158.

Lindzen, R. S., and K. K. Tung, 1976: Banded convective activity and ducted gravity waves. *Mon. Weather Rev.*, **104,** 1602 – 1617.

Long, R. R., 1953: Some aspects of the flow of stratified fluids. Part I: A theoretical investigation. *Tellus*, **5**, 42 – 58.

Long, R. R., 1954: Some aspects of the flow of stratified fluids. Part II: Experiments with a two fluids system. *Tellus*, **6**, 97 – 115.

Martin, C, R. A. Pielke, 1983: The adequacy of the hydrostatic assumption on sea breeze modeling over flat terrain. *J. Atm. Sci.*, **40**, 1472 – 1481.

Miles J. W., 1968a: Lee waves in a stratified flow. Part 1. Thin barrier. *J. Fluid Mech.*, **32**, 549 - 567.

Miles J. W., 1968b: Lee waves in a stratified flow. Part 2. Semi-circular obstacle. *J. Fluid Mech.*, **33**, 803 - 814.

Miles J. W., and H. E. Hupert, 1969: Lee waves in a stratified flow. Part 4. Perturbation approximations. *J. Fluid Mech.*, **35**, 481 – 496.

Miller, M. J., 1974: On the use of pressure as vertical co-ordinate in modelling convection. *Q. J. R. Meteorol. Soc.*,**100**, 155 – 162.

Miller, M. J., R. P. Pearce, 1974: A three-dimensional primitive equation model of cumulonimbus convection. *Q. J. R. Meteorol. Soc.*, **100**, 133 – 154.

Miller, M. J., A.A. White, 1984: On the nonhydrostatic equations in pressure and sigma coordinates. *Q. J. R. Meteorol. Soc.*, **110**, 515 – 533.

Miranda, P. M. A., 1990: Gravity waves and Wave Drag in Flow Past Three–Dimensional Isolated Mountains. A PhD Thesis. University of Reading, 191 pp.

Miranda, P. M. A., I. N. James, 1992: Non-linear three-dimensional effects on gravity-wave drag: Splitting flow and breaking waves. *Q. J. R. Meteorol. Soc.***118**, 1057 – 1081.

Monserrat, S, and A. J. Thorpe, 1996: Use of ducting theory in an observed case of gravity waves. *J. Atmos. Sci.*, **53,**1724 – 1736.

Ogura, Y., J. C. Charney, 1962: A numerical model of thermal convection in the atmosphere. *Proc. Int. Symp. Numerical Weather Prediction. Tokyo.* Met. Soc Japan, 431 – 451.

Ogura, Y., N. A. Phillips, 1962: Scale analysis of deep and shallow convection in the atmosphere. *J. Atm. Sci.*, **19**, 173 – 179.

Orlanski, I., 1976: A simple boundary condition for unbounded hyperbolic flows. *J. Comput. Phys.*, **21**, 251 – 269.

Orlanski, I., 1981: The quasi-hydrostatic approximation. *J. Atm. Sci.*, **38**, 572 – 582.

Phillips, N. A., 1957: A coordinate system having some special advantage for numerical forecasting. *J. Meteorol.*, **14**, 184 – 185.

Pielke, R. A., 1984: *Mesoscale Meteorological Modeling.* Academic Press, 612 pp.

Pinty, J.–P., et al, 1995: Simple tests of a semi–implicit semi–Lagrangian model on 2D mountain wave problems. *Mon. Weather Rev.*, **123,** 3042 – 3058.

Queney, P., 1948: The problem of airflow over mountains: a summary of theoretical studies. *Bull. Amer. Met. Soc.*, **29**, 16 – 26.

Raymond, W.H. and H. L. Kuo, 1984: A radiation boundary condition for multi-dimensional flows. *Q. J. R. Meteorol. Soc.*, **110**, 535 – 551.

Redelsberger, J. L., G. Sommeria, 1981: Methode de representation de la turbulence d'chelle infrieure a la maille pour un modele tridimentionnel de covection nuageuse. *Bound. Layer Meteor.*, **21**, 509 – 530.

Richie, H et all, 1995: Implementation of the Semi–Lagrangian method in a high–resolution version of the ECMWF forecast model. *Mon. Weather Rev.*, **123,** 489 – 514.

Robert, A. J., 1966: The integration of a low order spectral form of the primitive meteorological equations. *J. Met. Soc. Japan*, **44**, 237 – 245.

Rõõm, R. 1988: Evolutionary form of primitive equations in the isobaric coordinate space and free boundary effects. *Prepr. A-5(1988) of Estonian Academy of Sciences*, 30 pp.

Rõõm, R., 1989: The general form of dynamical equations of the atmosphere in the isobaric coordinate space. *Proc. Estonian Academy Sci., Phys. Math.*, **38**, 368 – 371.

Rõõm, R., 1990: General form of the dynamical equations for the ideal atmosphere in the isobaric coordinate system. *Izv. AN SSSR, Fiz. Atmos. i Okeana*, **26**, 17 – 26.

Rõõm, R. and A. Ülejõe, 1996: nonhydrostatic acoustically filtered equations of atmospheric dynamics in pressure coordinates. *Proc. Estonian Academy Sci., Phys., Math.*, **45**, 421 – 429.

Roulstone, I., S.J. Brice, 1995: On the Hamiltonian formulation of the quasi–hydrostatic equations. *Q. J. R. Meteorol. Soc.*, **121**, 927 – 936.

Salmon, R. 1983: Practical use of Hamilton's principle. *J. Fluid Mech.*, **132**, 431 – 444.

Salmon, R. 1988a: Hamiltonian Fluid Mechanics. *Ann. Rev. Fluid. Mech.*, **20**, 225 – 256.

Salmon, R. 1988b: Semi–geostrophic theory as a Dirac bracket projection. *J. Fluid. Mech.*, **196**, 345 –358.

Salmon, R., L. M. Smith, 1994: Hamiltonian derivation of the nonhydrostatic pressure–coordinate model. *Q. J. R. Meteorol. Soc.*, **120**, 1409 – 1413.

Sass, B. H., J. H. Christensen, 1995: A simple framework for testing the quality of atmospheric limited–area models. *Mon. Weather Rev.*, **123,** 444 – 459.

Scorer, R. S., 1949: Theory of waves in the lee of mountains. *Q. J. R. Meteorol. Soc.*, **75**, 41 – 56.

Scorer, R. S., 1953: Theory of airflow over mountains: II - The flow over a ridge. *Q. J. R. Meteorol. Soc.*, **79**, 70 – 83.

Scorer, R. S., 1954: Theory of airflow over mountains: III - Airstream characteristics. *Q. J. R. Meteorol. Soc.*, **80**, 417 – 428.

Scorer, R. S., 1956: Airflow over an isolated hill. *Q. J. R. Meteorol. Soc.*, **82**, 75 – 81.

Serrin, J., 1959: *Mathematical principles of Classical Fluid Mechanics.* In: Handbuch der Physik, Band VIII/1, Strömungmechanik I, Springer-Verlag, Berlin – Göttingen – Heidelberg. pp. 125 -263.

Simmons, A. J., D. M. Burridge, 1981: An Energy and angular–momentum conserving vertical finite-difference scheme and hybrid vertical coordinates. *Mon. Weather Rev.*, **109,** 758 – 766.

Smith, R. B., 1979: The influence of mountains on the atmosphere. *Adv. Geophys.*, **21**, 87 -230.

Tapp, M. C., P. W. White, 1976: A nonhydrostatic mesoscale model. *Q. J. R. Meteorol. Soc.*, **102**, 277 – 296.

Tjernström, M., L. Enger, A. Andren, 1988: A three–dimensional numerical model for studies of atmospheric flows on the meso-γ scale. *J. Theor. Appl. Mech.,* **7**, 167 – 194.

White, A.A. ,1989: An extended version of nonhydrostatic, pressure coordinate model. *Q. J. R. Meteorol. Soc.*, **115**, 1243 – 1251.

Williams, G. P., 1969: Numerical integration of the three-dimensional Navier-Stokes equations for incompressible flow. *J. Fluid Mech.*, **37**, 727 – 750.

Winninghoff, F., J., 1968: On the adjustment toward the geostrophic balance in a simple primitive equation model with application to the problems of initialization and objective analysis. Ph.D. Thesis. Dept. Met. Univ. of California, los Angeles.

Wurtele, M. G., R. D. Sharman and T. L. Keller, 1987: Analysis and simulations of a troposphere-stratosphere gravity wave model. Pat I. *J. Atmos. Sci.*, **44,**3269 – 3281.

Wurtele, M. G., A. Datta, and R. D. Sharman, 1996: The propagation of gravity-inertia waves and lee waves under a critical level. *J. Atmos. Sci.*, **53,**1505 – 1523.

Xue, M., A. J. Thorpe, 1991: A mesoscale numerical model using the nonhydrostatic pressure-based sigma-coordinate equations: Model experiments with dry mountain flows. *Month. Wea. Rev.*, **119**, 1168 – 1185.

Yang, X., 1993: A nonhydrostatic model for simulation of airflow over mesoscale bell-shaped ridges. *Bound.- Layer Meteor.*, **65**, 401 – 424.